

**Towson University
Office of Graduate Studies**

**EFFECTS OF STREAM RESTORATION BY LEGACY SEDIMENT REMOVAL
AND FLOODPLAIN RECONNECTION ON WATER QUALITY**

by

Patrick William McMahon

A thesis

Presented to the faculty

of Towson University

in partial fulfillment

of the requirements for the degree of

MASTER OF SCIENCE

Department of Environmental Science

Towson University
Towson, MD 21252

December 2020

TOWSON UNIVERSITY
GRADUATE STUDIES

THESIS APPROVAL PAGE

This is to certify that the Thesis prepared by

Patrick McMahon

Entitled

Effects of stream restoration by legacy sediment removal and floodplain reconnection on water quality

has been approved by the thesis committee as satisfactorily completing the thesis requirements for the degree of Master of Science in Environmental Science.



01/13/2021

Chairperson, Thesis Committee

Joel Moore

Date



January 13, 2021

Committee Member

Vanessa Beauchamp

Date



January 13, 2021

Committee Member

Ryan Casey

Date



13 Jan 2021

Committee Member

Christopher Salice

Date




Digitally signed by David R Ownby

Date: 2021.01.20 15:39:00 -05'00'

Dean of Graduate Studies

David Ownby

Date

Acknowledgments

This work was supported by a Restoration Research grant (#13974) from the Chesapeake Bay Trust (VBB, RAC, CJS, JM) and partially by the National Science Foundation ICER-1540631 (JM). I gratefully acknowledge Caroline Stanley, Colin McGill, Scott McGill, and others at Ecotone, Inc. for their assistance in site selection without which this project would not have been possible, for connecting us with property owners to gain site access, and for their willingness to share site design plans and other relevant information. I thank Melinda Marsh, Ginny Jeppi, Mary McWilliams, and Michael Dawson for assistance in the field and laboratory along with Mark Monk for invaluable support with laboratory procedures and instrumentation. Again, I thank Melinda Marsh for her work on the Plumtree Run Gage annual loads and storm analyses. I thank my committee (Vanessa Beauchamp, Ryan Casey, David Ownby, and Christopher Salice) for taking the time to help and review my thesis. Lastly, I would like to thank Joel Moore for his instrumental help and support through my Master's project.

Abstract

Stream restoration effects on water quality (WQ) are unknown, and approaches to restoration are diverse. In the mid-Atlantic region of the United States, European land-modifications resulted in the deforestation, erosion, and deposition of sediments into stream valleys – legacy sediments. During the 19th and 20th century, streams incised through legacy sediments (1) creating high banks subject to collapse, (2) removing connection to the floodplain, and (3) lowering water tables promoting adjacent upland soils. Legacy sediment removal (LSR) and floodplain reconnection (FR) projects propose WQ benefits by restoring degraded streams closer to their pre-European hydrologic condition. WQ was investigated at six restored LSR-FR projects and three control/regional sites. Baseflow nitrogen concentrations and fluxes at restored sites were elevated compared to forested controls, particularly in agriculture settings, with little apparent impact of restoration. Nutrient and sediment storm loads may be reduced at the restoration scale; however, regional effects of restoration were not observable.

Table of Contents

List of Tables	vii
List of Figures	viii
1. Introduction	1
1.1 Chesapeake Bay Health and Water Quality	1
1.2 Historic Land Alterations and Implications	4
1.3 Stream Restoration	6
2. Materials and Methods	12
2.1 Site Description	12
2.2 Base-Flow Discharge Measurements	15
2.3 Storm-Flow Discharge, primarily at First Mine Branch	17
2.4 Baseflow Sample Collection Methods	17
2.5 Stormflow Sample Collection Methods, primarily at First Mine Branch	18
2.6 Laboratory Analysis Methods	20
2.7 Baseflow and Storm Sampling	21
2.8 Calculations and Statistical Analysis	22
2.8.1 Baseflow and Stormflow Daily Load Calculations	22
2.8.2 Statistical and Storm Analysis	24
3. Goal	26
4. Results and Discussion	27
4.1 Baseflow Discharge Results and Discussion	27

4.2 Baseflow General Stream Characteristics.....	28
4.2.1 Baseflow pH Results and Discussion	28
4.2.2 Specific Conductance Results and Discussion	29
4.2.3 DO Results and Discussion.....	30
4.2.4 Temperature Results and Discussion	31
4.3 Baseflow Major Cation and Anion Results and Discussion	31
4.4 Baseflow Nitrogen Concentration/Daily Load Results and Discussion	33
4.5 Baseflow Dissolved Organic Carbon Concentration Results	36
4.6 Baseflow TDN and DOC Relationship Results and Discussion.....	37
4.7 Baseflow Total Suspended Solids Results and Discussion.....	41
4.8 Baseflow Total Dissolved Phosphorous and Ortho-Phosphate	43
4.9 Storm Assessment and Discussion at FMB and PTRG	43
4.9.1 FMB Storms.....	43
4.9.2 PTRG Storms	52
5. Conclusions.....	54
6. Tables	56
7. Figures.....	67
8. References.....	91
9. Curriculum Vitae	105

List of Tables

Table 1: Site Information	56
Table 2: Sampling Record.....	57
Table 3: Baseflow Discharge by Year.....	58
Table 4: Baseflow Stream Parameters.....	59
Table 5: Baseflow Major Cations.....	59
Table 6: Baseflow Major Anions	60
Table 7: Baseflow TDN, DOC, and TSS Concentrations and Daily Loads.....	60
Table 8: Post-Restoration Baseflow Significance Values – Concentration	61
Table 9: Post-Restoration Baseflow Significance Values – Daily Load.....	61
Table 10: Pre- and Post-Restoration Baseflow Concentrations and Daily Loads	61
Table 11: Pre-Post and Pre-Pre-Restoration Significance Values.....	62
Table 12: Phosphorous Concentrations by Site.....	62
Table 13: FMB Storm Loads.....	63
Table 14: FMB Storm Sample Information	63
Table 15: Temporal Trend in Peak (Min. for Nitrate) FMB Storm Concentration.....	64
Table 16: FMB Baseflow Compared to Stormflow Concentrations	64
Table 17: FMB Storm % Differences.....	65
Table 18: PTRG Mean Streamflow and Annual Loads	65
Table 19: PTRG Storm Sets	66

List of Figures

Figure 1: Watershed Maps and Watershed Location Maps	68
Figure 2: First Mine Branch (FMB) Rating Curve.....	68
Figure 3: FMB Calculated vs. Actual Discharge	69
Figure 4: FMB Continuous Discharge	69
Figure 5: Yearly Discharge and Area-Normalized Yearly Discharge.....	70
Figure 6: Baseflow Stream Parameters (pH, SC, DO, T)	71
Figure 7: Specific Conductance versus Chloride	72
Figure 8: Major Cation and Anions (Na^+ , Ca^{+2} , Mg^{+2} , Cl^- , HCO_3^- , SO_4^{-2}).....	73
Figure 9: Baseflow Ternary Diagrams	74
Figure 10: Baseflow Total Dissolved Nitrogen (TDN) Concentration by Site.....	74
Figure 11: Baseflow TDN and Nitrate Relationship	75
Figure 12: Pre- and Post-Restoration TDN, DOC, and TSS Concentration and Daily Load	76
Figure 13: TDN Daily Load by Site.....	77
Figure 14: Dissolved Organic Carbon (DOC) Concentration by Site	78
Figure 15: DOC:TDN Relationship	79
Figure 16: Total Suspended Solids (TSS) Concentration and Daily Load	80
Figure 17: Time Series of TSS.....	80
Figure 18: FMB 07/11/2019 Storm Dynamics	81
Figure 19: FMB 01/12/2020 Storm Dynamics	82
Figure 20: FMB 02/05/2020 Storm	83
Figure 21: Baseflow & Stormflow Concentration (C)-Discharge(Q) & C-C Relationships	84
Figure 22: Baseflow versus Stormflow Concentration Differences.....	85
Figure 23: FMB 07/11/2019 Upstream Sensitivity Analysis.....	86

Figure 24: FMB Stormflow Area-Normalized Load Differences	87
Figure 25: Plumtree Run Gage (PTRG) Nitrate-Discharge Relationship.....	87
Figure 26: PTRG C-C Relationships.....	88
Figure 27: PTRG Example Storm Event - 09/10/2015.....	89
Figure 28: PTRG Annual Loads	90

1. Introduction

1.1 Chesapeake Bay health and Water Quality

The Chesapeake Bay watershed includes regions of intense agriculture, suburban development, and major urban centers contributing to stream and estuary degradation (Ator et al., 2020). Decades of effort have been put towards the reduction of nutrients and sediments from nontidal stream tributaries in the 166,000 km² Chesapeake Bay watershed, including the development of the Environmental Protection Agency's 2010 Total Maximum Daily Load regulation to reduce nutrients and sediments from incoming tributaries (Williams et al., 2017, Ator et al., 2020). Despite these efforts to reduce nutrients and sediments from the upland watershed, the Chesapeake Bay has not met water-quality and ecological standards (Chesapeake 2018, Ator et al., 2020).

The Chesapeake Bay first showed symptoms of eutrophication in the 1950s (Kemp et al., 2005). Eutrophication is the process of over-production and decomposition of organic matter via harmful algal blooms (HABs). Microbial decomposition of HABs leads to low oxygen levels (hypoxia) in aquatic systems (Diaz 2001, Groffman et al., 2003, Kemp et al., 2005). Elevated nutrient inputs are a major cause of eutrophication (Brush 2009). In addition, elevated contributions of suspended sediments have caused the loss of submerged aquatic vegetation, increased turbidity, and the collapse of food webs (Boesch et al., 2001). Sources of nutrients and sediments include wastewater, agricultural fields, urban regions, degraded riparian regions, and altered stream channels (Carpenter et al., 1998).

The control of point source pollution discharges in the US began in 1972 and has yielded great improvements in water quality by directly limiting nutrient inputs from wastewater (Letson 1992, Carpenter et al., 1998). However, as point source pollution was reduced, non-point sources contributed a greater percentage of nutrients and suspended solids (Hobbie et al., 2017). Non-point sources – agricultural fields, legacy sediments, and urban activities – are now the largest sources of nutrients to aquatic systems (Carpenter et al., 1998, Walter and Merritts 2008, Janke et al., 2014, Hobbie et al., 2017). Nitrogen (N) and phosphorous (P) from non-point sources are the primary nutrients driving degradation in the Chesapeake Bay (Ator et al., 2020).

Non-point sources of N include the historic and present use of fertilizers, atmospheric deposition of nitrous oxides, and human/pet wastes (Carpenter et al., 1998). N largely travels through aquatic systems as dissolved inorganic nitrogen ($\text{DIN} - \text{NO}_3^-$) and dissolved organic nitrogen (DON). Both N species act as critical nutrients for HABs (Groffman et al., 2004, Petrone 2010). P is predominantly associated with soils and sediments. Soil initially acts as a sink for P via adsorption that can be mobilized during erosion events (Paul and Meyer 2009). P is mobilized in the particulate phase and transported during storm flows (Benitez-Nelson 2000, Duan et al., 2012). P in the particulate phase is largely not bioavailable, but physical, biological, and chemical redox reactions in anoxic environments, present in-stream or in the bottom of the Chesapeake Bay, promote the movement of P into the aqueous phase (Benitez-Nelson 2000, Orihel et al., 2017). Additionally, increasing temperatures, consistent with urban streams, promote the transition of particulate phosphorous (PP) to soluble reactive P (Duan et al., 2012). Much like N, P can be a limiting nutrient to HABs in estuaries (Petrone 2010).

Dissolved organic carbon (DOC) also may be relevant to understanding N and P dynamics. In-stream DOC originates from autochthonous and allochthonous sources. The majority of DOC inputs are from allochthonous or terrestrial inputs during stormflows; however, during baseflow, instream, riparian soils, and groundwater contributions can be substantial (Lambert et al., 2014). Land cover, specifically urban land-use (Worrall et al., 2012), is a strong indicator of DOC inputs into streams, while other predictors such as high wetland cover, frequent precipitation, typography, and organic soil content also increase DOC concentrations. Agriculture has a range of effects on DOC inputs into stream depending on the crops grown and farming practices (Stanley et al., 2012). Urban streams are known to transport increased DOC through altering connections to deeper groundwater pathways and upstream urban inputs (Petrone 2010 and Epstein 2016).

Riparian zones and floodplains are instrumental in processing nutrients and retaining sediments (Groffman et al., 2003), but these areas have been dramatically altered by land use changes. Stream incision in the Piedmont due to anthropogenic land-use changes and increased runoff from urban areas has left many streams decoupled from riparian regions and floodplains (Wittmann et al., 1996). Decreased residence time of water in the channel and floodplain has reduced the capacity of streams to attenuate storm flows, manage nutrients, and retain sediments (Groffman et al., 2003, Walsh et al., 2005). Anthropogenic alterations to watersheds and streams have resulted in large loads of N, P, and DOC that ultimately enter the Chesapeake Bay (Filoso and Palmer 2011, Filoso et al., 2015 Williams et al., 2017). N and P are exported in higher concentrations in urbanized and agricultural watersheds than forested and wetland environments, highlighting the role of land-use changes on nutrient export (Groffman et al., 2004,

Wollheim 2005, Janke et al., 2014). Additionally, historic and modern anthropogenic alterations to stream corridors in the Piedmont contribute to nearly 60% of the suspended sediment load to the Chesapeake (Hupp et al., 2013).

1.2 Historic Land Alterations and Implications

Prior to European settlement of the mid-Atlantic, much of the Piedmont region may have been characterized by a network of small multi-channel streams that flowed through a forested landscape containing abundant near-channel wetlands (Walter and Merritts 2008). Multi-channel streams wove through densely vegetated alluvial islands that divided and connected flows, contributing to a system of coupled wetlands (Wohl and Merritts 2007). Streams frequently overflowed stream banks depositing fine-grain sediments and organic matter into hydrologically connected floodplains (Jacobson and Coleman 1986, Walter and Merritts 2008, Merritts et al., 2011). European settlement activities such as deforestation, conversion to agricultural fields, and the construction and desertion of dams and ponds associated with mills led to the formation of single channel streams and stream entrenchment. As a result, floodplains became disconnected from their nearby streams, and adjacent wetlands were dramatically reduced (Walter and Merritts 2008, Voli et al., 2009). The start of this disconnection process in the Piedmont region was deforestation. Land clearing and vegetation burning caused increased erosion that resulted in the addition of sediments to valley-floor wetlands (Merritts et al., 2011). Conversion of forests, grasslands, and wetlands to agricultural fields further enhanced sediment transport by reducing sediment storage and accelerating sheet washing (Merritts et al., 2011). Much of this eroded sediment was captured by constructed mill dams during development and small-scale industrialization (Weitzman et al., 2014).

European colonists began building milldams and water-powered mills in the early 1700s. By the 1840s, tens of thousands of milldams and more than 64,000 water-powered mills had been built in the eastern United States (Walter and Merritts 2008, Weitzman et al., 2014). Mills were especially common in the mid-Atlantic Piedmont due to the region's proximity to shipping ports, agricultural fields, and suitable stream gradients (Walter and Merritts 2008). Once constructed, mills and mill dams produced a series of linked ponds that trapped fine-grained sediment and buried the surrounding floodplain and wetlands (Walter and Merritts 2008). Milldam sediments are now termed "legacy sediments" and are characterized by fine-grained sediment deposited on top of relic hydric soils (Weitzman et al., 2014). In the nineteenth and twentieth centuries, many of the silted-in dams were abandoned and breached. Evidence indicates that increased sediment export in northern Atlantic estuaries is largely due to mass transport of legacy sediments, and that failure of milldams led to increased erosion of legacy sediments that promote the incision of mid-Atlantic streams (Walter and Merritts 2008, Merritts et al., 2011, James 2013, Weitzman et al., 2014).

Stream incision lowers the stream channel below the floodplain surface formed by the legacy sediments and causes an increase in bank height (Merritts et al., 2011). Elevated stream banks leave a stream detached from the surrounding floodplain. During stormflows, erosional forces tend to be directed towards the floor and sides of the stream channel rather than spreading across the floodplain (Merritts et al., 2011, Hupp et al., 2013). Additionally, increased storm run-off associated with land use changes has intensified stream incision promoting bank collapse and transport of nutrient laden

sediments (Trimble 1997, Kaushal et al., 2008). Sediment-bound nutrients are a substantial driver of eutrophication in the Chesapeake Bay (Liang et al., 2013).

Legacy sediments also result in the formation of perched water tables that have little interaction with deeper groundwater. The lack of hydrologic connection between shallow and deeper groundwater affects infiltration of precipitation, groundwater recharge, nutrient cycling, and water temperatures (Gutshall and Oberholtzer 2011). Lack of hydrologic exchange between a stream and its floodplain impacts nutrient transport by limiting the amount of denitrification and P and N-immobilization (Carpenter et al., 1998). A reduction of floodplain-wetland residence time diminishes denitrification rates by minimizing stream exchanges with the floodplain's anaerobic environments.

Anaerobic microorganisms, known as denitrifying bacteria, are necessary to convert soluble inorganic N to atmospheric elemental N (Brush 2009). Likewise, an incised channel reduces interactions with the floodplain, inhibiting biological uptake of P and N, and further increasing nutrient export (Weitzman et al., 2014). Other evidence suggests that incision of streams through relic milldam sediments exposes soils to aerobic conditions that promote the oxidation of organic N, which can be easily leached from soils as inorganic nitrate (Weitzman et al., 2014). The compounded effects of legacy sediment transport, floodplain removal, and urbanization are major factors contributing to hypoxia within the Chesapeake Bay (Kaushal et al., 2008).

1.3 Stream Restoration

In an effort to reduce nutrient loading from non-point sources, the Environmental Protection Agency (EPA) in 2010 developed total maximum daily load (TMDL) regulations with the goal of reducing loads of total nitrogen (TN), total phosphorous

(TP), and total suspended solids (TSS) to the Chesapeake Bay (<https://www.epa.gov/chesapeake-bay-tmdl>). The creation of TMDL regulations recognized stream restoration projects as a best management practice (BMP) for reducing nutrient loads into the Chesapeake Bay (Williams et al., 2017). Traditional stream restoration practices rely on stabilization remedies and geomorphological alterations to address erosional aspects, while often overlooking the role of ecological processes (Palmer et al., 2014). Engineered solutions frequently attempt to control the movement of water through streams rather than address the historic and present ecological degradation of the site. Thus, restoration techniques that focus on restoring ecosystem structure, chemical interactions, and biological processes have emerged in the restoration community, including legacy sediment removal (LSR) and floodplain reconnection (FR) (Beechie et al., 2010, Palmer et al., 2014).

The goal of LSR-FR is to remove some or all of the legacy sediments deposited from European land alterations and to restore the stream to its historical elevation (<https://landstudies.com/>). Bank sediments are removed, and the stream is reconnected to its natural floodplain where frequent spillover can occur. Removal of legacy sediments and floodplain reconnection facilitate a rejoining of surface to groundwater. Additionally, stream restoration can reduce erosion by decreasing bank stress and permitting stream expansion into the floodplain-wetland complexes. N and P loads can be attenuated through increased sediment retention, denitrification, and N/P immobilization via plant uptake and microbial integration (Carpenter et al., 1998, Kaushal et al., 2008, Filoso and Palmer 2011, Weitzman et al., 2014). N exports may be mitigated through increased interaction with organic-carbon rich soils in the attached floodplain promoting

denitrification (Kaushal et al., 2008, Williams et al., 2017). Removal of sediments also eliminates a major P source. Recent data from Big Spring Run in the Chesapeake watershed showed median total P reductions of 0.15 mg/L from pre to post restoration, and sediment reductions of 69.3% from upstream (above restoration) to downstream (below restoration) (Langland et al., 2020).

Big Spring Run data indicate legacy sediment and floodplain reconnections mitigate nutrient export in an agricultural setting. However, differing land use (agricultural, suburban, urban) may influence the success of a given restoration. Due to the unknown role of impervious surface coverage (ISC) on stream restoration parameters, this study will sample watersheds with a wide range of ISC, 1.15% to 56.6%. The Environmental Protection Agency has identified runoff from urban ISC as the leading source of stream degradation (U.S. EPA 2000). In 2005, Walsh describes the “urban stream syndrome” as streams that are progressively degraded due to runoff from urban ISC. Urban and, to a lesser extent, heavily managed agricultural (low ISC) streams possess a suite of characteristics that are different from their forested counter-parts, such as: a flashy storm hydrograph, incised stream channels, increased loadings of nutrients and other contaminants, elevated dissolved solutes, altered geomorphology, and changes in species abundance and composition (Groffman et al., 2004, Walsh et al., 2005, and Paul and Meyer 2009). ISC associated with urban streams causes large differences in discharge between baseflow and stormflow. Impervious surfaces promote runoff and reduce infiltration. Urban runoff has been shown to increase stream discharge during storms by 2 to 5 orders of magnitude greater than forested catchments (Booth and Jackson 1997). Increased storm discharge has implications for the concentrations of TN,

TP, and TSS. Greater overland flow promotes high discharge events that can further erode stream banks and transport nutrient laden sediment downstream (Booth and Jackson 1997, Duan et al., 2012). Large storms contribute 85% of sediment and nutrient loads (N and P) into waterways (Shields et al., 2008, Filoso et al., 2015, and Williams et al., 2017). The positive benefits of LSR-FR may be off-set by watershed urbanization. As little as 1% imperviousness in a region can cause harm to waterways through altered hydrology, habitat structure, biodiversity, and water quality (Schueler 1994, Moore et al., 2017). This study hopes to not only model the efficacy of these restoration projects as a function of restoration type, but to determine the limits of success in relation to increased impervious surface coverage.

While stream restoration is increasingly utilized, it is not immediately apparent that these projects achieve their goal. Project monitoring efforts are often not completed, incomplete, or vary widely between projects (Kondolf and Micheli 1995, Bash and Ryan 2002, Bernhardt et al., 2005). A study that observed data on ~3700 restoration projects across the U.S., only 10% indicated that any form of restoration monitoring was occurring, and the majority of projects have no clear goal for restoration (Bernhardt et al., 2005).

Of the streams that do undergo monitoring, most restoration studies focus on engineering techniques, geomorphological characteristics, and longevity. For instance, a study by Brown (2001) assessed over 24 different stream restoration practices in >15% ISC conditions that were broadly classified into four design functions: bank protection, grade control, flow deflection/concentration, and bank stabilization/bioengineering. The study focused on more than 450 individual structures (i.e. rootwad or weir) within these

design types and was completed using a rapid, semi-qualitative questionnaire. The findings suggest over 90% of the restoration's structures were effective in maintaining structural integrity; 78% of the structures met the design objective, while habitat enhancement was identified as a lacking quality with less than 60% of the projects reaching their habitat creation goals. Analysis of structural integrity is critical from an engineering and habitat-creation perspective but does not acknowledge the role of sediment and nutrient export that have large hydrogeochemical implications for the health of downstream waterways.

The U.S. Army Corps of Engineers largely relies on strict hydraulic engineering (Copeland et al., 2001, Kail et al., 2007). Studies find that the role of “soft” engineering tactics, which emphasize bioengineering over rigorous form, have increased functionality over the “hard” structural technique to restoration (Beechie et al., 1996, Roni et al., 2002, Lake et al., 2007). Legacy sediment and floodplain reconnection projects fall under the umbrella of “softer” (non-traditional) construction methods with a focus on designs that mitigate nutrient and sediment exports while reconnecting groundwater pathways (<https://landstudies.com/>). Legacy sediment and floodplain reconnection practices have been largely unstudied; understanding the water quality mitigation capacities of these systems, particularly during storm events, is critical information with this technique being increasingly implemented.

Studies on the regenerative stormwater conveyance approach that includes restoration of stream-wetland complexes indicate that these systems are effective in reducing TN from urban watersheds. However, TP and TSS reduction was limited. William's study compared samples from pre-restoration and post-restoration systems

during the rising and falling limbs of storm-events (>0.254 mm rainfall) (Williams et al., 2017). Filoso and Palmer assessed eight restored streams with various restoration approaches (geomorphological restoration, riparian restoration, step-pool creation, and vegetated floodplains establishment) in the coastal plain of Maryland. Sites were sampled above and below the restoration projects during both baseflow and stormflows. The results indicate that restorations may have the ability to reduce TN during baseflow and stormflow conditions though reductions varied substantially between reaches (Filoso and Palmer 2011). Another Filoso study, sampling upstream and downstream of restored stream-wetland complexes, suggested that restoration projects are ineffective at reducing TSS (Filoso 2015). The research presented in our study will attempt to support and fill in knowledge gaps between past research in relation to total dissolved nitrogen (TDN), total dissolved phosphorous (TDP), and TSS transport from baseflow and stormflow conditions. Additionally, our study will span across varying watersheds with the goal of determining where these restoration projects produce the greatest reductions in N, P, and sediments. The hope is this study will help to focus restoration techniques in the environments best suited for success.

This study attempts to find answers to the following questions:

- Are LSR-FR projects successful at mitigating nutrient and sediment export?
- Is there a relationship between percent impervious surface cover and nutrient export reduction capabilities from these projects?
- What is the magnitude of difference between sediment and nutrient exports between baseflow and stormflow conditions?
- Does restoration “age” play a role in restoration success?

2. Materials and Methods

2.1 Site Description

Six restored and three reference stream sites were selected in the Maryland Piedmont region to examine the effect of LSR-FR restoration projects on nutrient export (Fig. 1, Table 1). All restorations were completed by Ecotone Inc. Limiting the projects to one contractor reduced variation since construction practices and structures were likely to be consistent across the sites. Restoration completion dates ranged from 2014 through 2018. Three sites were completed prior to the study period (Fig. 1b) and three sites were under construction during the initial period of the grant (Fig. 1c). The three sites under construction during the first year of the grant allowed for pre-and post-construction data collection. Studying pre-restoration granted insight into the benefits of stream restoration from current, degraded, conditions. Furthermore, by selecting a range of streams differing in restoration ages, the role of longevity in legacy sediment and floodplain reconnection restorations on nutrient export could be examined. The restored sites covered a broad spectrum of characteristics: ISC, forest cover, drainage area, project length, and land use (Table 1). Two control sites, one forested and one predominantly forested, were selected to determine the effect of landscape on water quality parameters, and a regional control site downstream of the most urban restored site was examined to investigate larger-scale improvements (Fig. 1d, Table 1).

First Mine Branch (Agricultural): First Mine Branch (FMB) was restored in May and June 2017 (during the study period). FMB is mostly agricultural with the remaining being forested (Table 1, Fig. 1c). Land use adjacent to the restored reach is active agriculture on one side of the channel with disbursed outdoor recreation (shooting

facilities) and forest on the other side. Upstream of the restored site was row crop/pasture and forest. Prior to restoration, the channel at FMB was deeply incised with 0.5-2 m banks and a riparian forest buffer approximately 10–30 m in width. During restoration of 731 linear meters of channel, the banks were cut to be consistently ~0.5 m in height, toe wood was installed around meanders, log vanes were constructed instream, and several low-radius meanders were removed, shortening the stream. Toe wood is a practice that uses un-milled wood (structural component) and soil lifts (bankfull surface) to create a natural armored floodplain surface (Reynolds 2020). Log vanes are structures used to re-center the thalweg of the stream reducing bank erosion and increase meander integrity (Bhuiyan et al., 2010). New high-radius meanders were constructed, and oxbow wetlands were created in the floodplain.

Cabbage Run (Agricultural): Cabbage Run (CBR) was restored roughly three years prior to baseflow sampling. The watershed was predominantly agricultural with smaller portions of pasture and low-density development (Table 1, Fig. 1b). Based on design plans (408 linear meters), approximately 0 – 1 m high of bank and floodplain sediments were removed and several meanders were armored with live stakes and toe wood, producing a mean bankfull depth of ~0.5m. Live staking is process of integrating long hardwood cuttings into the stream bank that quickly establish root systems for bank stabilization (Zahawi and Holl 2009). The restored stretch continues to have row crops directly adjacent (few meters) to the steam in areas, and there has been evidence of bank collapse in several portions.

Beetree Run (Agricultural): Beetree Run (BTR) was restored one year prior to baseflow sampling. The immediate site is surrounded by adjacent forest and retired

agriculture (little evidence of agriculture onsite); upstream is a mix of agriculture, pasture, low-density development and forest (Table 1, Fig. 1b). Construction (1620 linear meters) consisted of bank armoring meanders with toe wood, instream log vanes, and removal of legacy sediments in select areas. Evidence of bank collapse was present at the beginning and end of the restoration site.

North Stirrup Run (Pasture): North Stirrup Run (NSR) was restored approximately two years before baseflow sampling. The restored site consists of active pasture where cows graze frequently. Upstream is a mix of forest, cultivated crops, and pasture (Table 1, Fig. 1b). Restoration (792 linear meters) included the removal of 0 – 1 m high of legacy sediments in select areas, armoring high-radius meanders with toe wood, and installing several log vanes instream. The restoration project created a narrow (<10 m) herbaceous riparian buffer.

Bear Cabin Branch (Suburban): Bear Cabin Branch: BCB was completed in April of 2018 and contains the most pre-restoration data. Prior to restoration, the land was largely grassland with scattered riparian trees and upstream medium density development. The land was historically agricultural (Table 1, Fig. 1c). The stream was deeply incised with banks as high as 2.5 m. Construction (1120 linear meters) removed bank sediments (~1.5 m high in areas), armored meanders with toe wood, installed several log vanes through the project, and created a large adjacent wetland nexus.

Plumtree Run (Urban): Plumtree Run (PTR) was restored in July and August of 2017. The landscape is highly urbanized with medium and high-density development (Table 1, Fig. 1c). The site is surrounded by major and secondary roads, including a parking lot and an adjacent school. The upstream portion of the stream flows from a

culvert, and a tributary that contains an upstream stormwater pond on the school's property; downstream flows into three culverts that empty into an incised small riparian-forested stream. Prior to construction, the surrounding riparian area was a mature forest with bank heights up to 2.5 m in depth. Construction (377 linear meters) removed banks sediments 0 – 1.5 m high, armored meanders with toe wood, and installed several instream log vanes. The surrounding riparian area became mostly native herbaceous species with an adjacent wetland in the central portion of the project.

Controls (Forested): Pond Branch (POBR) and Baisman Run (BARN) are located in Oregon Ridge Park. POBR is a small 100% forested stream that drains into BARN. BARN is mostly forested with low density development and low pasture in the area (Table 1, Fig. 1).

Regional Control (Urban): Plumtree Gage (PTRG) is located roughly 1700 m downstream of the PTR restoration project. PTRG is largely developed with medium to high-density housing/commercial businesses. The immediate surrounding area of the sample site was forested and pasture (Table 1, Fig. 1).

2.2 Base-Flow Discharge Measurements

Discharge was measured, and samples were collected upstream and downstream of each restored reach. Baseflow discharge was typically measured using the sodium chloride slug injection method. Salt dilution is preferable to current metering when dealing with smaller low-flow streams and can be expected to be within 5% precision under favorable conditions (Day 1977, Moore 2005). The downstream stations were visited first since salt dilution gauging was used. 60 ± 0.05 g of table salt was dissolved in 4 liters of on-site collected stream water. In streams with greater specific conductance

during winter months (PTR) 120 ± 0.05 g was used. The 4 liter salt solution was injected upstream of a specific conductance (SC) probe from a measured distance (19ft-95 ft). A YSI ProDSS (DSS), calibrated ≤ 24 hours prior to sampling, logged SC every second. Discharge measurement locations are selected to ensure that the salt solution is well mixed in the stream. Reaches were selected to provide lateral mixing in a short distance while containing minimal pools or backwater areas. When possible, the DSS was placed in a region where flow became constricted, forcing the salt solution to interact with the measuring probe (Moore 2005). The DSS monitored the change in SC from original stream conditions to elevated SC as a result of the NaCl injection and the return to background stream SC. A Thermo Orion A325 meter, calibrated ≤ 24 hours prior to sampling, was used upstream of the injection site to determine any changes in background SC values. When SC returned to the pre-test values, conductivity logging stopped. Discharge was determined from the change in SC as the salt slug moved through the stream system:

$$C_{\text{slug}} = k(SC_{\text{ms}} - SC_{\text{bg}}) \quad (1)$$

where C_{slug} (mg/L) is the concentration of salt in the water as a result of the slug, SC_{ms} (mS/cm) is the measured SC, SC_{bg} (mS/cm) is the background SC, and k is a proportionality constant determine by the relationship of Cl (mg/L) to SC (mS/cm) ($k = 307.8$) (Moore 2005). The area under the curve was calculated as:

$$A = \sum C_{\text{slug}} * t_{\text{int}} \quad (2)$$

where A is the area under the curve and t_{int} (s) is the time interval between measurements.

Lastly, discharge was calculated using the following equation:

$$Q = M / A \quad (3)$$

where Q is discharge (L/s), and M is the mass of Cl in 60 or 120 g of salt (mg) (<http://www.fathomscientific.com/introduction-to-sd-gauging/>). The mass of chloride was used because Cl moves through aqueous systems conservatively and does not bind to stream sediments (<http://www.es.lancs.ac.uk/people/nickc/104/case16.htm>). The area velocity approach, measured using an OTT MF Pro (an electromagnetic current meter), was also used on selected sampling dates to verify the dilution slug method.

2.3 Storm-Flow Discharge, primarily at First Mine Branch

When flow was higher, particularly during storms, discharge was measured using the area-velocity method via the OTT MF Pro. Following the MF Pro's manual, in accordance with USGS and ISO methods, a permanent cross-sectional area was identified and divided into the proper sections that were then measured for velocity (<http://www.ott.com/en-us/products/water-flow-3/ott-mf-pro-water-flow-meter-968/>). Upstream and downstream reaches were measured and sampled throughout the course of the storm.

2.4 Baseflow Sample Collection Methods

Baseflow grab samples for TSS were collected using 1000 mL high density polyethylene bottles (HDPE). All grab samples were collected while wearing nitrile gloves to avoid contamination. TSS was collected first in an effort to minimize disturbance to the stream. Prior to collection, TSS sample bottles were triple-rinsed on-site with unfiltered stream water. Following the Environmental Protection Agency's (EPA) criteria for stream sampling, TSS samples were collected facing upstream and containing no headspace to minimize effects of storage on the sample (Dohner 1997).

Baseflow samples for water chemistry were in-field filtered (0.45 μm). DOC and

TDN samples were collected in a pre-ashed (500 °C for >4 hours) glass amber vial with no headspace. Alkalinity was collected in a 60 mL low-density polyethylene (LDPE) bottle containing no headspace; cation-anion samples were collected in a 15 mL LDPE bottle with headspace preferred. Alkalinity and cation-anion bottles were triple-rinsed with on-site filtered stream water prior to collection. All samples were placed on ice during transport. Samples were stored at 4°C in the laboratory prior to analysis.

2.5 Stormflow Sample Collection Methods, primarily at First Mine Branch

Storm flow sampling at First Mine Branch (FMB) occurred before, during, and after precipitation events. The goal was to capture samples that were representative of the storm hydrograph. Water samples during storm events were collected both manually and automatically. Manual collection of the entire storm hydrograph was difficult to achieve. Discharge measurements and manual grab samples were exclusively used for rating curve data and C-Q relationships. Manual stormflow TSS samples were collected using the same method as baseflow samples. Samples for DOC, TDN, alkalinity, and cations-anions were gathered using an on-site triple-rinsed 250ml wide mouth HDPE bottle. Samples were in-lab filtered (0.45 μm) within 24 hours and placed into their respective storage vials/bottles. All samples were stored on ice in the field and at 4 °C in the lab until analysis could occur.

ISCO 6712 and ISCO 2700 full-size portable samplers were deployed with the same sampling timing and frequency programed at upstream and downstream locations prior to storm events and collected as soon as possible after storm completion. The ISCOs collected samples on a time basis with a sampling frequency that attempted to predict the entire length of the storm. ISCOs were loaded with ice during the sampling

process, and samples were placed on ice upon retrieval. TSS samples were subsampled from the ISCO bottles after rigorous agitation and stored at 4°C. DOC/TN, alkalinity, and cation-anion samples were subsampled from ISCO bottles and filtered (0.45 μm) in the lab within 24 hours into the proper amber vials or LDPE bottles, and stored at 4°C in the lab until analysis.

A rating curve for FMB was developed. Staff plates were installed at the upstream and downstream ends of the restoration in locations where geomorphological features were relatively stable in an effort to minimize changes in the cross-sectional area of the stream. Staff plates and pressure probes were regularly monitored. Accumulated sediment at the bottom of the staff plates was removed to minimize changes in stage height during the production of the rating curves and collection of pressure data. During baseflow and stormflow events, stage (m) and discharge (m^3/s) was measured with an OTT MF Pro using the methods described in section 2.3. Due to variability in stage height during stormflow events, three stage measurements were taken during the discharge measurement: 1) before 2) during - middle 3) after, then averaged for stage height. Changes in stream height that exceeded an increase of 0.03 m or 0.1 ft during the discharge measuring process were not used in the creation of the rating curve.

A rating curve (Fig. 2) was established for both upstream and downstream (n: 13 upstream – 15 downstream). Rating curves followed a logarithmic pattern with an R^2 of 0.8001 FMBU and 0.8958 FMBD (Fig. 2). Standard error (SE) associated with the two rating curves is as follows: FMBU 0.016, FMBD 0.007. When comparing actual to theoretical discharge measurements, the SE was 0.099 upstream and 0.052 downstream (Fig. 3). Stage height was determined from continuous U20 water level sensors deployed

from 04/23/2019 – 03/11/2020 taking a measurement every 5 minutes. Discharge was determined using the logarithmic function from the rating curves for both upstream and downstream reaches (Fig. 4). Data gaps were present due to issues with pressure loggers.

2.6 Laboratory Analysis Methods

TSS was determined by filtering a known volume of sample through a pre-weighed and prepared glass fiber disc, in compliance with standard methods for wastewater method 2540 (Standard Methods 2005). TSS glass fiber discs were prepared by ashing at 500°C for >4 hours and pre-washing prior to filtration with E-pure: 18.2 MΩ-cm. Discs were dried at 104°C and weighted in a labeled aluminum pan. A known volume of sample was filtered through the glass fiber discs. After filtration, glass fiber discs were dried at 104°C and reweighed to determine mg/L TSS. TSS analysis was monitored for accuracy by including a known check standard every 10-20 samples. If check standard concentrations contain >10% error from the known concentration, then samples were remeasured or excluded.

Alkalinity or dissolved inorganic carbon (DIC) was determined using the Gran titration method (Radtke 1998). Titration to a pH 3.0 endpoint was completed with a Mettler-Toledo G20 autotitrator with Rondolino autosampler. Accuracy was monitored by including a gravimetrically prepared 25:1 Na₂CO₃ check standard measured along with the samples. Uncertainty was typically <3–5%. Dissolved organic carbon (DOC or NPOC) and TDN was determined using a Shimadzu TOC-Vcsh NC analyzer. Carbon and N check standards were measured regularly during sample runs to determine accuracy; if check standard concentrations deviated greater than 10%, then samples were remeasured. Cation and anion concentrations (Ca²⁺, Mg²⁺, Na⁺, K⁺, NH₄⁺, Cl⁻, NO₃⁻, PO₄³⁻, SO₄²⁻)

were measured with an ion chromatograph (Dionex ICS-5000) with 5 ppm and 100 ppm check standards being measured regularly for accuracy. If average check standard concentrations were >10% different than expected, samples were remeasured. Charge balance error (CBE) was also completed for major cations and anions; samples with CBE >15% were reanalyzed. Ammonia, nitrate+nitrite, TDP, and orthophosphate, were analyzed by the SEAL AQ1 Discrete Analyzer (AQ1). Ammonium, nitrate+nitrite, and ortho-phosphorous (and total dissolved phosphorus TDP) were analyzed using methods 350.1, 353.2, and 365.1 of the EPA's protocols. Silica was also measured with the AQ1 following Std. Methods 4500-SiO₂(20th).

2.7 Baseflow and Storm Sampling

Baseflow sampling occurred twice per month prior to construction and for three months following construction in an attempt to capture sufficient data pre-and post-construction (Table 2). Subsequently, the sampling frequency was once a month for all sites, except during the growing season (June – August) in 2018 and 2019 where sampling was twice per month. Sites that were restored prior to the grant (CBR, BTR, NSR) were sampled once a month except during the 2018 and 2019 growing seasons when these sites were sampled twice per month (Table 2).

Storm sampling occurred at FMB due to private land ownership and elevated nutrient and TSS concentrations as a result of agriculture. A total of 157 individual samples (manually and automatically) were collected during stormflows post-restoration from FMB (84 upstream – 73 downstream) from 08/17/2017 – 02/07/2020. Pre-restoration data was not used in analysis due to a lack of rating curve data. Manual discharge was measured using an MF pro or determined using a rating curve (n: 13

upstream – 15 downstream) previously established (refer to section 2.5). Three storms were sampled from baseflow conditions to stormflow then a return to baseflow conditions: 07/11/2019, 01/12/2020, and 02/05/2020. Storms were measured for TDN, NO_3^- , NH_4^+ , NPOC, TDP, PO_4^- , TSS, and major cations and anions. NO_3^- , NH_4^+ , TDP, and PO_4^- were analyzed from frozen samples to minimize speciation and volatilization. Discharge was determined from the rating curves; The three storms were within the lower and upper stage range of the rating curve minimizing error associated with stormflow discharge.

2.8 Calculations and Statistical Analysis

2.8.1 Baseflow and Stormflow Daily Load Calculations

N, DOC and, sediment daily loads (g/km^2) during baseflow conditions (L_b) were calculated by:

$$L_b = ((C_b * Q_b * T_b) / A_w) * 1 \text{ day} \quad (4)$$

where C_b is the concentration of the given parameter at the sampling time (mg/L), Q_b is instantaneous discharge (L/s), T_b is 86,400 seconds/day, and km^2 is the watershed area. Both C_b and Q_b were assumed to be constant for the whole day. Daily fluxes were normalized to watershed area (A_w) to allow for cross site analysis. Fluxes were converted to loads by multiplying by 1 day.

Daily loads (g or kg / km^2) during storm flow conditions (L_s) from ISCO storm samplers were calculated by:

$$\text{Daily } L_s = (\Sigma((C_s * Q_s * T_s)_1 + (C_s * Q_s * T_s)_2 + \dots (C_s * Q_s * T_s)_n) / A_w) / D_s \quad (5)$$

where C_s is the instantaneous concentration of a parameter; Q_s is the instantaneous discharge measured from the rating curve; T_s is the time step between discharge

measurements (300 s); the denominator is the watershed area (km²); and D_s is the number of days the storm lasted. Loads were calculated using the sample concentration spread evenly before and after the collection time in 5-minute intervals, multiplied by the discharge at that interval. Loads were normalized to watershed area (A_w) to account for the differences in watershed area between the upstream and downstream ends of the restored reaches. Loads were normalized to 24 hours (D_s) to remove effects of storm length when analyzing different storms.

The %load decreased or increased across the restored stream reach was calculated by:

$$\% \text{ Difference in LOAD} = ((\text{OUTPUT} - \text{INPUT}) / \text{INPUT}) * 100 \quad (6)$$

where a negative number for %LOAD suggests a retention, and a positive number suggests an increase in load between upstream and downstream sites.

Discrete water quality and high-frequency Plumtree Run gage (PTRG: #01581752) data were downloaded from the USGS National Water Information Survey (NWIS) using the *dataRetrieval* (De Cicco et al., 2018) library in R from October 2013 through December 2019. Discrete data included nitrate, TDP, and TSS concentrations. High-frequency data consisted of discharge and turbidity measured every five minutes; daily mean discharge and turbidity were also downloaded. Precipitation data (15-minute interval) was recorded at Atkisson Reservoir (#01581753) ~1700m away from PTRG.

Missing data in the high-frequency data were filled by linear interpolation for gaps lasting ≤ 1 hour, and daily mean values were used for missing data > 1 hour. 104 days lacked daily mean turbidity values from 2013-2020. Daily mean turbidity was

estimated using a regression model with daily mean discharge as the predictor ($R^2 = 0.72$).

Nitrate, TDP, and TSS were converted to 5-minute high-frequency concentration data using highly correlated concentration discharge (C-Q) and concentration-concentration (C-C) relationships determined from discrete samples. Concentration data for NO_3^- , TDP, and TSS were summed to produce daily and annual loads using the *dplyr* package (Hadley et al., 2019) in R. Daily and annual loads were used to investigate restoration success at the regional control site: PTRG.

2.8.2 Statistical and Storm Analysis

All statistical analysis was completed in R using interface (RStudio 2019). The two-sided unpaired Wilcoxon rank-sum test (Wilcoxon test) was used to use to statistically analyze baseflow samples across sites, years, and pre- and post- analysis, for all parameters. Unpaired Wilcoxon tests are used when data sets are independent from one another (Derrick et al., 2019). A two-sided paired Wilcoxon test was used for intra-site comparisons (upstream and downstream) as the data was collected from the same stream, on the same day, and within a small temporal window for upstream-downstream samples. Paired Wilcoxon tests are used when the data are dependent on one another (Brien and Fleming 2019). The Wilcoxon test was used to analyze baseflow concentrations and daily loads because (1) the majority of sample populations did not pass the Shapiro-Wilks Normality Test (Shapiro-Wilks). Normality Test tests whether data follows a normal distribution, the Shapiro-Wilks is the most the most powerful and preferred method of testing for normality (Mendes and Pala 2003). A Wilcoxon test is valid for any distribution (parametric and non-parametric) and is less sensitive to outliers

(Wild 1988). (2) The Wilcoxon test provides statistical power when sample populations are small (LaMorte 2017): the majority of pre and post data was $n < 30$. (3) The Wilcoxon test is used to test the shape of two populations, which is considered to be synonymous with comparing population medians (Wild 1988 and Shier 2004). Median values were compared rather than means.

FMB stormflow conditions were characterized by producing C-Q and C-C relationships to understand the trends observed in nutrients and suspended sediments. Temporal relationships of peak concentrations to peak discharges were also investigated to determine the nature of nutrient and sediment dynamics as storm events occur. Stormflow nutrient and sediment loads were compared by using percent difference from upstream and downstream daily loads ((k)g/km²). Due to a low storm population ($n = 3$ up-down paired storms), statistical testing lacked power. Analysis of percent difference can offer insight into the observations and the general success of restoration projects during storm events. PTRG was assessed by interpreting the hydrological response to three pre- and three post-restoration precipitation events and drawing connections to peak discharge, precipitation amount, and precipitation duration. Annual loads for six years (2014-2019) were also observed to determine if loads decreased regionally post-restoration.

3. Goal

The goal of this thesis was to determine the functionality of LSR-FR projects as a novel and useful approach to sediment and nutrient reduction. This research aimed to determine the limitations of restoration success by observing ISC and restoration age as potential factors that could influence sediment and nutrient export. In doing so the aim was to produce knowledge that can assist the restoration community in developing and constructing more targeted restorations with an increased possibility for success.

4. Results and Discussion

4.1 Baseflow Discharge Results and Discussion

Baseflow discharge across all sites was lowest in 2017 (Table 3). Discharge increased substantially in 2018 during the highest precipitation year on record (Sweet et al., 2019). Most sites, with exception of the (sub)urban sites, experienced an increase from 2018 to 2019 in baseflow discharge as well (Fig. 5a). The annual precipitation records from NOAA indicate annual rainfall was 38.28 inches, 71.82 inches, and 38.16 inches for 2017, 2018, and 2019, respectively.

After normalizing discharge measurements to watershed area ($\text{m}^3/\text{s}/\text{km}^2$), the study sites fit three distinct categories: (1) three agricultural sites (FMB, CBR, BTR) + the pasture site (NSR), (2) the suburban site (BCB), and (3) the urban site (PTR) (Fig. 5b). Agricultural and pasture sites with low ISC ($<8\%$) exhibited an increase in median baseflow discharge each year (Fig. 5b). By contrast, the two sites with higher ISC had a decrease in median baseflow discharge from 2018 to 2019. The regional PTRG control followed a similar pattern in discharge across years to the restored PTRD site. Forested regional controls (POBR and BARN) had a slight increase in baseflow discharge from 2018 to 2019, similar to the agricultural grouping (Table 3). Broadly, upstream baseflow discharge measurements closely mirrored downstream locations with downstream locations having a slight increase in discharge in all sites except BCB and PTR (Table 3). Pre-restoration baseflow discharge was lower than post-restoration baseflow with the difference being statistically significant ($p<0.05$) in a few cases (Table 3). However, since the record high precipitation in 2018 is the main driver of this difference, pre- and post-restoration discharge patterns will not be discussed.

Understanding temporal discharge changes through a study are integral as precipitation trends can alter rates of biogeochemical cycling and stream export of nutrients (Thompson et al 2011, Koenig et al., 2017, Ide et al 2019). Baseflow increases from 2017 to 2018 and 2019 (in the agricultural + pasture environments) are the result of inputs to groundwater from precipitation (Fig. 5a, b). Higher 2019 baseflow discharge in agricultural and pastoral landscapes may be expected due to groundwater travel times in low ISC watersheds (Hamilton et al., 2012). In the (sub)urban setting, the decrease in median baseflow from 2018 to 2019 is likely due to lower infiltration into groundwater as a result of ISC (Konrad 2002). Restoration did not appear to have a marked effect on upstream versus downstream discharge, although further research would be needed to determine the effect of restoration.

4.2 Baseflow General Stream Characteristics

4.2.1 Baseflow pH Results and Discussion

pH values were circumneutral across the sites and followed no consistent trend along the landscape gradient (Fig. 6a). The regional POBR located in Oregon Ridge Park composed of 0% ISC and 100% forest has maintained a median pH of ~6.9 since the mid 1960s (Moore et al., 2017). FMB, BTR, BCB, PTR exhibit statistically higher ($p < 0.05$) median pH values than the POBR control. NSR and CBR were similar in median pH to the regional control POBR (Fig. 6a, Table 4). Intra-site comparison indicates that all sites, excluding BTR, contain a significant change in pH between upstream and downstream conditions ($p < 0.05$): FMB, CBR, and PTR are more acidic downstream, while NSR and BCB are more alkaline downstream (Table 4).

All median pH values fall within the State of Maryland's instantaneous numeric threshold (Steele et al., 2004) range of 6.5 – 8.5 (Fig. 6a). Given that all sites were underlain with similar, non-carbonate bedrock, pH differences were likely the result of land modification, although drivers are uncertain. Agricultural sites with higher pH (FMB and BTR) are probably the result of current and past liming practices (Oh et al., 2006, Hamilton et al., 2007). Sites considered (sub)urban consistently had higher pH values than the remaining sites, largely the result of concrete infrastructures (Weigman et al., 1993, Conway 2007, Moore et al., 2017). pH increases along the agricultural to urban gradient are unclear; however, it is hypothesized that anthropogenic inputs or vegetation changes are largely the result (Conway 2007).

4.2.2 Specific Conductance Results and Discussion

Specific conductance appears to follow ISC: 100% forested control (POBR) was substantially lower in SC than the remaining sites and minor increases (<1% - 10%) in ISC caused elevated SC. Abundant ISC (>10%) produced the greatest SC. Study sites significantly differ from one another ($p < 0.05$) but fall within a similar range of 200 - 300 $\mu\text{S}/\text{cm}^3$. PTR (48.6 – 97.1% ISC) exhibits significantly ($p < 0.05$) elevated SC when compared to the other restoration reaches (Fig. 6b). Intra-reach comparison yields little significance between upstream and downstream comparison, except in FMB and BTR where a decrease in SC occurred ($p < 0.05$) (Table 4).

Stream SC largely mirrors Na and Cl concentrations, suggesting differences in specific conductance are tied to salt applications (Fig. 7). A connection between specific conductance differences and road salt applications has been well documented along the northern to mid-Atlantic coast (Cooper 2014, Long et al., 2015, Baker et al., 2019, Moore

et. al., 2020). The forested control POBR experienced SC that were typical of undisturbed forest (Helvey et al., 1976, Moore et al., 2017, Baker et al., 2019). Even mild anthropogenic changes have resulted in elevated SC (Moore et al., 2017). Elevated SC levels in agricultural settings (FMB, CBR, and BTR) are largely the result of fertilizer application and, to a lesser extent, deicing salts (Helvey et al., 1976, Dow et al., 2000, Calvi 2014, Baker et al., 2019); while, deicing salts are the main driver of SC in (sub)urban sites (Cooper et al., 2014, Long et al., 2015, Moore et al., 2017).

4.2.3 DO Results and Discussion

Baseflow Dissolved oxygen (%DO) in the restoration reaches is significantly higher than the 100% forested POBR regional control (94%) ($p < 0.05$) (Fig. 6c). BARN, possessed a median %DO equal to or less than most study sites. The median DO% of the restoration reaches spanned from 94.95 – 110.75%. Intra-reach differences in DO were not significant upstream and downstream of restoration (Table 4). %DO can have implications for stream health and N retention and removal.,

Relatively high DO at all sites likely indicates that conditions are not ideal for substantial denitrification, although some denitrification can occur in streams with measurable DO (Kaushal et al., 2008 and Lu et al., 2008). Additionally, the removal of riparian tree-cover during restoration results in more light inputs to the restored reaches, and in-stream photosynthetic activity is likely increased, contributing to higher %DO. The lowest DO values are observed at the urban site (PTR), which is the smallest stream and has the lowest discharge, possibly leading to in-stream denitrification zones, which will be discussed in sections 4.4.1 and 4.6.1.

4.2.4 Temperature Results and Discussion

Baseflow water temperatures are not significantly different than the 100% forested control site, POBR (Fig. 6d). BCB is the exception with a significantly ($p < 0.05$) higher temperature from the regional controls and the other restoration reaches. Upstream and downstream intra-site variations are not significant (Table 4). Though temperature may influence nutrient export and microbial uptake (Manning et al., 2017 and Schaefer et al., 2007), the lack of significant differences at baseflow suggests that temperature does not play a substantial role in biogeochemical processes across sites and between upstream and downstream reaches.

4.3 Baseflow Major Cation and Anion Results and Discussion

Major cation results indicate (sub)urbanized landscapes, specifically urban, contained higher dissolved cations compared to agricultural and mixed land use landscapes. Median and total cation concentrations differ substantially along the agricultural to urban gradient (Fig. 8). All restored sites contained concentrations significantly ($p < 0.05$) higher than POBR. The sites cluster into two main groups: non-urban and urban (PTR). Ca^{2+} concentrations were highest in all sites followed by Na^+ , Mg^{2+} , and K^+ , respectively, with the exception of NSR that possessed higher median $[\text{Na}^+]$ to $[\text{Ca}^{2+}]$ (Fig. 9, Table 5). Generally, median sodium increased as ISC increased (Fig. 8a). Non-urban sites had similar median $[\text{Ca}^{2+}]$ and $[\text{Mg}^{2+}]$ with much higher $[\text{Ca}^{2+}]$ and $[\text{Mg}^{2+}]$ at the urban site (Fig. 8bc). Potassium was highest at the most agricultural (FMB) site; $[\text{K}^+]$ at the remaining sites shows reasonably similar concentrations (Table 5). Upstream and downstream of the restoration sampling locations largely decreased in [cation] but remained similar (Table 5).

Similar to cations, the urban site contained the highest concentrations of major anions compared to other landscapes. Median anion concentrations shifted in relative anion species and total anion concentration along the agricultural to urban transition (Fig. 8, Table 6). All sites contained [anion] significantly ($p < 0.05$) higher than POBR (Table 6). Agricultural sites (>50%) contained highest concentrations of $[\text{HCO}_3^-]$, followed by $[\text{Cl}^-]$, $[\text{SO}_4^{2-}]$, and lastly, $[\text{NO}_3^-] - \text{N}$. As sites become more mixed usage and (sub)urban (<50% Ag), relative Cl^- concentrations increased (Fig. 9). In the most urban site $[\text{Cl}^-]$ and $[\text{HCO}_3^-]$ were $\sim 4+$ and $\sim 2+$ times higher than the remaining sites, respectively. $[\text{Cl}^-]$ exhibited a steady increase in concentration as agricultural practices decreased and urbanization increased. All sites exhibited significant concentration differences ($p < 0.05$), with the exception of CBRD and NSRD (Fig. 8c). $[\text{HCO}_3^-]$ was more variable along the agricultural/urban gradient: the most urban and most agricultural site contained higher concentrations. Similarly, $[\text{SO}_4^{2-}]$ was highest in agricultural and urban sites (Fig. 8f). $[\text{NO}_3^-]$ diminished in concentration as site became less agricultural (Table 6). Upstream and downstream [anion] were significantly different ($p < 0.05$) but did not vary substantially (Table 6).

Since underlying geology was relatively similar among sites, stream chemistry was primarily influenced by the surrounding agricultural or urban environments altering baseflow chemistry between the restored sites. All restored sites had high concentrations of cations and anions relative to the forested controls (Table 5, 6). Given the lack of carbonate bedrock, high $[\text{Ca}^{2+}]$, $[\text{HCO}_3^-]$ and $[\text{SO}_4^{2-}]$ in agricultural sites are consistent with liming of soils (Oh 2006). In (sub)urban sites, parallels between elevated $[\text{Ca}^{2+}]$, $[\text{HCO}_3^-]$, and $[\text{SO}_4^{2-}]$ suggest concrete weathering is driving the concentration increases

(Shanley et al., 1994, Mason et al., 1999, Moore et al., 2013, Moore et al., 2017).

Weathering of silicate rocks may also contribute to elevated concentrations of HCO_3^- where concrete sources are not present. Elevated $[\text{Na}^+]$, $[\text{Mg}^{2+}]$, and $[\text{Cl}^-]$ as ISC increases is likely the result of long-term stream-chemistry effects from road deicing salts during winter months (Casey et al., 2013, Moore et al., 2017). Accounting for geological consistencies, variations in stream inorganic chemistry has been shown to be linked to anthropogenic land uses largely affecting ion and nutrient baseflow chemistry (Dow 2016, Moore et al., 2017).

4.4 Baseflow Nitrogen Concentration/Daily Load Results and Discussion

TDN concentrations (mg/L) are highest in the agricultural landscapes and decrease as sites become more (sub)urban (Fig. 10, Table 7). [TDN] was equivalent to $[\text{NO}_3^-]$ during baseflow conditions (Fig. 11a, b); [TDN] data was used rather than nitrate data because the data set was more complete. Restored sites are significantly ($p < 0.05$) greater in [TDN] than forested controls, except PTR, which is similar to BARN (Fig. 10a). Restored sites fit two categories: agricultural ($>50\%$) and non-agricultural ($<50\%$). Agricultural sites FMB, CBR, and BTR contained significantly ($p < 0.05$) elevated median TDN concentrations relative to the non-agricultural sites: NSR, BCB, and PTR (Fig. 10a). FMB and BTR were similar in median concentration, while CBR showed lower [TDN] relative to the other agricultural sites (Fig. 10a). Sites considered pasture, suburban, and urban possessed significantly ($p < 0.05$) lower median [TDN]s than all agricultural sites ($p < 0.05$). NSR and BCB were not significantly different from one another in [TDN]. NSR and BCB were significantly ($p < 0.05$) higher in concentration than the most urban site, PTR (Fig. 10a). PTRG median concentration (2.52 mg/L)

suggests significant ($p < 0.05$) inputs of TDN between the restoration reach and the downstream regional control (Fig. 10a).

Baseflow TDN concentrations decreased from upstream to downstream locations at FMB, BTR, BCB, and PTR ($p < 0.05$); CBR and NSR increased [TDN] from upstream to downstream (Table 7, 8). Pre and post construction analysis of downstream locations yielded a significant ($p < 0.05$) increase at BCBD and no significant differences in [TDN] at FMBD and PTRD. Pre-construction n was relatively small at FMBD and PTRD (Fig. 12, Table 10).

Baseflow N daily loads (g/km^2) mirror the trend observed in TDN concentrations (Fig. 10b). Agricultural sites exhibited significantly ($p < 0.05$) higher TDN daily loads than non-agricultural/(sub)urban sites. FMB, CBR, and BTR were similar in TDN daily load (Fig. 10b, Table 7). NSR and BCB had similar daily loads despite large agricultural and watershed differences. PTR had significantly ($p < 0.05$) lower TDN daily loads than the other non-agricultural sites (Fig. 10b). The agricultural and pasture sites did not reveal a baseflow daily load reduction in TDN between upstream and downstream of the restoration site. However, the (sub)urban sites, BCB and PTR, demonstrated a significant ($p < 0.05$) reduction in TDN daily load from upstream to downstream of the restoration projects (Figs. 10b, 13, Table 7, 9). Pre- and post-restoration analysis indicates that all downstream sites experienced an increase in TDN daily load; however, BCBD was the only site that was significantly higher ($p < 0.05$). Pre-construction n were low in FMBD and PTRD (Fig. 12ad, Table 10). Lastly, data did not suggest that older restoration projects had any additional retention capabilities than those recently installed. Patterns associated with [TDN] and TDN daily load were consistent between recently restored and

projects restored 4-6 years ago (Figs. 10, 13, Table 7). Hydrogeochemical processes may take decades to respond to physical stream changes (Meals et al., 2010, Hamilton 2012). Long groundwater residence times are particularly important with respect to N dynamics as isotopic tracers often suggest baseflow stream water is over a decade old. Decades may be required to flush soluble nitrate from groundwater reservoirs (Hamilton 2012).

The agricultural sites regularly exhibit higher concentrations of NO_3^- (Coulter et al., 2004). Conversely, urban and suburban sites routinely exhibit lower $[\text{NO}_3^-]$ (Kaushal et al., 2008, Filoso and Palmer 2011). Nitrate contributions are largely the result of agricultural practices (fertilizer); to a lesser degree, urban activities and atmospheric deposition play a role in N surface water transport (Carpenter et al., 1998). As shown, the results indicate decreasing nitrate concentrations and daily loads along the agricultural to urban land-use gradient. Variation in N sources, quantity, and groundwater pathways in the urban setting may account for lower concentrations and loads of NO_3^- along this gradient (Hope et al., 2005, Aitkenhead-Peterson et al., 2009, Mouri et al., 2012).

N reduction was variable across the six sampled sites (Table 7). FMB and BTR showed a significant ($p < 0.05$) decrease in [TDN] (Table 7, 8). Studies have shown streams with ample [DOC] and $[\text{NO}_3^-]$ can provide conditions for denitrification (Kaushal et al 2008, Newcomber-Johnson et al., 2014). However, FMB and BTR contain higher $[\text{NO}_3^-]$ than the studies mentioned, and low $\text{NO}_3^-:\text{DOC}$ ratios suggest denitrification was not a major driver in the reduction (Smith et al., 2017). Higher downstream discharges (Table 3, 8) most likely caused a N dilution effect from up to downstream in FMB and BTR, accounting for the decrease (Rose et al., 2017, Williams et al., 2017). However, discharge increases are not a suitable explanation for all [TDN] decreases: BCB and PTR

demonstrated N decreases but did not show increases in discharge between upstream and downstream locations (Table 3, 7, 8). N reductions observed at the (sub)urban sites may be the result of increased N uptake and denitrification rates due to conducive nitrate to labile carbon ratios (Kaushal et al., 2008, Smith et al., 2017, Williams et al., 2017). Denitrification conditions were potentially present at PTR due to water residence times associated with low discharge, high [DOC] (Table 7), and the most variable %DO (Fig. 6c) (Craig et al., 2008, Knapp et al., 2009, Filoso and Palmer 2011), potentially explaining the significant ($p < 0.05$) decrease in TDN concentration and daily load. Significant ($p < 0.05$) reductions in TDN daily loads (Table 7, 9) at the two most (sub)urban sites were potentially the result of decreased post-restoration discharge along the restored reach (Table 3), which would decrease daily loads. Although N reductions from restoration are not entirely clear, the results suggest focusing restoration projects in urban landscapes with low [TDN] and high [DOC] may contribute to baseflow N reduction (Mayer et al., 2003, Newcomer 2014). In contrast, pre-restoration data from upstream to downstream also indicate a significant ($p < 0.05$) decrease at FMB, BCB, and PTR (Table 10, 11) indicating baseflow N dynamics have not changed substantially after restoration.

4.5 Baseflow Dissolved Organic Carbon Concentration Results

Broadly, non-purgeable dissolved organic carbon (DOC) does not dramatically change along the agricultural gradient (Fig. 14). Non-urban sites (FMB, CBR, BTR, NSR, and BCB) fall between the [DOC]s of the regional controls: POBR and BARN. Non-urban sites [DOC] are significantly ($p < 0.05$) related in median concentrations, and fall within a narrow range, 0.92 – 1.83 mg/L (Fig 14, Table 7). The urban site, PTRU/D,

contains a significant ($p < 0.05$) increase in DOC compared to the non-urban sites, 2.09/2.66 mg/L (Fig. 14). PTRG is not significantly different from the PTR site in [DOC] (Fig 14). Upstream and downstream [DOC]s in the non-urban sites do not substantially vary from one another (Table 7, 8). PTR exhibits a significant ($p < 0.05$) increase in [DOC] between upstream and downstream locations (Table 7, 8). Analysis of pre and post restoration suggests [DOC] increased across the three studies restored during the granting period (Fig. 12b, e, Table 10, 11). The increases in [DOC] were not significant ($p > 0.05$). FMBD and PTRD contained low pre-construction n values making statistical strength limited.

4.6 Baseflow TDN and DOC Relationship Results and Discussion

TDN and DOC concentration (mmol/L) relationships from the six downstream locations and three control-sites follow an agricultural, pasture/suburban, and urban pattern (Fig. 15a). BARN closely mimics the [DOC]-[TDN] pattern observed in suburban sites; while, POBR has higher [DOC] and lower [TDN], more closely relating to the urban site (Fig. 15a). Agricultural sites show high median [TDN] concentrations and low [DOC]; suburban sites (NSR and BCB) exhibit lower [TDN] concentrations and similar [DOC] to the agricultural sites; lastly, the urban site (PTR) contains the lowest [TDN] and the highest [DOC]. PTRG follows a general trend similar to the pasture/suburban landscapes. Upstream and downstream relationships are similar (Table 7).

The molar ratio (mmol:mmol) of DOC to TDN (DOC:TDN) remain similar across the agricultural to suburban gradient, with a slight increase in the pasture-suburban environment, and a sharp increase in the urban setting (Fig. 15b). POBR possessed a median ratio of 11.47 DOCmmol:TDNmmol due to low [TDN], and BARN presents a

molar ratio similar to the suburban landscape. DOC:TDN relationships have implications for the retention/removal and export of N in the system (Lu et al., 2009, Mayer et al., 2010, Taylor and Townsend 2010, Asmala et al., 2013, Grebliunas and Perry 2017, Smith 2017, and Ward 2017). Agricultural and pasture/suburban landscapes largely have DOC:TDN values <1 ; while, the urban site contains DOC:TDN relationships >1 (Fig. 15b, Table 7). PTRG possessed a median ratio significantly ($p<0.05$) lower than PTR, due to [TDN] increases (Table 7). Upstream and downstream analysis show significant increases ($p<0.05$) intra-site in FMB and BCB (Table 7, 8); however, increases in DOC:TDN ratios are small. PTR median DOC:TDN ratio increased significantly ($p<0.05$) from upstream to downstream by nearly a factor of 2 (Table 7, 8). Pre-and-post restoration analysis showed a non-significant decrease ($p>0.05$) in DOC:TDN ratios at BCB $<1:1$, while a non-significant increase ($p>0.05$) was present in FMB and PTR (Table 10). FMBD and PTRD have a low pre-construction sampling size, making statistical power low (Table 10). Significant ($p<0.05$) increases in DOC:TDN ratios seen at the three sites restored during the study period, but not at the three sites restored previously, could potentially suggest restoration has altered hydrogeochemical properties in the short term, whereas older restorations have stabilized. Increases in DOC as a result of restoration may be due to unearthing historic wetland sediments and reestablishing shallow groundwater pathways (Petrone 2010). Increased labile [DOC] as a result of restoration may promote increased N removal, although the dynamics are not well understood (Zarnetske et. al. 2011, Barnes et. al 2012).

Ratios of DOC:TDN (NO_3^-) indicate whether TDN will be nitrified and exported as NO_3^- or metabolized/denitrified in the stream setting (Grebliunas and Perry 2017, and

Smith 2017). Inorganic N transformations are linked to the availability of organic carbon stocks (Barnes et al., 2012); specifically, denitrification rates in streams are connected to labile DOC inputs (Inwood et al., 2005). Ratios of 1:1 are shown to produce the greatest denitrification rates (Taylor and Townsend 2010, Asmala et al., 2013, and Smith et al., 2017).

Agricultural, pasture, and suburban streams exhibited DOC:TDN molar ratios less than 1:1 (Fig. 15b), which indicate N transport from the system was likely to occur. In FMB, CBR, BTR, NSR, and BCB (DOC:TDN <1:1) denitrification was carbon limited and labile DOC concentrations were too low to produce sufficient energy to denitrifying bacteria. Ratios 1:1 or greater, as shown in PTR (Fig 15b), suggest catabolism/denitrification of TDN (NO_3^-) may have occurred in the stream and nearby sediments retaining or removing N from the waterway (Lu et al., 2009, Mayer et al., 2010, Taylor and Townsend 2010, Asmala et al., 2013, Grebliunas and Perry 2017, Smith et al., 2017, and Ward et al., 2017). In ratios >>1:1 nitrate is limited, and denitrification rates decrease, although microbial heterotrophic uptake continues to take place (Smith 2017), which may be the case in PTR. Though median DO is >100% at PTR with sizeable variation (Fig. 6c), denitrification has been shown to occur even in conditions where DO concentrations are measurable (Lu et al., 2009), and experimentally to occur quite rapidly with short water residence time (Grebliunas and Perry 2016). The decrease observed in [TDN] from PTRU to PTRD may be indicative of denitrification or microbial uptake. Pre-restoration data from upstream to downstream also indicate a significant ($p<0.05$) decrease at PTR (Table 10, 11) indicating denitrification may have been occurring prior to restoration as well.

One of the goals of LSR-FR restoration is to reestablish shallow riparian groundwater pathways through relic wetlands, which has shown to increase labile DOC capable of reducing N (Petrone 2010). However, [DOC] increases are not apparent in the upstream/downstream analysis of the agricultural – suburban watersheds (Table 7). The most urban site, PTR, was consistent with the urban stream syndrome - high DOC inputs through urban pollution and shallower groundwater pathways (Walsh 2005). [DOC] is higher in the urban setting suggesting restoration may have a positive effect on [DOC] (through the lens of N removal) when constructed in the urban environment (Fig. 14). Increased DOC inputs through PTRU/D (Table 7, 8), altering the DOC:TDN ratio (Fig. 15b, Table 7, 8), suggest increased uptake/denitrification of N maybe occurring between the upstream and downstream reaches. Discharge values are significantly lower at the PTR compared to other sites (Table 3), which may promote anaerobic-denitrifying conditions (Craig et al., 2008). However, pre-restoration upstream and downstream TDN:DOC also indicate >1 ratios and a similar increase between reaches. At the regional level, PTRG showed substantial inputs of [TDN] (Table 7), despite greater discharge, shown to have a dilution effect on N concentrations (Rose et al., 2018), suggesting larger regional N reductions are limited (Fig. 15b).

Baseflow N removal is limited in the agricultural -suburban sites. Although N may be attenuated through conducive DOC:TDN ratios promoting N-uptake and denitrification in the urban environment (Mayer 2003, Newcomer et al., 2014), pre-restoration conditions did not substantially vary from post-restoration (Table 7, 10). Additionally, little to no effect was observed at the regional scale.

4.7 Baseflow Total Suspended Solids Results and Discussion

Baseflow TSS mg/L are broadly similar across all six sampled sites; landscape differences have limited effect on baseflow TSS concentrations. All sites fall in a similar concentration as POBR and BARN (Fig. 16a). Intra-site comparison between upstream and downstream reaches of the restoration show significant ($p < 0.05$) increases in [TSS] in the three sites that were restored during the study period (FMB, BCB, and PTR) (Table 7, 8). Intra-site comparison on streams restored prior to the study period indicate no significant differences at CBR and BTR. NSR showed a significant decrease ($p < 0.05$). Pre and post analysis of [TSS] suggests a significant ($p < 0.05$) increase in FMBD. BCB and PTRD did not experience a significant change (Table 10, 11). Most TSS concentration data were near detection limits (2 mg/L) during baseflow.

Baseflow daily load (g/km^2) comparison between sites indicate there is a trend between elevated daily loads in agricultural sites and a lower daily load in pasture and (sub)urban sites (Fig. 16b). Agricultural and pastures sites were similar to the forested controls, (sub)urban sites demonstrated a lower baseflow TSS daily load. FMB, CBR, and BTR contained significantly ($p < 0.05$) higher median daily loads compared to NSR, BCB, and PTR, with the most urban site (PTR) containing the lowest median daily load (Fig. 16b). Intra-site comparison during baseflow indicates nearly all sites increased in TSS daily loads, though only FMBU/D and BCBU/D were significantly ($p < 0.05$) higher (Fig. 16, Table 7, 8). NSR showed a significant decrease in daily load. Pre- and post-restoration analysis suggests TSS daily loads at FMB, BCB, and PTR increased. FMBD and PTRD had n values of 4 and 7, respectively (Table 10, 11). Statistical testing on

FMBD and PTRD was limited. FMBD and BCB showed a significant ($p < 0.05$) increase in baseflow TSS daily load following restoration.

Generally, agricultural sites exported greater [TSS] and daily loads during baseflow than pasture and (sub)urban sites (Fig. 16), which is not consistent with other research although many factors (discharge, soil type, clay content, slope, bank height, and fraction of agricultural land) are attributed to sediment mobilization (Coulter et al., 2004, Mallin et al., 2009, Sandström et al., 2020). Higher baseflow discharges (Fig. 5a, b) and agricultural practices (i.e. tilling, low ground cover, etc.) in the agricultural setting may explain elevated [TSS]. However, discharge is not the only variable governing baseflow TSS concentration and daily load across sites as BCB has a high baseflow discharge, but lower TSS than agricultural sites (Fig. 5, 16). At the most urban site, PTRD, low discharge and upstream piping of water may explain low [TSS] and daily load. ISC suggests lower TSS export during baseflow; and long-term age did not play a role in the retention of TSS.

Upstream and downstream analysis show median [TSS] significantly increased ($p < 0.05$) in the three sites constructed during the study period, but not within the sites restored prior to the study (Table 7, 8). FMB, BCB, and PTR had elevated [TSS] following restoration that eventually returned to pre-restoration conditions (Fig. 17). Possible explanations of increased [TSS] and daily load can be attributed to unstable banks following construction practices (Williams et al., 2017, Mattern et al., 2020) as well as agricultural practices in the case of FMB (Fig. 17, Table 10, 11). LSR restoration projects show limited ability to retain sediments during baseflow conditions; in fact, restoration projects likely increase TSS following construction (Williams et al., 2017).

4.8 Baseflow Total Dissolved Phosphorous and Ortho-*Phosphate*

Baseflow total dissolved phosphorus (TDP) was significantly greater than ortho-phosphate (PO_4^-) ($p < 0.05$). However, both P species were present in low concentrations during baseflow (0.0025 – 0.079 mg/L). Baseflow was largely ignored as a substantial contributor of P in this study. Stormflow produced substantial phosphorus export, 1 - 2 magnitudes greater than baseflow, and is therefore discussed only through the lens of storm export (Table 12).

4.9 Storm Assessment and Discussion at FMB and PTRG

4.9.1 FMB Storms

Three complete storms with water chemistry and sediment data were sampled at FMBU/D from baseflow to peak(s) through a return to baseflow on 07/11/2019 (1st), 01/12/2020 (2nd), and 02/05/2020 (3rd). The three complete storms sampled exhibited (1) differences in precipitation amounts, (2) variation in storm duration, (3) differences in peak discharge and total storm volume, and (4) some seasonal variation (Table 13, 14). These storms represent 3 of 27 storm events (stage: FMBU > 0.25 m and FMBD > 0.15 m) at the site from 04/23/2019 – 03/11/2020 (Fig. 4); note there were data gaps at FMBD during that period.

Local precipitation data was not available for 07/11/2019 at the USGS rain gage closest to White Hall, MD, but a nearby rain gage in Bel Air, MD measured 11.46 cm over 0.40 days (USGS 01581753 Atkisson reservoir near Bel Air, MD). Precipitation for the 01/12/2020 and 02/05/2020 events was 0.84 cm over 1.5 days and 3.3 cm over 2.3 days, respectively (USGS 394205076320201 rain gage in Deer Creek Basin at Norrisville, MD). The first storm hydrograph consisted of a rapid (<30 min) increase to

peak discharge and then a slower return to baseflow conditions within a few hours (Fig. 18). Steep increases in discharge are the result of high precipitation in a short period. The second storm had a lower peak discharge than the 07/11/2020 event due to a smaller precipitation amount over a longer period (Fig. 19). The hydrograph shows a slower increase to peak discharge then an eventual return to baseflow over the next few hours. The third storm had 4 separate discharge peaks, and the last peak was substantially larger than the previous three discharge peaks (Fig. 20). In all cases, FMBD peak discharge was 0 – 20 minutes behind FMBU peak discharge (Table 15).

Stream chemistry differed between stormflow and baseflow. Log – log TDN-Q relationships indicate there are weak dilution signals for up and downstream sites; low R^2 values for upstream and downstream (0.04931 and 0.1366) suggest more factors influence N concentration than discharge alone (Fig. 21a). Likewise, upstream and downstream log-log NO_3^- -Q relationships have weak dilution signals and low R^2 values (0.2231 and 0.2365). Chemostatic relationships in N species account for the considerable N loads exported during storm events (Table 13). Log-log TDP-Q relationships indicate an increase from baseflow to stormflow, but the R^2 are low (0.2427 and 0.1964) and concentration signals are not strong (Fig. 21b), suggesting discharge is not the main driver of TDP export. Log-log TSS concentration discharge relationships indicate a strong concentration signal as discharge increases (R^2 0.6684-upstream and 0.5292-downstream). [TSS] is heavily influenced by increasing discharge (Fig 21c). Log TDP and log TSS relationships suggests that TDP increases are tied to TSS suspension (Fig 21d). Increased TDP concentrations may be tied to TSS mobilization, which has implications for downstream export (Ekka et al., 2006).

Baseflow concentrations were significantly ($p < 0.05$) different than stormflow conditions based on parameter (Table 16). During baseflow, [TDN] and $[\text{NO}_3^-]$ are largely equivalent (Fig. 11). By contrast, during storm events, $[\text{NO}_3^-]$ diluted more than [TDN] (Fig. 22a, Table 16). Conversely, $[\text{NH}_4^+]$ was shown to increase from an undetectable level to substantial concentrations during storm events, accounting for less of a dilution in TDN (Fig. 22a). [TDP] and $[\text{PO}_4^-]$ were nearly undetectable during baseflow. During stormflow, [TDP] and $[\text{PO}_4^-]$ increased by an order(s) of magnitude (Fig. 22b, Table 16). [TSS] marks the greatest change in stream parameters as concentrations increased exponentially (Koskelo et al., 2018, Rose et al., 2018) during storm events (Fig. 22c, Table 16).

Nutrient and sediment concentrations across storm events can be described through three patterns. First, concentrations of [TDN] and $[\text{NO}_3^-]$ gradually decreased as stormflow increased and slowly returned to pre-stormflow concentrations, albeit slightly lower concentrations, as discharge subsided (Fig. 18a, 19a, 20a). Minimum concentrations occurred after peak discharge (Table 15). Additionally, in the 1st (FMBU) and 2nd (FMBU/D) storm, [TDN] and $[\text{NO}_3^-]$ initially increased slightly before peak discharge (Fig. 18a, 19a). Second, NH_4^+ , DOC, TDP, and PO_4^- exhibited concentration increases as discharge increased, followed by a slow decrease to baseflow concentrations after peak discharge (Fig. 18abc, 19abc, 20ab). Temporally, NH_4^+ , DOC, TDP, and PO_4^- peak concentrations occurred after peak discharge (Table 15). TDP peak concentrations occurred between 0-35 min after peak TSS concentrations (Table 15). Lastly, TSS showed a steep increase in concentration after peak discharge, followed by an immediate decrease in concentration after peak concentration (Fig. 18d, 19d, 20d, Table 15).

Time series data suggests concentration dynamics varied depending on the parameter, storm, and site. Comparing FMBU and FMBD across the three storms, downstream [TDN] and $[\text{NO}_3^-]$ were lower than upstream concentrations during the 07/11/2019 storm (Fig. 18a). Decreases in $[\text{NO}_3^-]$ between upstream and downstream during the 2nd storm were less visible (Fig. 19a). The 3rd storm was similar to the 7/11/2019 storm and downstream $[\text{NO}_3^-]$ was consistently lower than upstream conditions (Fig. 20a). $[\text{NH}_4^+]$ upstream and downstream concentrations were largely similar throughout the storms (Fig. 18a, 19a, 20a).

Intra-site comparison of [DOC] in the 1st and 2nd storm (3rd storm excluded due to lack of data) showed similar concentration changes across the event (Fig. 18b and 19b). Upstream concentrations of TDP and PO_4^- are consistently elevated relative to downstream during peak discharges. On the rising and falling limbs, P dynamics are more variable between up and downstream sites (Fig. 18c, 19c, 20b). Upstream and downstream [TSS] varied between the sites for the three different storms. In storm 1 and 2, upstream contained elevated [TSS], while in the 3rd storm [TSS] was greater in the downstream site (Fig 18d, 19d, 20c).

When performing load analyses, the 7/11/2019 storm samples exhibited atypical results in FMBU from the FMBD storm samples. Concentrations and loads for the upstream location appeared to lag, temporally, when compared to the downstream sample site and the other storms sampled. A sensitivity analysis was performed on load calculations for the upstream locations to better represent the true timing of the storm, which was most likely the result of mislabeling samples or an incorrect ISCO start time. Sensitivity analysis was performed for a subtraction of 15, 30, 45, and 60 minutes from

the recorded sample times (Fig. 23). A decrease of 30 minutes appeared to best reflect the hydrogeochemical response to storm conditions. For example, samples labeled as 15:30 were adjusted in time to 15:00, which resulted in concentration-discharge patterns that better matched the patterns for the other storms. Load analysis for 07/11/2020 in the following results refers to the 30 minutes shift in time, although all results are presented in tables 13 and 17.

Load analysis for the various parameters from the three storms indicate a decrease in load from upstream to downstream (Fig. 24). Across the three storms, N loads (g/km^2) of TDN and NO_3^- indicate a reduction of 21% - 37.55% from upstream to downstream (Table 13 and 17). NH_4^+ loads vary between increases and decreases between the storms, and % differences from upstream to downstream are <15%, suggesting uncertainty (Table 13, 17). TDP and PO_4^- loads (g/km^2) decrease from upstream to downstream across all storms; however, % differences exist between -12% through -17.07% providing little confidence to the reduction (Table 13, 17). TSS loads (kg/km^2) suggest a decrease between the upstream and downstream sites in all three storms. Percent differences in TSS load are more variable than the other parameters with a range from -9.87% through -35.52, contributing to restoration uncertainty in TSS load reduction (Table 13, 17).

Storms are of major concern when assessing restoration success because large loads of nutrients and suspended solids are transported during stormflows (Mark et al., 2004, Coulter et al., 2004, Burcher and Benfield 2006, Davis et al., 2015, Filoso et al., 2015, Williams et al., 2017, Koskelo et al., 2018, Mattern et al., 2020). FMB baseflow concentrations of TDN and NO_3^- were diluted with increasing discharge and different water sources (Fig. 21, 22, Table 17). The chemostatic relationship observed in log

[TDN] and log discharge can potentially be explained by increases in other N species, differences in water sources, and variations in storms events (Koskelo et al., 2018). From a daily load perspective, N increases were generally ~1.5 to ~3 times greater during stormflow due to large Q volumes (Table 7, 13). In the yearly budget, N is likely exported greater during baseflow conditions as concentration is higher and baseflow comprises roughly ~60-70% of the annual discharge (Filoso and Palmer 2014, Koskelo et al., 2018). NH_4^+ , TDP, and PO_4^- concentrations and loads increased from nearly undetectable to substantial nutrient source during stormflow conditions (Fig. 22, Table 16). NH_4^+ increases were likely the result of upstream riparian and soil matrix throughflow (Koskelo et al., 2018). TDP and PO_4^+ increases are related to high [TSS] (Fig. 21c, d) and throughflow (interflow) subsurface pathways during storm events (Benitez-Nelson 2000, Duan et al., 2012 Orihel et al., 2017, Koskelo et al., 2018, Rose et al., 2018). Baseflow TSS loads increased at greatest by nearly 3 magnitudes during stormflow (3 kg to >3000 kg), indicating an exponential increase with discharge (Table 7, 13, Fig. 21d)(Koskelo et al., 2018, Rose et al., 2018). Stormflows contribute substantially to the FMB N, P, and TSS export budget.

Three general trends were observed during stormflows. The first trend (dilution), exemplified by TDN and NO_3^- (Fig. 18a,19a, 20a)., are the result of groundwater NO_3^- dilution by surface water run-off and shallow soil-water throughflow (Scudlark et al., 1998, Vanni et al., 2001, Fox et al., 2014, Koskelo et al., 2018). TDN dilutes less than NO_3^- because of increases in other N species, such as NH_4^+ (Volk e. al., 2006). Baseflow largely consists of groundwater and shifts to a greater proportion of precipitation, soil

water, and overland flow during storm events, diluting N concentrations (Rose et al., 2018).

The second pattern observed in NH_4^+ , DOC, TDP, and PO_4^- (an elongated increase and decrease in concentration), reflect the chemical nature of these species (Fig. 18a, b, c; 19a, b, c; 20a, b, c). Ammonium and P typically bind to soil particles and are released through chemical desorption processes as precipitation infiltrates and saturates the upland and riparian soils (Koskela et al., 2018). TDP and PO_4^- are also related to TSS transport, but desorption processes in-stream require additional conditions for P release resulting in a delayed response from TSS (Benitez-Nelson 2000, Duan et al., 2012 Orihel et al., 2017). DOC is likewise flushed from the surrounding soil matrix during throughflows in storm events (Lambert et al., 2014). These parameters rely on sufficient infiltration through the soil matrix before flushing into the stream channel, producing a gradual increase and decrease in concentration through the storm event.

Third, TSS exhibited a steep increase and decrease in concentration centered during or after peak discharge (Fig. 18d, 19d, 20c). Concentrations of TSS changed the most dramatically out of all the parameters. The steep increases and decreases are likely due to physical erosion, souring, bank collapse, and re-suspension of bedloads as water velocity increased (Kuhnle et al., 2006, Thompson 2008, Koskela et al., 2018, Mattern et al., 2020). Differences in concentration patterns throughout the storm have implications for load contributions and the strategies used to ensure restoration practices reach their desired goals.

Upstream and downstream comparison of event loads suggest that restoration may result in reduced nutrient and TSS export during storm events (Fig 24, Table 13, 17).

Cumulative errors through the results make it difficult to conclusively evaluate reductions through the restoration as storm uncertainty was high. Furthermore, a lack of additional upstream and downstream storm sample sets renders confident conclusions challenging. Downstream daily loads (g/km^2) were consistently lower in TDN, NO_3^- , TDP, PO_4^- , and TSS than upstream for the three storms (Fig. 24). Reductions in parameters varied between -5% through -39%, which was similar to the observed trend in area-normalized storm discharge volume reductions (Table 17).

TDN and NO_3^- loads expressed the most consistent decreases with all reductions from upstream to downstream >20% (Table 17). N load removal from upstream to downstream may be the result of increased water residence time and improving interactions with bioreactive surfaces (Roley et al., 2012). Decreasing bank heights from ~2 m to a consistent 0.5 m at FMB increased overbank events leading to greater interaction with the floodplain area. Increasing floodplain riparian surface area with stormflow discharge plays a key role in N retention and removal (Newcomber-Johnson et al., 2014). Furthermore, reconnecting shallow groundwater pathways promotes DOC flushing during storm events (Fig. 18b, 19b), which may promote rapid denitrification during storm events (Mayer et al., 2003, Lu et al., 2008, Grebliunas and Perry 2016).

TDP and PO_4^- were also reduced from upstream to downstream locations. Percent reduction varied from -12% through -39% (Table 17). Load reductions in P may be tied to reductions in sediments as P is likely sorbed to sediments (Davis et al., 2015) and is desorbed when in contact with more anoxic conditions during stormflows (Filoso et al., 2015). A reduction in TSS loads through the restoration may have implications for P retention.

TSS load reductions were variable: 23%, 36% and 10% for the three storms (Table 17). Inconsistent reductions in TSS have been reported in other restoration projects during stormflows (Filoso and Palmer 2015, Williams et al., 2017). Seasonality and storm size contribute to the variability in TSS load reduction (Filoso and Palmer 2015). Peak storm discharge, total volume of discharge, and length of storm appear to have influences on the amount of load (Koskelo et al., 2018); however, relationships are hard to determine within this study. Our data may suggest shorter high-intensity events promote reduction in TSS loads (Table 17). As stage height increases rapidly, the floodplain is more readily accessed, and sediments are deposited. Low bank height may be a key factor in TSS reduction: increasing connectivity to floodplains has the potential to retain sediments. Lowering floodplains permit more frequent flooding, not solely during bankfull events, that can substantially increase floodplain retention of sediments (McMillian and Noe 2017).

The reductions observed at FMB are positive but only suggestive without pre-restoration data or further post-restoration data. Other factors, outside of the nutrient and sediment dynamics listed above, may contribute to smaller loads at the downstream end. With similar peak discharges at the upstream and downstream reaches but a 32% larger downstream watershed area, area normalized exports are expected to decrease. Additionally, decreases from upstream to downstream area-normalized discharge (Table 17) may account for some of the reductions witnessed.

4.9.2 PTRG Storms

PTRG baseflow and stormflow results were collected from USGS continuous sensor data at site 01581752 Plumtree Run near Bel Air, MD. PTRG was used to

investigate larger regional changes from the PTR restoration project (summer 2017). During storm events, nitrate diluted as discharge increased (Fig. 25). TDP was closely linked to TSS: as TSS concentrations increased, TDP increased (Fig. 26). TSS followed a flushing pattern as discharge increased (Fig. 27). Nitrate, TDP, and TSS patterns throughout individual storms followed the three trends and temporality described for FMB (Section 4.9.1, Table 15). Annual loads over the course of six years for nitrate were shown to vary by a factor of $\sim 2.5\times$, while TSS and TDP varied by $\sim 7.5\times$ (Fig. 28, Table 19). Total annual load rankings for each year were the same and were reflective of mean annual discharge (Fig. 28, Table 18). Annual NO_3^- exports were generally consistent throughout the year indicating N contributions were constant and baseflow driven (Fig. 28a). Conversely, TDP and TSS annual exports show large increases at discrete times indicating storm events are the main driver of TDP and TSS export (Fig. 28bc). In addition to observing annual loads, six paired pre- and post- restoration storms were selected based on similar precipitation amounts. Higher NO_3^- , TDP, and TSS loads occurred in five of the six post restoration storms; three of the five storm events had substantially higher loads post-restoration in TDP and TSS (Table 19).

PTRG higher post restoration event loads are likely the result of greater precipitation/discharge years following restoration. The restored PTR reach accounts for $\sim 15\%$ of the regional control watershed area; however, the effects of restoration were obscured by high variability in mean annual discharge (and total annual discharge) affecting annual load export (Table 18), providing little insight into the success of the PTR-LSR restoration project. The six pre- and post-restoration storms suggest precipitation, precipitation duration, and peak discharge are the important factors in N,

TDP, and suspended sediment exports (Table 19). Peak discharge appears to be the main driver of NO_3^- , TDP, and TSS loads. Observing the paired storms, the storm with higher peak discharge (5 of 6 storms) generally exported more nutrients and sediments (Table 19), which can promote uncertainty in drawing conclusions on restoration success. However, increased loads due to greater peak discharges may be a function of loads derived from Q-C relationships (Fig. 25, 26). To a lesser extent, total precipitation and precipitation intensity further complicate comparative analysis between pre- and post-restoration storms suggesting restorations may reduce storm inputs at the restoration scale, but there is unknown to no effect at the larger regional scale (Thompson et al., 2018).

5. Conclusions

The LSR-FR projects in this study showed minimal hydrogeochemical response to restoration during baseflow; during stormflow, at the restoration-scale, projects may have reduced nutrient and sediment loads, but regionally these reductions are not detectable. N was determined to have a larger baseflow contribution to the annual load budget than during stormflow. Agricultural and pasture restored sites saw little to no difference during baseflow as a result of restoration practices. Baseflow retention and removal of N may have occurred in the (sub)urban streams where N concentrations were low and dissolved organic carbon concentrations were higher facilitating denitrification, but pre-restoration data suggests these conditions were present before restoration. P and TSS contributions were low during baseflow and exported magnitudes higher during stormflow conditions. Analysis of storm events (FMB) suggest N, P, and sediments may be retained/removed during storms; however, due to the stochastic nature of individual storms and uncertainty inherent in calculating discharge from rating curves additional research is needed to determine success. Larger-scale regional reductions (PTRG) in nutrients and sediments were largely obscured due to variations in precipitation and discharge between years before and after restoration. Furthermore, restoration age from the beginning of the study, zero through five years, did not appear to have additional benefits after initial streambank stabilization. A long-term timescale was not established to observe any additional age-related benefits of restoration: restored stream systems may take decades to respond to physical changes (Meals et al., 2010, Hamilton 2012). Assessing the true effectiveness of stream restoration projects was challenging due to: a

lack of sufficient pre- and post-restoration data; variability in weather/climate year to year; and adequate time-intensive storm sampling.

6. Tables

Table 1: Site information

Site	Drainage Area (km ²)	%Agriculture	% ISC	% Developed	ISC +DEV	%Forest	Usage
FMBU	2.93	73.05	0.53	4.25	4.78	22.7	Active Agriculture
FMBD	3.88	68.74	0.47	4.86	5.33	26.4	Active Agriculture
CBRU	4.40	57.8	2.19	31.5	33.69	10.7	Active Agriculture
CBRD	4.97	59.9	1.97	28.1	30.07	12.0	Active Agriculture
BTRU	6.03	52.7	4.24	33	37.24	14.3	Retired Agriculture
BTRD	6.55	55.1	3.90	30.4	34.3	14.5	Retired Agriculture
NSRU	1.83	48.76	0.78	7.44	8.22	43.8	Pasture
NSRD	2.25	55.3	0.65	7	7.65	37.7	Pasture
BCBU	7.07	25.6	10.2	52.5	62.7	21.9	Suburban
BCBD	8.18	29	8.98	49.4	58.38	21.6	Suburban
PTRU	0.88	0	97.1	97.1	145.9	3.29	Urban
PTRD	0.96	0	48.6	95.5	144.5	5.01	Urban
PTRG	6.37	12.3	27.0	82.3	109.3	5.40	Urban
BARN	3.85	11.4	1.11	25.2	26.31	71.7	Reforested
POBR	0.33	0	0	0	0	100	Reforested

Information on upstream and downstream reaches for six restored sites. The table includes two reforested controls (POBR and BARN) and a regional watershed site PTRG to test larger watershed improvement from the PTR restoration. % agriculture was determined by subtracting 100% from %developed and %forested.

Table 2: Sampling Record

2017												
Stream Name	Jan	Feb	Mar	Apr	May	Jun	Jul	Aug	Sep	Oct	Nov	Dec
First Mine Branch	24th	7th & 21st	7th & 28th	4th & 11th & 25th (St)	Construction	Construction	7th & 17th & 31st	14th & 29th (St)	11th & 25nd	10th	6th	4th
Plum Tree Run + Gauge	25th	7th & 21st	7th & 28th	11th & 25th	8th & 23rd	5th & 19th(St) & 30th(gauge)	Gauge: 7th 17th and 31st (Cnstrn)	Gauge: 4th & 14th & 31st (Cnstrn)	Gage: 12th & 27th (Cnstrn)	11 & 27	10th & 20nd	6th & 20th(Gauge)
Bear Cabin Run	25th	21st	28th	X	8th & 23rd	5th	7th & 17th & 31st	14th & 31st	12th & 27th	9th (St) & 27th & 29th (St)	10th & 20nd	Construction
Bee Tree Run	-	-	-	-	-	-	X	X	22nd	13th	6th	6th & 20th
North Stirrup Run	-	-	-	-	-	-	-	-	-	-	21st	21th
Cabbage Run	-	-	-	-	-	-	-	-	-	-	21st	21th
2018												
Stream Name	Jan	Feb	Mar	Apr	May	Jun	Jul	Aug	Sep	Oct	Nov	Dec
First Mine Branch	9th	6th	6th	10th	1st	3rd (RC) + 5th + 11th(RC/St) + 19th	2th & 18th	1st and 14th	9th(RC/St) & 13th	12	6(RC) + 9th (St) + 30th	19th
Plum Tree Run + Gauge	11th(Gauge) + 22(Gauge) + 24(Gauge)	13th (Gauge)	13th + Gauge	17th	8th	6th + 20th	11th & 2th	2nd + 21(St)st + 22nd(St) (Gauge) 22	20th	18	16th	26th
Bear Cabin Run	Construction	Construction	Construction	Construction	8th	6th + 20th	11th & 26th	2nd + 21st	20th	18	16th	26th
Bee Tree Run	9th	6th	6th	10th	1st	5th + 19th	2th & 18th	1st + 14th	13th	12	30th	19th
North Stirrup Run	31	20th	27th	24th	17th	6th + 20th	11th & 26th	2nd + 21st	26	26	29th	26th
Cabbage Run	31	20th	27th	24th	17th	6th + 20th	11th & 26th	2nd + 21st	26	26	29th	26th
Pond Branch	11th	13th	13th	17th	30th	5th + 19th	2nd & 18th	1st + 14th	13th	12	30th	19th
Baisman Run	11th	13th	13th	17th	30th	5th + 19th	2nd & 18th	1st + 14th	13th	12	30th	19th
2019												
Stream Name	Jan	Feb	Mar	Apr	May	Jun	Jul	Aug	Sep	Oct	Nov	Dec
First Mine Branch	11th	12(RC/St) + 14th	1(RC) + 5th + 21(st)	2nd (RC) + 26(RC/St)	9th	4th + 18	2 + 11 (St) + 23 (St)	6	X	16(st) + 22(St)	X	X
Plum Tree Run + Gauge	25th	19th	6(g) + 19th	4th(g) + 18th	2(Gauge) + 21	11(+g) + 25(+g)	9(+g)	13(+g)	Gauge: 11 + 30	Gauge: 17 + 29	Gauge: 14	X
Bear Cabin Run	16th	19th	19th	18th	21	11 + 25	3 + 9	6 + 14	X	X	X	X
Bee Tree Run	11th	14th	5th	2nd	9th	4th + 18	2	6	X	X	X	X
North Stirrup Run	16th	19th	19th	18th	21	11 + 25	9	13	X	X	X	X
Cabbage Run	16th	19th	19th	18th	21	11 + 25	9	13	X	X	X	X
Pond Branch	11th	15th	5th + 19th	2nd + 20	9th	5th + 19	3 + 19 + 31	13 + 14 + 27	11 + 30	17 + 29	14	X
Baisman Run	11th	15th	5th + 10(St) + 25(st)	2nd + 17 + 20	9th + 22	5th + 19	3 + 19 + 31	13 + 14 + 27	11 + 30	17 + 29	14	X
2020												
Stream Name	Jan	Feb	Mar	Apr	May	Jun	Jul	Aug	Sep	Oct	Nov	Dec
First Mine Branch	11th(St)	5th (St)	X	X	X	X	X	X	X	X	X	X

St = Storm sampling

RC = Rating curve sampling;

+g = gage sampling

X = no sampling

Table 3: Baseflow Discharge by Year

Site	2017 Discharge	<i>n</i> 2017	2018 Discharge	<i>n</i> 2018	2019 Discharge	<i>n</i> 2019	Pre- restoration Discharge	<i>n</i> <i>Pre</i>	Post- Restoration Discharge	<i>n</i> <i>Post</i>
FMBU	0.024*	18	0.04*	17	0.065*	9	0.028*	12	0.037	33
FMBD	0.031	18	0.061	15	0.111	9	0.038	12	0.052	33
CBRU	0.043	2	0.077*	15	0.097*	9	N/A	N/A	N/A	N/A
CBRD	0.047	2	0.088	17	0.125	9	N/A	N/A	N/A	N/A
BTRU	0.069	7	0.086*	18	0.167	9	N/A	N/A	N/A	N/A
BTRD	0.046	6	0.130	18	0.175	9	N/A	N/A	N/A	N/A
NSRU	0.010	2	0.025*	16	0.041	9	N/A	N/A	N/A	N/A
NSRD	0.015	2	0.033	16	0.040	9	N/A	N/A	N/A	N/A
BCBU	0.056	16	0.163	11	0.114*	11	0.056 ⁺	19	0.129 ⁺	22
BCBD	0.057	17	0.116	11	0.093	11	0.058 ⁺	22	0.106 ⁺	22
PTRU	0.003	15	0.005	16	0.005	9	0.003	13	0.003	30
PTRD	0.002	16	0.004	17	0.004	9	0.003 ⁺	14	0.004 ⁺	29
PTRG	0.0375	12	0.066	18	0.061	20	N/A	N/A	N/A	N/A
BARN	N/A	N/A	0.052	16	0.065	24	N/A	N/A	N/A	N/A
POBR	N/A	N/A	0.004	14	0.005	19	N/A	N/A	N/A	N/A

Discharge measurements (m^3/s) taken through the study period. CBR and NSR only contained two discharge measurements during 2017 so conclusions on discharge increases are difficult to statistically represent.

Bold: Denotes statistical significance between years

*: Denotes significance between upstream and downstream sites

+ : Denotes significance between Pre and Post data

Table 4: Baseflow Stream Parameters

Site	Median pH	Median SC (uS/cm)	Median Temp (°C)	Median DO (%DO)	<i>n</i>
FMBU	7.32 *	260.2*	16.3	94.95 (32)	33
FMBD	7.24	251.3	17	97.2	33
CBRU	7.07 *	237.6	16.7	98	25
CBRD	6.915	240.55	16.6	100.1	26
BTRU	7.33	279.8 *	14.9	98.45 (28)*	29
BTRD	7.39	261.5	14.9	100.65 (28)	29
NSRU	6.86 *	212.9	15.85	97.6	26
NSRD	6.915	208.0	16.4	99.95	26
BCBU	7.365*	297.2	20.1	107.4	22
BCBD	7.575	289.4	21.3	110.8	22
PTRU	7.52*	912.1	15.7	104.8	30
PTRD	7.3	882.0	15.5	102.7	30
PTRG	7.75	573.4	18.2	99.15 (36)	61
BARN	7.17 (41)	178.25	13.5	98.35 (24)	42
POBR	7.02 (34)	28.1	15.3	94 (23)	34

Discrete in-field measurements for up and downstream reaches of the restoration projects during baseflow.

*: Denotes significance between upstream and downstream sites

(*n*): Indicates variation in *n* from the population

Table 5: Baseflow Major Cations

Site	Median [Na ⁺]	Median [Ca ²⁺]	Median [Mg ²⁺]	Median [K ⁺]	<i>n</i>
FMBU	11.17*	21.01*	8.86	3.87*	29
FMBD	10.41	20.59	8.96	3.54	29
CBRU	13.645*	16.78	6.605	2.315	27
CBRD	13.16	16.75	6.96	2.36	26
BTRU	17.87*	18.18*	8.48*	1.74*	25
BTRD	16.71	16.99	8.11	1.73	25
NSRU	13.82*	12.13	5.86	1.41	22
NSRD	13.02	12.02	5.68	1.38	22
BCBU	17.99	20.13*	5.545	2.28	14
BCBD	18.73	19.78	8.355	2.23	14
PTRU	39.14	82.90*	30.51*	1.95	23
PTRD	39.31	77.54	28.91	1.99	23
PTRG	41.22	37.08	14.13	1.67	49
BARN	16.64	7.24	4.52	1.67	48
POBR	1.98	1.06	0.83	1.01	39

[Median] (mg/L) for up and downstream reaches of the post-restoration projects during baseflow.

*: Denotes significance between upstream and downstream sites

Table 6: Baseflow Major Anions

Site	Median [Cl ⁺]	Median [HCO ₃ ⁻]	Median [NO ₃ ⁻] - N	Median [SO ₄ ²⁻]	<i>n</i>
FMBU	25.93*	59.50*	6.35*	15.96*	33
FMBD	25.50	58.05	5.92	14.61	33
CBRU	34.93	29.21*	5.21*	14.21*	26
CBRD	33.72	30.56	5.49	14.71	26
BTRU	40.11*	46.32*	6.34*	9.11	29
BTRD	37.22	44.71	6.10	9.18	29
NSRU	34.89*	27.32*	2.90*	10.17*	(26)
NSRD	33.28	29.085	2.98	10.135	(26)
BCBU	55.64*	39.13*	3.07*	10.305	(22)
BCBD	54.53	40.17	2.94	10.375	(22)
PTRU	232.59*	127.73	1.88*	38.03*	(29)
PTRD	216.56	127.21	1.16	34.075	(29)
PTRG	130.07	55.24	1.87	22.24	49
BARN	36.66	16.84	1.57	3.43	48
POBR	2.140	11.20	0.16	1.10	39

[Median] (mg/L) for up and downstream reaches of the restoration projects during baseflow from the ion chromatography instrument. Nitrate is reported as nitrogen.

*: Denotes significance between upstream and downstream sites

(*n*): Indicates minor variation in *n* from the population

Table 7: TDN, DOC, and TSS [Median] and Median Daily Load (g/km²)

Site	Median [TDN]	Load TDN	Median [DOC]	Load DOC	DOC:TDN	<i>n</i>	Median [TSS]	Load TSS	<i>n</i>
FMBU	6.40*	6935.59	1.78	1592.95	0.31*	33	2.842*	3038.92*	31
FMBD	6.01	6343.05	1.84	2233.93	0.36	33	6.103	8631.36	31
CBRU	5.30*	7831.77	1.07	1819.51	0.24	26	2.041	2904.86	24
CBRD	5.37	8935.01	1.02	1606.31	0.20	26	2.201	3545.97	24
BTRU	6.13*	9448.12	0.92	1464.93	0.19	29	4.158	7075.41	26
BTRD	5.90	8771.25	0.95	1335.98	0.19	29	3.810	7480.82	27
NSRU	2.80*	3425.31	1.16*	1801.18	0.45	26	3.074*	4510.29*	24
NSRD	2.85	4082.11	1.32	1679.62	0.54	26	1.900	2303.77	24
BCBU	2.96*	4311.45*	1.55	2270.12	0.63*	22	1.058*	1674.65*	19
BCBD	2.72	3062.02	1.78	1663.57	0.69	22	3.053	2516.37	19
PTRU	1.91*	712.80*	2.09*	766.45	1.40*	29	2.126*	702.79	28
PTRD	1.42	477.45	2.65	815.40	2.64	29	3.152	1104.84	28
PTRG	2.52	1876.66	2.05	1580.43	0.93	45	0.500	613.81	36
BARN	1.78	2134.48	1.02	1489.84	0.61	(36)	2.990	4164.57	25
POBR	0.19	216.64	1.80	2450.99	11.47	(36)	4.271	3863.90	20

*: Denotes significance between upstream and downstream site

(*n*): Indicates minor variation in *n* from the population

Table 8: Post-Restoration Baseflow Significance Values [Concentration]

Parameter	FMBU/D	CBRU/D	BTRU/D	NSRU/D	BCBU/D	PTRU/D
Discharge	3.107e-06↑*	0.0002036↑*	0.01007↑*	0.001147↑*	0.1627	0.3339
[TDN]	5.633e-07↓*	3.667e-05↑*	2.681e-06↓*	0.03465↑*	6.33e-05↓*	2.701e-06↓*
[DOC]	0.8443	0.4927	0.7538	0.02141↑*	0.0037	2.699e-06↑*
DOC:TDN	0.001187↑*	0.1007	0.2941	0.1645	0.0003538↑*	7.451e-09↑*
[TSS]	0.0001451↑*	0.3301	0.9393	0.02965↓*	0.001025↑*	0.001025↑*

Discharge and concentration significance values for up and downstream sites

*: Denotes statistical significance between upstream and downstream of the restoration sites

↑↓: Indicates an increase (↑) or a decrease (↓) between upstream and downstream of the restoration reaches

Table 9: Post-Restoration Baseflow Significance Values Daily Load

Site/Parameter Load	FMBU/D	CBRU/D	BTRU/D	NSRU/D	BCBU/D	PTRU/D
TDN	0.5366	0.6528	0.7493	0.3032	0.001262↓*	4.211e-05↓*
DOC	0.16	0.5249	0.2383	0.2304	0.0822	0.01911↑*
TSS	6.266e-05↑*	0.5838	0.4992	0.04568↓*	0.009453↑*	0.08593

Daily load significance values for up and downstream sites

*: Denotes statistical significance between upstream and downstream of the restoration sites

↑↓: Indicates an increase (↑) or a decrease (↓) between upstream and downstream of the restoration reaches

Table 10: Pre- and Post-Restoration Baseflow Concentrations (mg/L) and Daily Loads (g/km²)

Site/Parameter	FMBD Pre	FMBD Post	<i>n</i> Pre Post	BCBD Pre	BCBD Post	<i>n</i> Pre Post	PTRD Pre	PTRD post	<i>n</i> Pre Post
[TDN]	5.660	6.010	7 33	2.330*	2.723	16 21	1.500	1.420	9 29
Load TDN	4352.96	6343.052	7 33	1442.98*	3062.024	16 21	355.05	477.45	9 29
[DOC]	1.640	1.840	7 33	1.690	1.780	16 21	2.260	2.745	9 29
Load DOC	1314.71	2233.93	7 33	1112.22*	1663.57	16 21	602.10	815.40	9 29
DOC:TDN	0.352	0.360	7 33	0.832	0.694	16 21	1.758	2.644	9 29
[TSS]	1.761*	6.103	4 31	2.139	3.053	15 19	3.206	3.152	7 28
Load TSS	1230.53*	8631.36	4 31	1298.55*	2516.37	15 19	749.52	1104.84	7 27
Site/Parameter	FMBU Pre	FMBU Post	<i>n</i> Pre Post	BCBU Pre	BCBU Post	<i>n</i> Pre Post	PTRU Pre	PTRU post	<i>n</i> Pre Post
[TDN]	6.17	6.4	7 33	2.495	2.985	16 22	1.85	1.91	8 29
Load TDN	4234.60	6935.59	7 33	1541.58	4311.45	16 22	445.5	712.8	7 29
DOC	1.870	1.780	7 33	1.695	1.550	16 21	2.265	2.09	8 29
DOC:TDN	0.560	0.310	7 33	0.782	0.630	16 22	1.445	1.404	8 29

*: Denotes statistical significance between upstream and downstream of the restoration sites

Table 11: Significance Values Pre-Post and Pre-Pre-Restoration

Site/ Parameter	Pre-Post FMBD	Pre-Post BCBD	Pre-Post PTRD	Pre – FMBU/D	Pre- BCBU/D	Pre-PTRU/D
[TDN]	0.8170	0.005959↑*	0.5253	0.01563↓*	0.0005834↓*	0.007813↓*
Load TDN	0.1802	0.00000663↑*	0.09073	0.03125↑*	0.03864↓*	0.01563↓*
[DOC]	1.0000	0.9633	0.2154	0.8125	0.4954	0.02344↓*
Load DOC	0.1105	0.008392↑*	0.08638	0.2969	0.8209	0.8125
DOC:TDN	0.9445	0.2290	0.1238	0.8125	0.09344↑*	0.01563↑*
[TSS]	0.04149↑*	0.3857	0.8852	0.8125	0.1205	0.1422
Load TSS	0.03222↑*	0.0362↑*	0.3021	0.625	0.107	0.4185

*: Denotes statistical significance between upstream and downstream of the restoration sites

↑↓: Indicates an increase (↑) or a decrease (↓) between upstream and downstream of the restoration reaches

Table 12: Phosphorous Concentrations

Site	Baseflow Median PO ₄ ³⁻ mg/L	HDL <i>N</i>	BDL <i>N</i>	Significance	Storm Flow Median PO ₄ ³⁻ mg/L		BDL/ censored <i>N</i>	Storm Flow TP mg/L		BDL/ censored <i>N</i>
Pre- FMBU	0.031 ⁺	6	0	0.03969↓ (Pre-Post)						
Pre- FMBD	0.0305 ⁺	6	0	0.0002647↓ (Pre-Post)						
FMBU	0.007	16	11	0.002584	0.461	77	3	0.5495	76	0
FMBD	0.0025	10	18		0.254	60	5	0.332	73	0
CBRU	0.0025	1	13	0.9604						
CBRD	0.0025	1	14							
BTRU	0.0025	0	18	1						
BTRD	0.0025	0	17							
NSRU	0.0025	1	13	0.4025						
NSRD	0.0025	3	12							
Pre- BCBU	0.0025	7	8	0.2043 (Pre-Post)						
Pre- BCBD	0.00425	7	7	0.2518 (Pre-Post)						
BCBU	0.0025	2	7	0.958						
BCBD	0.0025	3	7							
Pre- PTRU	0.006	5	4	0.1209 (Pre-Post)						
Pre- PTRD	0.0025	2	7	0.9155 (Pre-Post)						
PTRU	0.0025	5	14	0.7618						
PTRD	0.0025	4	14							

+ indicates significance between pre-post upstream or downstream

Pre FMBU to Pre FMBD significance = 0.4375

Pre BCBU to Pre BCBD significance = 0.3621

Table 13: FMB Storm Loads

Site	Peak Discharge (m ³ /s)	Volume Discharge (m ³ /km ²)	TDN (g/km ²)	NO ₃ ⁻ (g/km ²)	NH ₄ ⁺ (g/km ²)	TDP (g/km ²)	PO ₄ ⁻ (g/km ²)	TSS (kg/km ²)
07/11/2020								
FMBU	0.545	1279.2331	16152.6397	15653.9372	318.4994	1201.4004	1358.6325	2514.7498
FMBU(15)	0.545	1279.2331	16024.6838	15545.5176	413.7161	1358.5026	1528.5006	3290.4414
FMBU(30)	0.545	1279.2331	15702.2853	15315.1194	483.3857	1549.3485	1748.4681	3710.1344
FMBU(45)	0.545	1279.2331	15087.1285	14809.2023	529.9532	1831.8992	2090.2445	3719.9479
FMBU(60)	0.545	1279.2331	14780.7377	13972.7091	529.6756	1922.4817	2240.0086	3398.9521
FMBD	0.566	1131.4428	12173.9712	9677.7161	490.6533	1328.6433	1197.5788	2822.4144
01/12/2020								
FMBU	0.246	3526.3443	13503.5563	12668.6510	834.9053	1314.9139	1075.6835	717.1325
FMBD	0.220	2781.4280	10545.1749	9617.3806	927.7944	1106.5646	938.1273	448.3702
02/05/2020								
FMBU	0.773	9374.2771	20395.8754	19771.3350	624.5404	1241.4709	1518.2641	894.4224
FMBD	0.524	6380.1124	12938.2075	12346.3110	591.8965	1092.4975	923.8670	877.4327

Cumulative storm loads normalized to 24 hours for three sampled storms. Loads were normalized to 24 hours to compare across the three different storms. TDN loads were approximated for the 2nd and 3rd storms by adding NO₃⁻ to NH₄⁺.

Table 14: FMB Storm Sample Information

Storm	Storm Duration (Days)	Precip. (cm)	TDN (n)	NO ₃ ⁻ (n)	NH ₄ ⁺ (n)	TDP (n)	PO ₄ ⁻ (n)	TSS (n)
07/11/2019	0.40	11.46	13 13	12 13	13 13	13 12	13 13	13 13
01/12/2020	1.48	0.838	0 0	12 11	12 11	12 11	12 11	13 11
02/05/2020	2.27	3.200	0 0	15 15	15 15	15 15	15 15	9 9

Listing format: FMBU (n) | FMBD (n)

Table 15: Temporal Trend in Peak (Min. for NO₃⁻) FMB Storm Concentrations

Storm	Diff. Q (Hrs:min)	Diff. NO ₃ ⁻ (Hrs:min)		Diff. NH ₄ ⁺ (Hrs:min)		TDP (Hrs:min)		TSS (Hrs:min)	
Site	Up - Dn	FMBU	FMBD	FMBU	FMBD	FMBU	FMBD	FMBU	FMBD
07/11/2019	+0:15	+1:55	+0:40	+0:25	+0:10	+0:25	+0:40	+0:25	+0:10
01/12/2020	+0:15	+1:50	+3:05	+1:20	+1:35	+1:20	+2:05	+0:50	+1:35
02/05/2020	+0:20	+1:25	+1:05	+1:25	+1:05	+1:25	+1:05	+1:25	+1:05
02/05/2020	+0:15	+2:20	+2:05	+2:20	+2:05	+2:20	+2:05	+2:20	+2:05
02/05/2020	+0:00	+1:35	+1:35	N/A	+1:35	+1:35	+1:35	+1:35	+1:35

Information based on upstream and downstream peak discharges. The 07/11/2020 storm used concentrations adjusted to 30minutes prior for FMBU. Note: Temporal resolution of 02/05/2020 storm was low due to water sampling infrequency.

+ : Signifies After Peak Discharge

- : Signifies Before Peak Discharge

Table 16: FMB Baseflow Compared to Stormflow Concentrations (mg/L)

Site/Parameter	Baseflow	25% Storm	Median Storm	75% Storm	<i>n – base storm</i>
FMBU [TDN]	6.400*	4.675	5.415	6.02	33 48
FMBD [TDN]	6.010*	3.935	4.550	4.990	33 40
FMBU [NO ₃ ⁻]	6.352*	4.499	5.280	5.895	33 68
FMBD [NO ₃ ⁻]	5.925*	2.982	4.285	4.851	33 58
FMBU [DOC]	1.780*	4.300	6.670	9.860	33 61
FMBD [DOC]	1.840*	3.693	6.340	8.675	33 58
FMBU [PO ₄]	0.007*	0.107	0.461	1.041	27 77
FMBD [PO ₄]	0.0025*	0.078	0.254	0.537	28 60
FMBU [TDP]	0.052*	0.1825	0.550	0.996	9 76
FMBD [TDP]	0.036*	0.113	0.322	0.675	11 73
FMBU [TSS]	2.842*	44.094	163.623	618.769	31 70
FMBD [TSS]	6.103*	53.567	173.600	616.1905	31 75

*: Denotes statistical significance between median baseflow and stormflow concentrations

Table 17: FMB Storm % Differences

Site	Volume Discharge (%)	TDN (%)	NO ₃ ⁻ (%)	NH ₄ ⁺ (%)	TDP (%)	PO ₄ ⁻ (%)	TSS (%)
07/11/2019							
FMBU/D	-11.55	-24.63	-38.18	54.06	10.59	-11.85	12.23
FMBU(15)/D	-11.55	-24.03	-37.75	18.56	-2.20	-21.65	-14.22
FMBU(30)/D	-11.55	-22.47	-36.87	1.50	-14.25	-31.51	-23.93
FMBU(45)/D	-11.55	-19.31	-36.65	-7.42	-27.47	-42.71	-24.13
FMBU(60)/D	-11.55	-17.64	-30.74	-7.37	-30.89	-46.54	-16.96
01/12/2020							
FMBU/D	-21.12	-21.91	-24.09	-89.50	-15.85	-12.79	-37.48
02/05/2020							
FMBU/D	-31.94	-36.56	-37.55	-5.23	-12.00	-39.15	-9.87

Bold indicates the time stamp chosen for FMBU on 07/11/2019

(+) Indicates upstream < downstream

(-) Indicates downstream < upstream

Uncertainty was estimated to be 20%

Table 18: PTRG Mean Streamflow and Annual Loads

Calendar Year / Period	PTRG mean m ³ /s	PTRG NO ₃ ⁻ kg/yr	PTRG TDP kg/yr	PTRG TSS kg/yr
2014	0.1584 (3)	6617.39 (3)	553.98 (3)	588,565.17 (3)
2015	0.1674 (2)	7006.89 (2)	557.69 (2)	600,281.67 (2)
2016	0.1006 (5)	5278.29 (5)	238.67 (5)	253,617.43 (5)
2017	0.0832 (6)	4533.41 (6)	175.83 (6)	152,122.90 (6)
2018	0.2013 (1)	7809.30 (1)	807.77 (1)	988,778.48 (1)
2019	0.138 (4)	6251.90 (4)	406.65 (4)	421,763.47 (4)

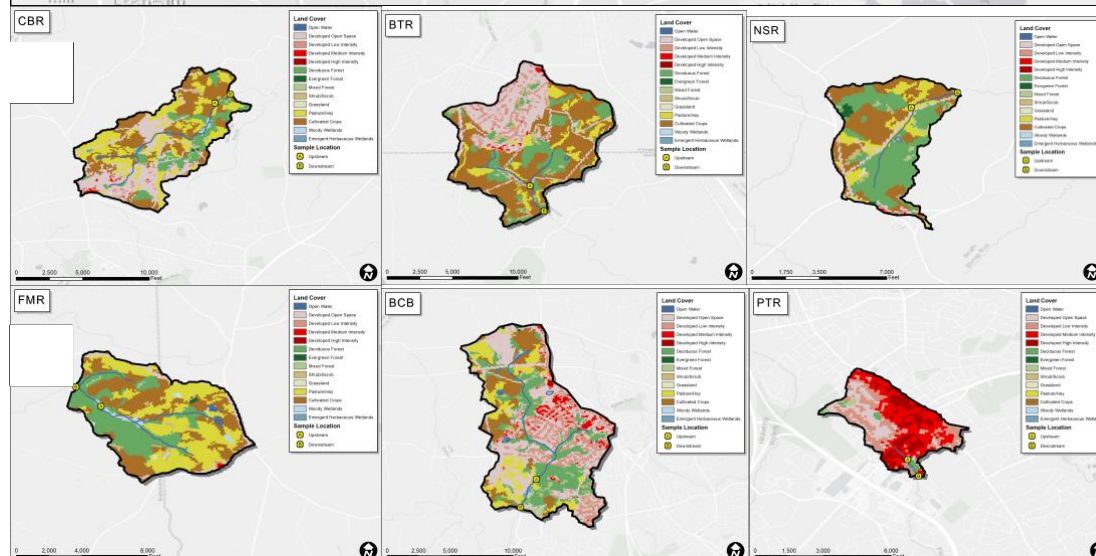
Gaps in the high-frequency data less than or equal to 1-hour, were filled via linear interpolation of the surrounding points. If data gaps were greater than 1-hour, daily mean Q from USGS were used.

Rankings are present in parentheses

Data sources: PTRG https://waterdata.usgs.gov/md/nwis/uv/?site_no=01581752&agency_cd=USGS

Table 19: PTRG Storm Sets

Storm Set	Start Time	End Time	Peak Discharge (m ³ /s)	Pre or Post Restoration	Total Precip. (cm)	Precip Duration (hr)	TSS Load (kg)	TDP Load (kg)	NO ₃ ⁻ Load (kg)
1	7/30/2015 14:35	8/1/2015 16:05	5.324	Pre	73.548	0.75	6590	6.44	56.95
1	6/19/2019 22:10	6/22/2019 22:50	5.748	Post	71.613	1.50	9688	9.25	72.76
2	9/10/2015 3:55	9/12/2015 16:35	3.256	Pre	108.39	12.75	5356	6.64	75.62
2	7/27/2018 8:50	7/29/2018 12:25	16.310	Post	115.48	13.75	45224	32.48	89.02
3	11/6/2014 0:10	11/7/2014 6:15	0.963	Pre	45.161	11.25	550	1.08	35.60
3	11/7/2017 12:20	11/11/2017 9:10	0.864	Post	49.677	10.75	607	1.16	50.05
4	7/8/2016 17:15	7/11/2016 14:20	1.209	Pre	70.322	2.75	1424	1.68	39.85
4	7/17/2019 18:10	7/22/2019 13:35	16.679	Post	61.935	2.25	24422	20.65	116.1
5	10/4/2014 0:45	10/5/2014 18:40	0.728	Pre	26.452	8.50	217	0.41	24.98
5	1/12/2020 1:20	1/14/2020 15:20	1.379	Post	27.097	7.50	1050	1.56	46.05
6	1/10/2014 8:55	1/13/2014 16:55	3.936	Pre	80.645	38.75	11006	11.96	106.4
6	2/5/2020 23:55	2/9/2020 18:35	1.928	Post	79.355	37.25	3097	4.87	92.37



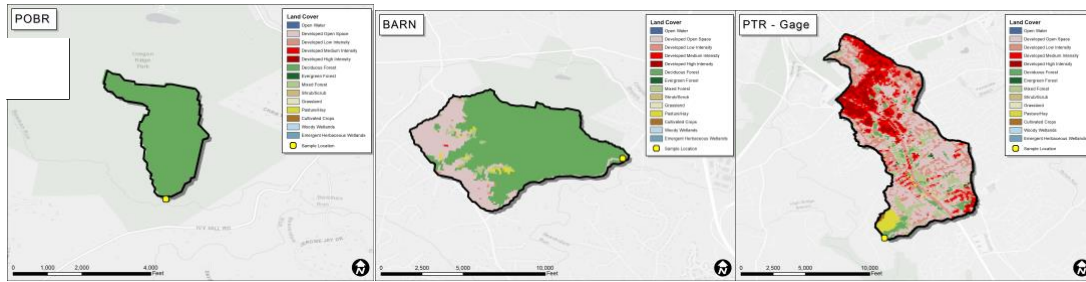


Fig. 1 (A) Map of the six restored watersheds with upstream and downstream locations indicated (BTR = Beetree Run, BCB = Bear Cabin Branch, CBR = Cabbage Run, FMB = First Mine Branch, NSR = North Stirrup Run, PTR = Plumtree Run). The map also includes the forested (BARN = Baismen Run and POBR = Pond Branch) and regional control (PTRG = Plumtree Run Gage). (B) Zoomed-in maps of the three sites restored pre-grant period. (C) Zoomed-in maps of the three sites restored during-grant period. (D) Zoomed-in maps of the three sites control sites.

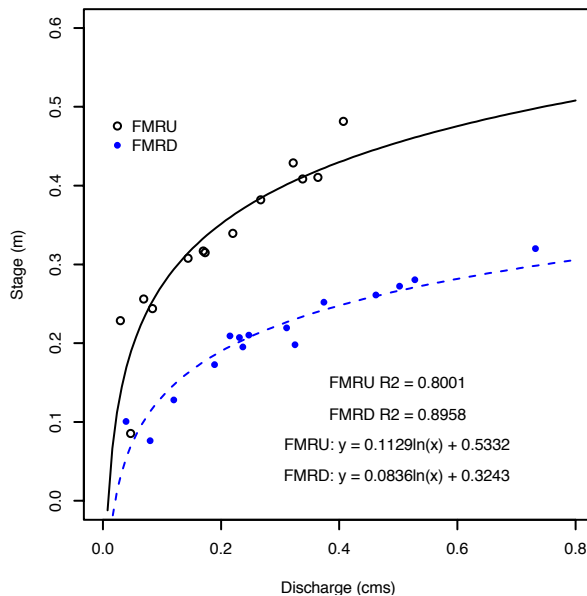


Fig. 2: Plot of upstream and downstream stage height (m) and discharge ($\text{m}^3/\text{s} = \text{cms}$) relationship. The logarithmic regression equation shown was evolved to calculate discharge (cms) from stage height (m). FMBU $n = 13$, FMBD $n = 15$

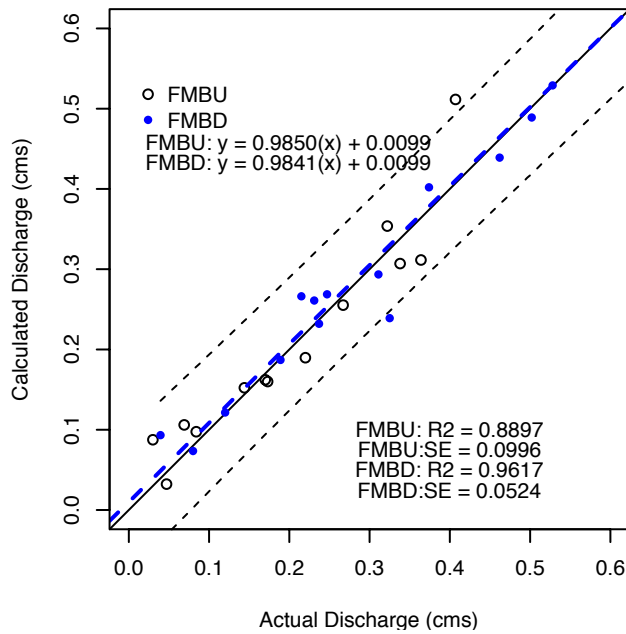


Fig. 3: Plot of calculated discharge ($\text{m}^3/\text{s} = \text{cms}$) versus discrete discharge measurements. The dashed lines indicate a 95% prediction interval: the estimated interval that a future observation will fall within that range. As shown, R^2 values are high, and standard error (SE) is low.

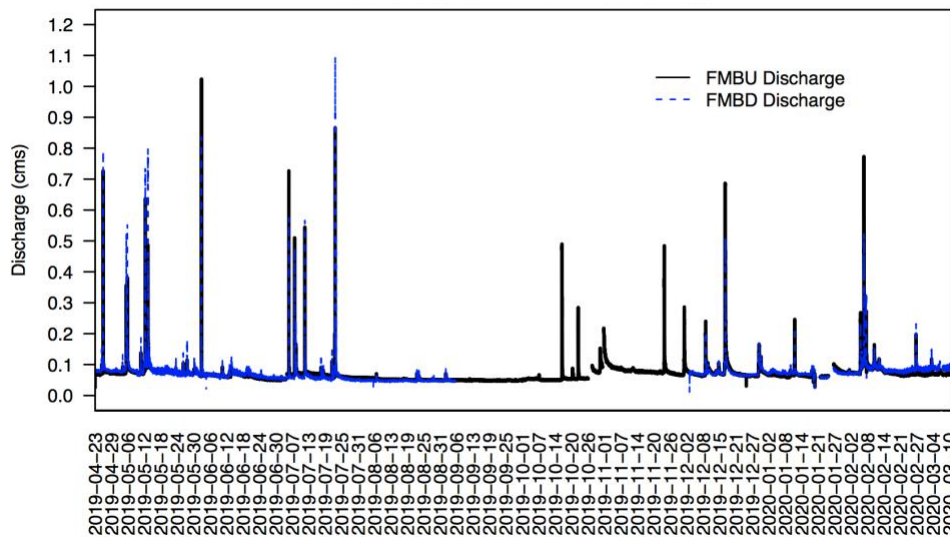


Fig. 4: Discharge calculated from rating curves (Fig. 2) from 04/23/2020 – 03/10/2020. Gaps in data were due to issues with HOBO U20 pressure loggers.

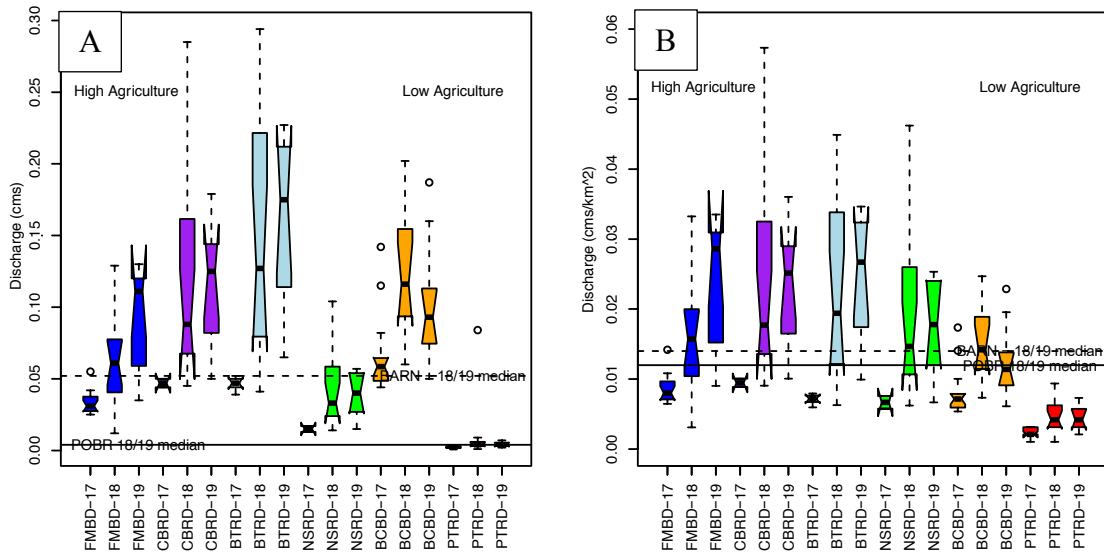


Fig. 5: (A) Baseflow discharge (m^3/s) by year from the downstream reaches of the six restoration sites. Discharge from 2017 to 2018 is shown to increase in all sites across the agricultural gradient. Increases from 2018 to 2019 are consistent in the agricultural and pastures sites; while, a median decrease is observed in the (sub)urban sites. NSRD, BTRD, and CBRD have less than 10 samples in 2017; meaningful interpretation is limited. Median discharge values from a 100% forested control site, POBR, are represented by a solid line; median discharge values from a 71.7% forested, BARN, site are represented by a dashed line. (B) Baseflow discharge was normalized by watershed area ($\text{m}^3/\text{s}/\text{km}^2$). Discharge becomes less variable as an outcome of the modification; the same trend is observed across the sites. Upstream mirrored downstream sites with reduced discharge except in BCB and PTR. POBR and BARN experienced a median increase in baseflow discharge from 2018 to 2019.

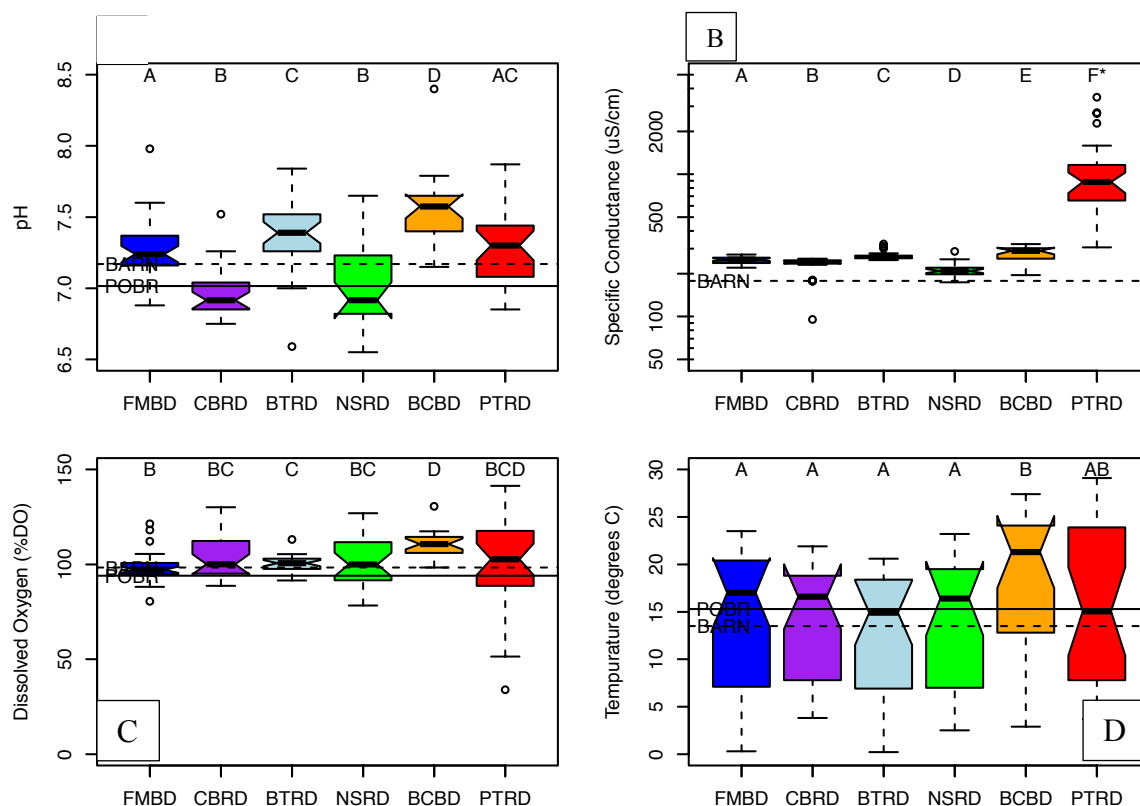


Fig. 6: (A) Baseflow pH from the six downstream restored reaches through the duration of the sampling period 2017 – 2019. pH varied across the agricultural gradient. Upstream did not vary substantially from downstream. Median pH for the control sites are represented as lines, POBR (solid) and BARN (dashed). (B) Baseflow Specific Conductance (SC) (uS/cm) from the six downstream sites during the sampling period. Agricultural median values did not vary substantially; while, SC was shown to increase as sites because more (sub)urban. Upstream sites mirrored downstream sites with the exception of FMB and BTR that experienced a decrease in SC from up to down. BARN is shown as a dashed line, and POBR contained a median SC value of 28.33 uS/cm³. (C) Temperature (°C) across the six downstream sites indicate no substantial variance in temperature across the sites. Upstream mirrored downstream locations – controls follow the same line type. (D) Dissolved Oxygen (%DO) shown in the six downstream sites. No trend is observed across the agricultural gradient. Upstream followed downstream in DO%. Controls are symbolized by their line type.

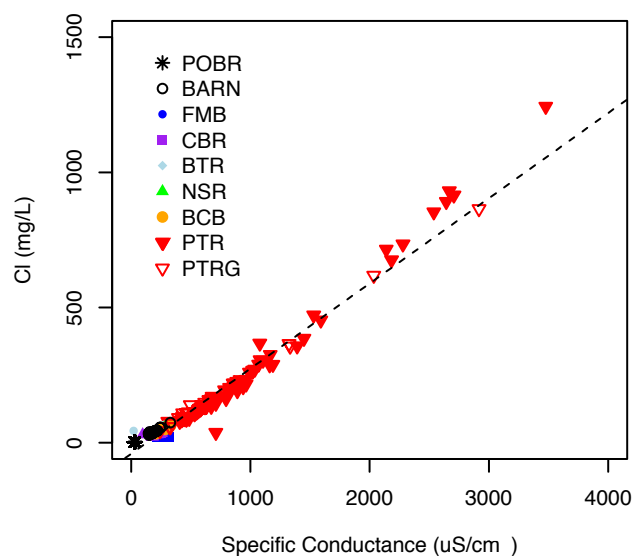


Fig. 7: Plot of conductivity and Cl. Chloride concentrations are approximately 1/3rd of specific conductance. The dashed line is a linear model of the data.

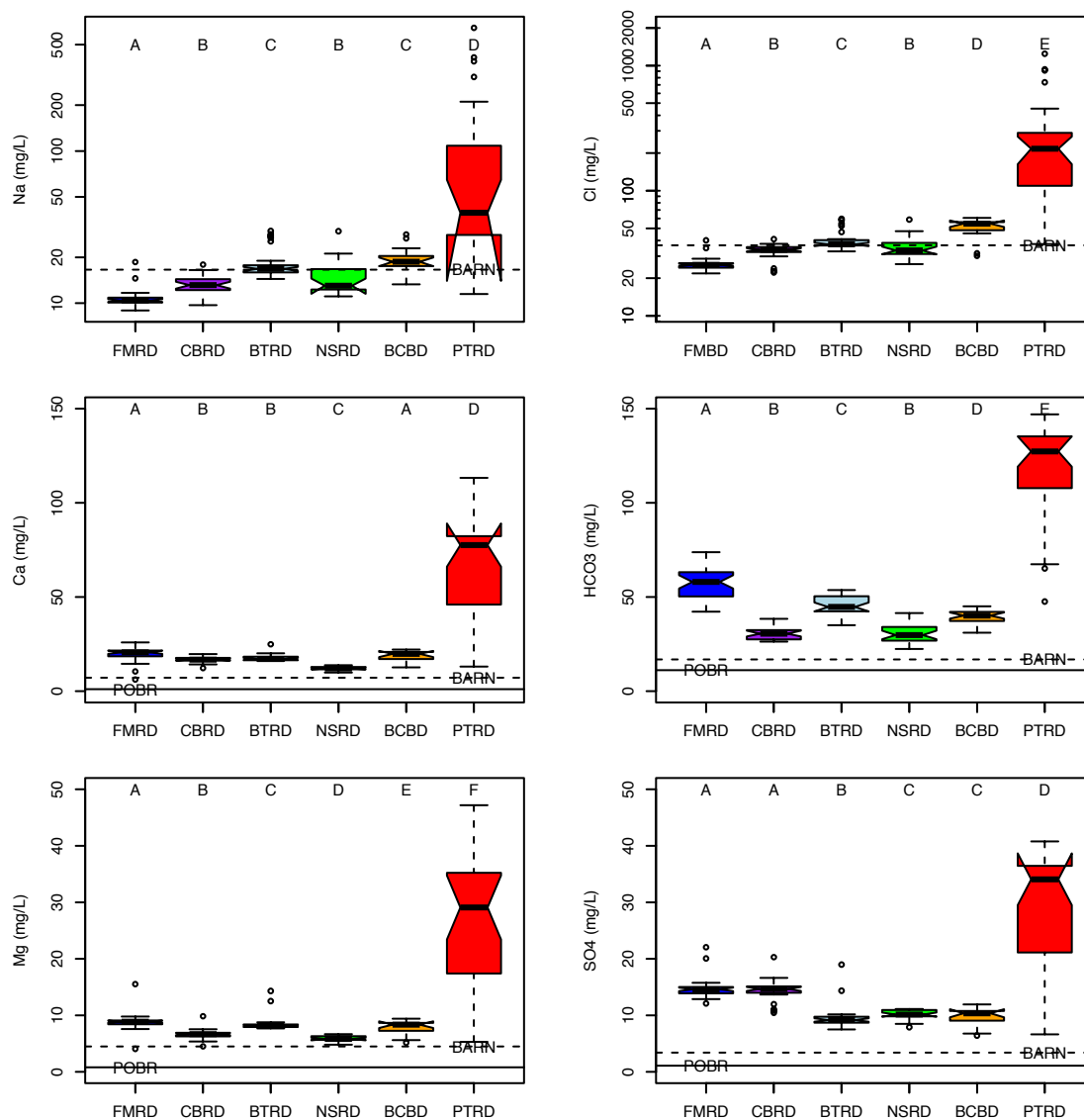


Fig 8: Shows the major cation and anion concentrations (mg/L) during baseflow in the six downstream reaches of the restored sites. Upstream and downstream median concentration differences were largely not significant. POBR and BARN are lines on the plot. K^+ and NO_3^- are not shown; concentrations are available in Table 5 & 6.

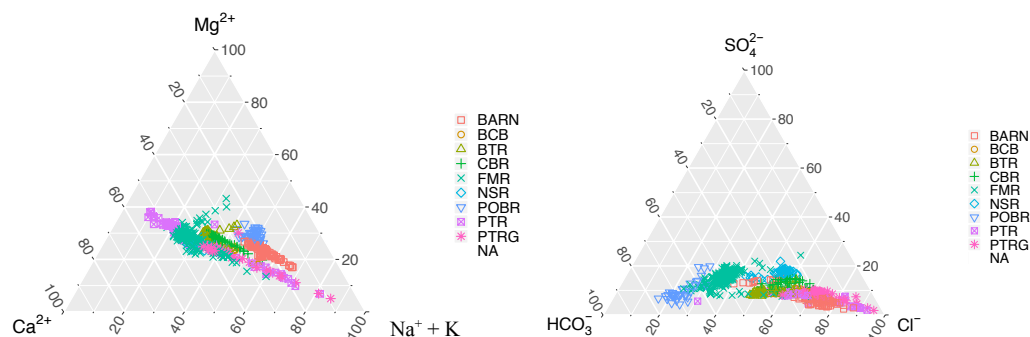


Fig. 9: Ternary diagrams of all sites for baseflow major ions. The figure highlights the baseflow geochemical properties of all sites including controls and regional controls.

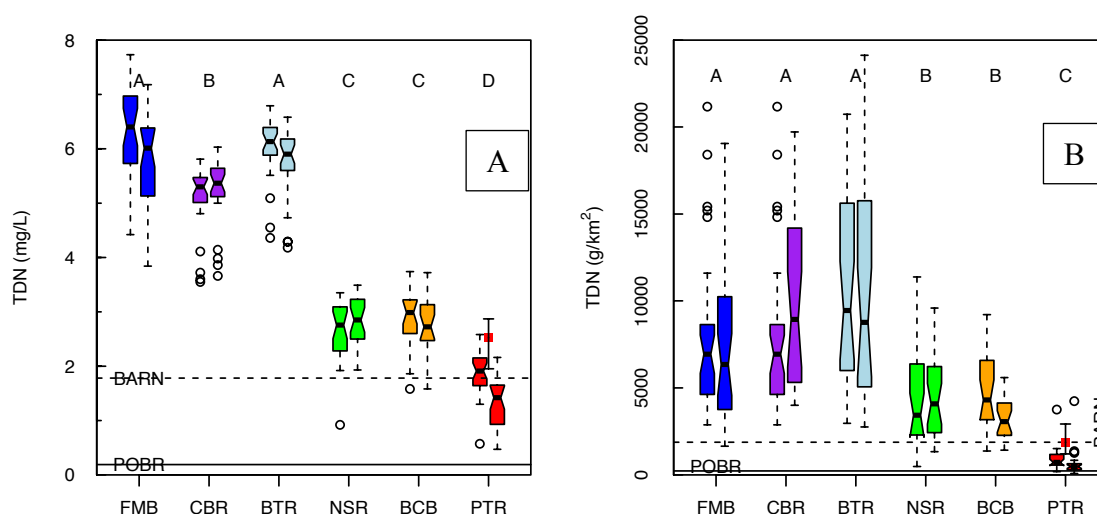


Fig. 10: Concentrations of TDN (mg/L) across the six different upstream and downstream sites during baseflow. [TDN] exist along the agricultural, pasture/suburban/urban gradient with greatest concentrations in the agricultural landscape. Letters along the top of the plot indicate significant differences between sites ($p < 0.05$). Upstream and downstream comparison show no significant changes, except in the most urban setting - PTR. PTRG indicated an increase in median [TDN] from PTRU/D. Median [TDN] values from a 100% forested control site, POBR, are represented by a solid line; median [TDN] values from a 71.7% forested, BARN, site a represented by a dashed line. (B) Load comparison (g/d/km^2) across the six sampled upstream and downstream of the restoration reaches; load was greatest in the agricultural setting, followed by pasture/suburban and urban. Upstream and downstream reaches were not significantly different with the exception of PTR. Downstream regional site PTRG was significantly higher ($p < 0.05$) in TDN load from PTRD. Controls follow the same symbols. Upstream samples are the first boxplots above each stream heading; downstream samples are the second boxplot above each stream heading. Inter-site comparison was completed using only downstream reaches.

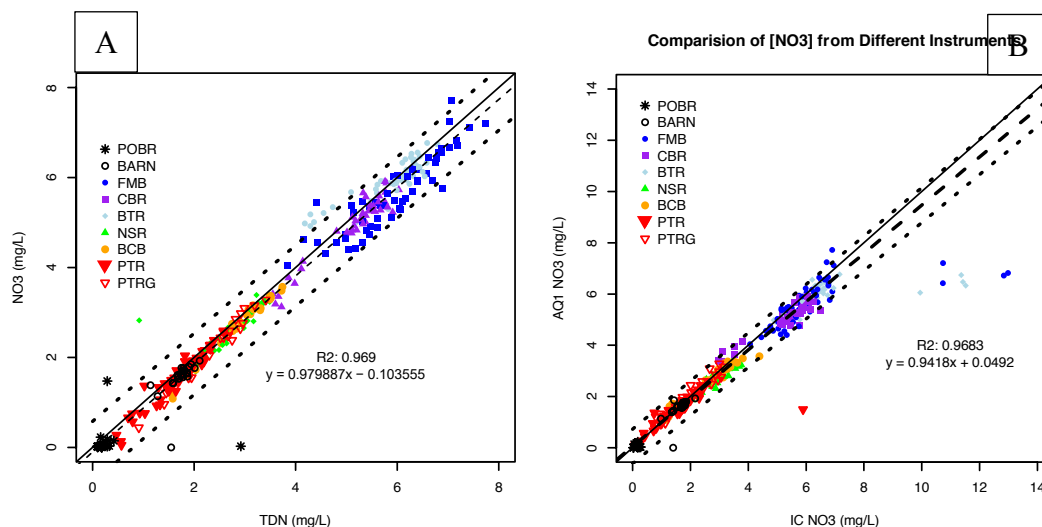


Fig 11: (A) Baseflow TDN and NO_3^- concentrations across the sites through the study period. The plot indicates that TDN almost exclusively moves through the system as NO_3^- during baseflow conditions. A solid 1:1 line represent exact equivalence. A thin dashed line represents the linear model, and the thicker dashed lines encompassing the linear model represent the prediction interval. Prediction intervals indicate the estimated interval that a future observation will fall within that range. (B) Baseflow NO_3^- concentrations from two different instruments AQ1 and the IC across the sites through the study period. The plot indicates the instruments recorded similar values for nitrate. Any data that was not available on one specific instrument could be interchanged with the other. High recorded values for NO_3^- in the IC were from two dates 12/19/2018 and 01/10/2019 only at FMB and BTR. These values were removed from the R^2 and equation. High values are predicted to be user contamination. A solid 1:1 line represent exact equivalence. A dark thicker dashed line represents the linear model, and the thicker dashed lines encompassing the linear model represent the prediction interval.

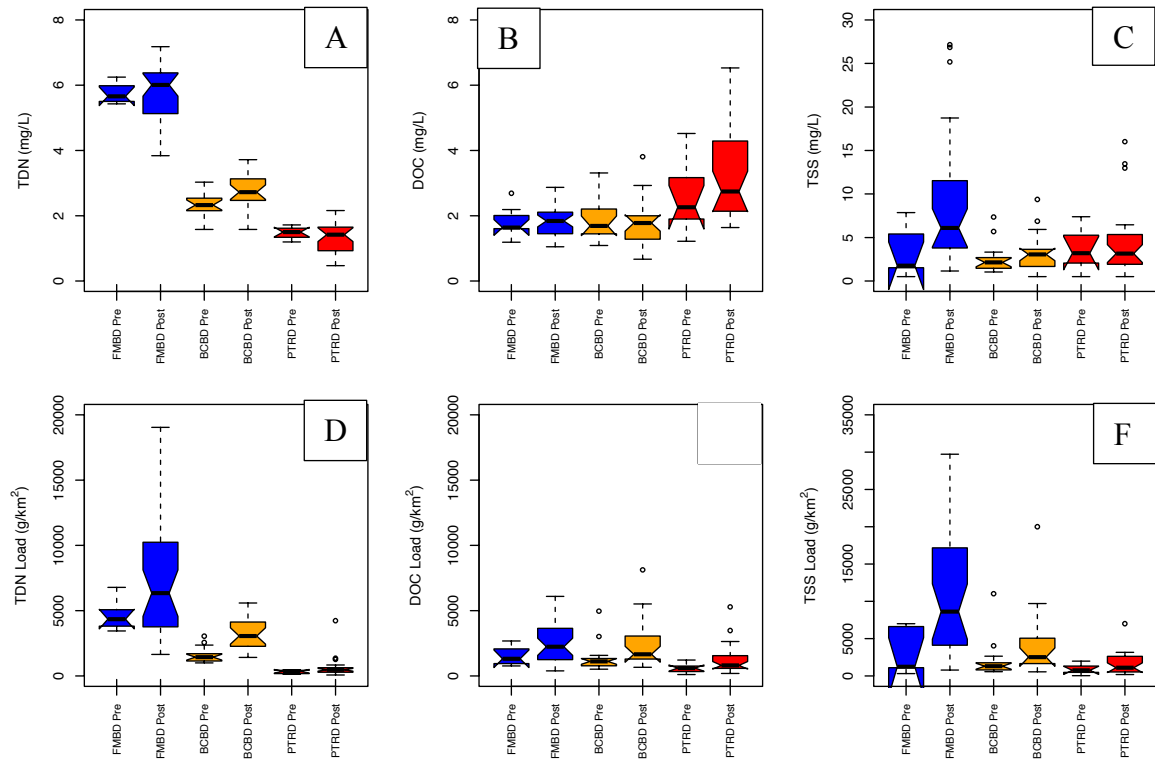


Fig. 12: (A, B, C) Downstream pre and post baseflow restoration for TDN, DOC, and TSS concentrations. There was no significant difference between pre and post restoration values ($p < 0.05$). (D, E, F) Downstream pre and post restorations fluxes normalized to watershed area for TDN, DOC, and TSS. Significant differences ($p < 0.05$) between pre and post restoration values are listed in table 8. FMB and PTR pre-restoration data possessed a small sample size affecting statistical power.

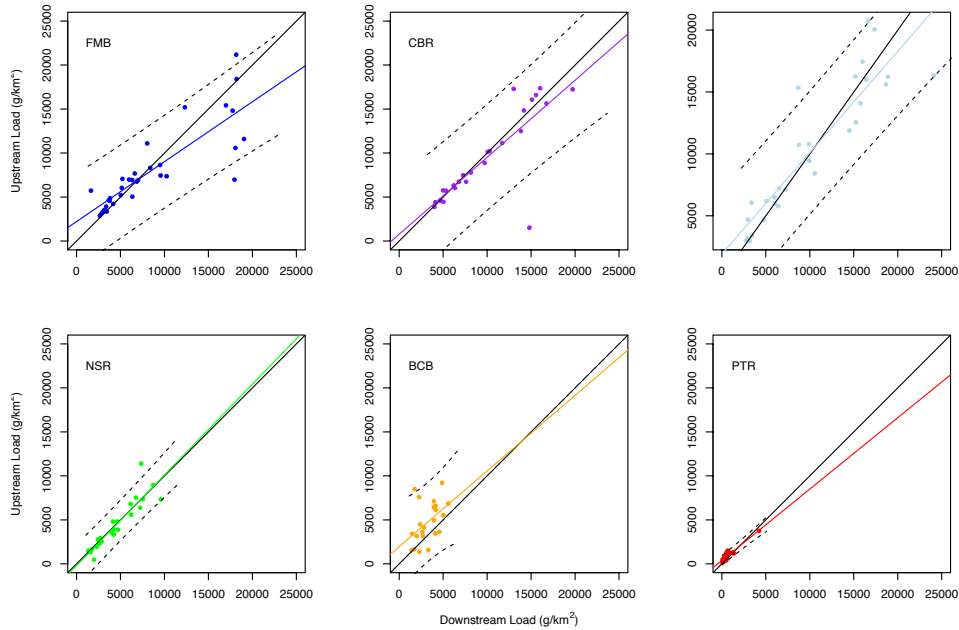


Fig. 13: Indicates the upstream (y-axis) and downstream (x-axis) baseflow daily flux of TDN in g/d/km^2 . A solid 1:1 line represent exact equivalence. A colored solid line represents the linear model, and the dashed lines encompassing the linear model represent the confidence interval. Confidence intervals indicate the upper and lower confidence bounds (95%) from the data. Data that is leaning towards the upstream (y-axis) suggest TDN flux decreases through in the restoration project. Data that is closer towards the downstream (x-axis) suggests that there is an increased daily flux of nitrogen through the restoration project. Outliers are largely the result of measuring soon after storm events.

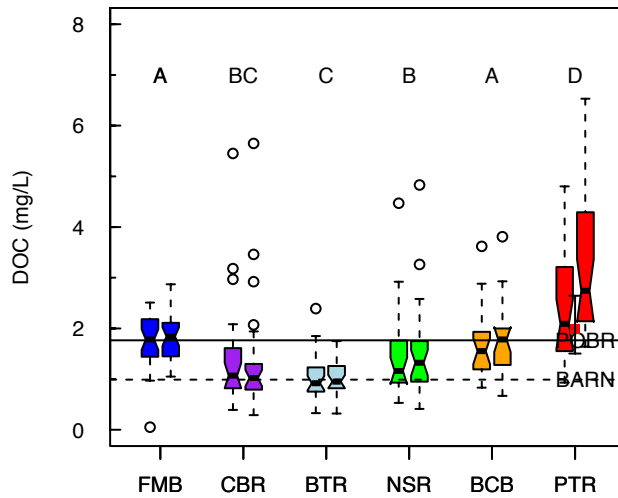


Fig. 14: Baseflow concentrations of DOC (mg/L) across the six upstream and downstream sites. Concentrations across agricultural to suburban sites were within a narrow concentration. Letters at the top of the plot indicate significant differences ($p < 0.05$). PTR (urban) is the exception with higher DOC concentrations relative to the remaining sites. Intra-site comparison yielded little median [DOC] variation between upstream and downstream of the restoration reaches. Again, PTR was the exception with a higher concentration in the downstream reach. PTRG is represented as a red dot and falls within the PTRU/D range. POBR and BARN are represented as their respective lines.

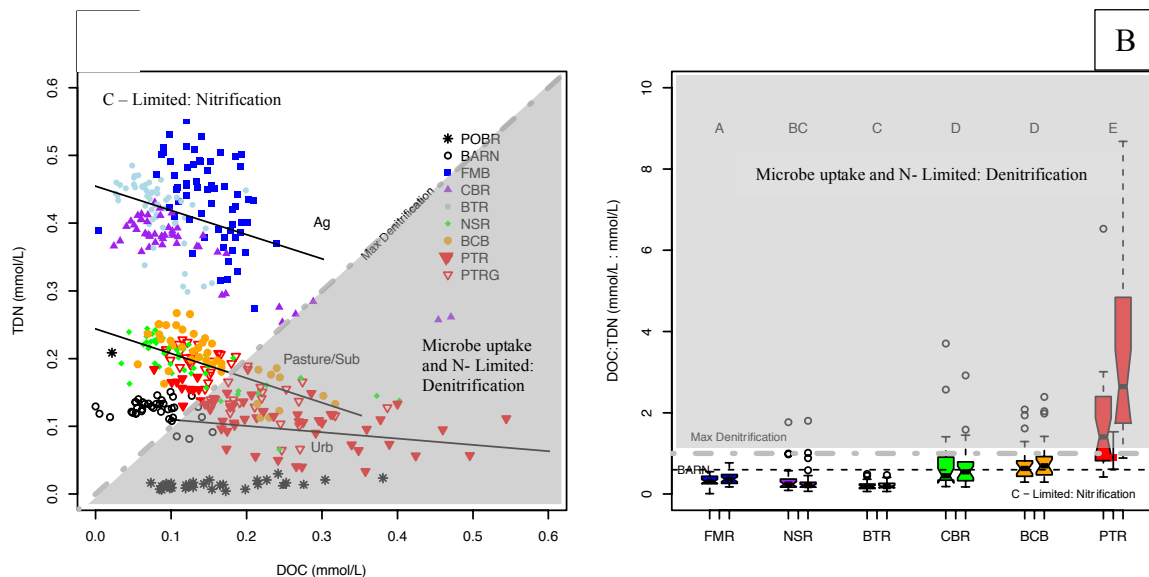


Fig. 15: (A) Baseflow concentration of TDN (mmol/L) to concentration of DOC (mmol/L) of upstream and downstream sampled sites. Sites follow three distinct groupings: agricultural (FMB, EDW, and BTR), pasture/suburban (RIG and BCB), and urban (PTR). PTRG the downstream region site more closely mirrors the suburban landscape with higher [TDN] than the urban site. Controls are also included: BARN is similar to the urban site in [TDN], while containing less [DOC] and POBR is significantly lower in [TDN] concentration. A gray dashed 1:1 line indicates a molar ratio of 1:1 for [DOC]:[TDN]. Research has indicated that increase [DOC] to [TDN] can promote denitrification in these conditions. Increased [TDN] to [DOC] is indicative of nitrogen transport in stream systems. (B) The ratio of DOC (mmol/L) to TDN (mmol/L). Letters at the top of the plot indicate significance between downstream sites. Ratios across the sites vary but are generally below the 1:1 line (grey dashed line) indicating denitrification is limited in these landscape and nitrogen transport is occurring. PTR is the only site that exhibits the conditions for denitrification. Upstream and downstream ratios are not significant, with the exception of FMB, BCB, and PTR where an increase in millimolar ratios is experienced: increased denitrification. PTRG is shown as a red square point - below the denitrification threshold. BARN is shown as a black dashed line more similar to the agricultural and pasture/suburban sites. POBR (not shown) had a median ratio of 11.47 DOC mmol/L:TDN mmol/L – indicative of denitrification. Upstream samples are the first boxplots above each stream heading; downstream samples are the second boxplot above each stream heading. Inter-site comparison was completed using only downstream reaches.

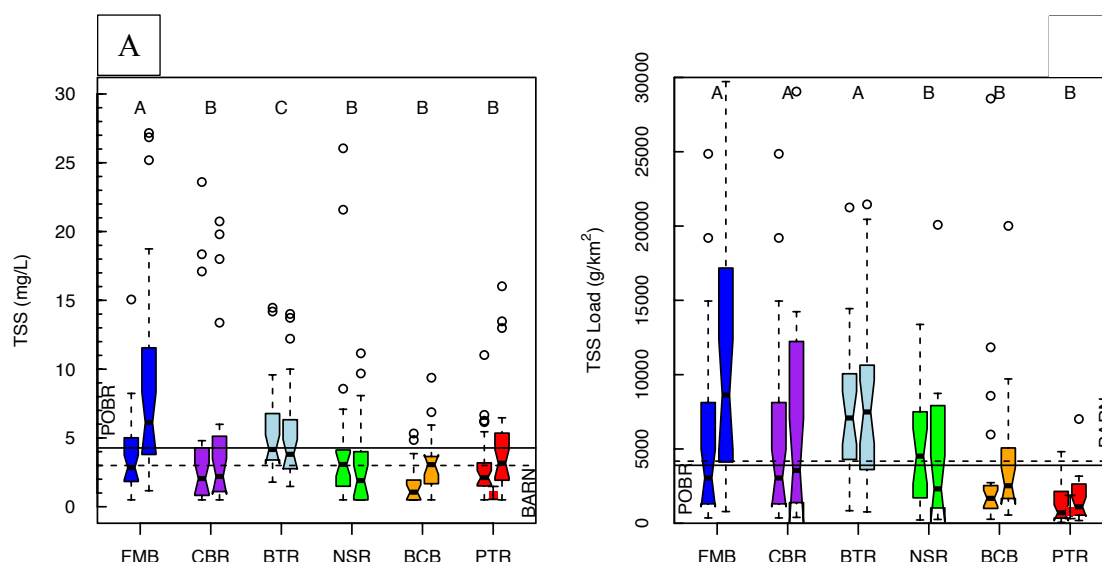


Fig. 16: (A) TSS concentration between sites and upstream and downstream of the restoration locations. Concentrations did not vary substantially between sites; letters at the top of the plot indicate a significant difference between sites ($p < 0.05$). FMB, BCB, and PTR showed a significant ($p < 0.05$) increase between upstream and downstream concentrations. BCB and PTR showed significant increases ($p < 0.05$) in load from upstream to downstream. Extremely high values were removed from the plot. See table 7, 8 and 9 for more details.

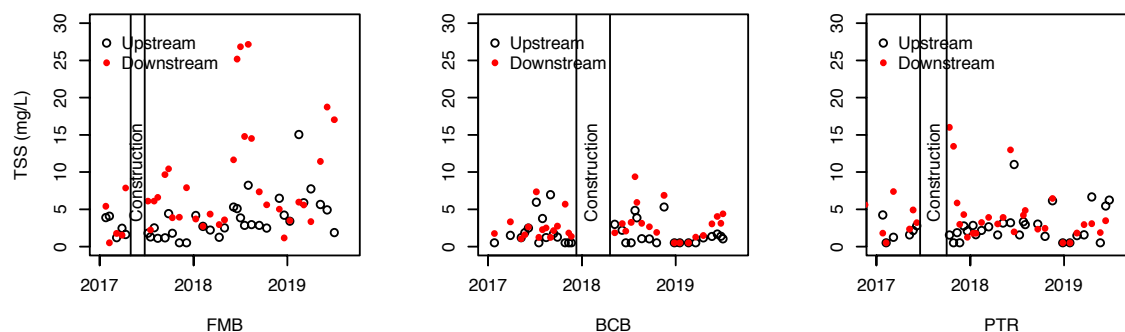


Fig. 17: Time series of TSS (mg/L) shown from pre-post restoration from the three sites restored during the granting period.

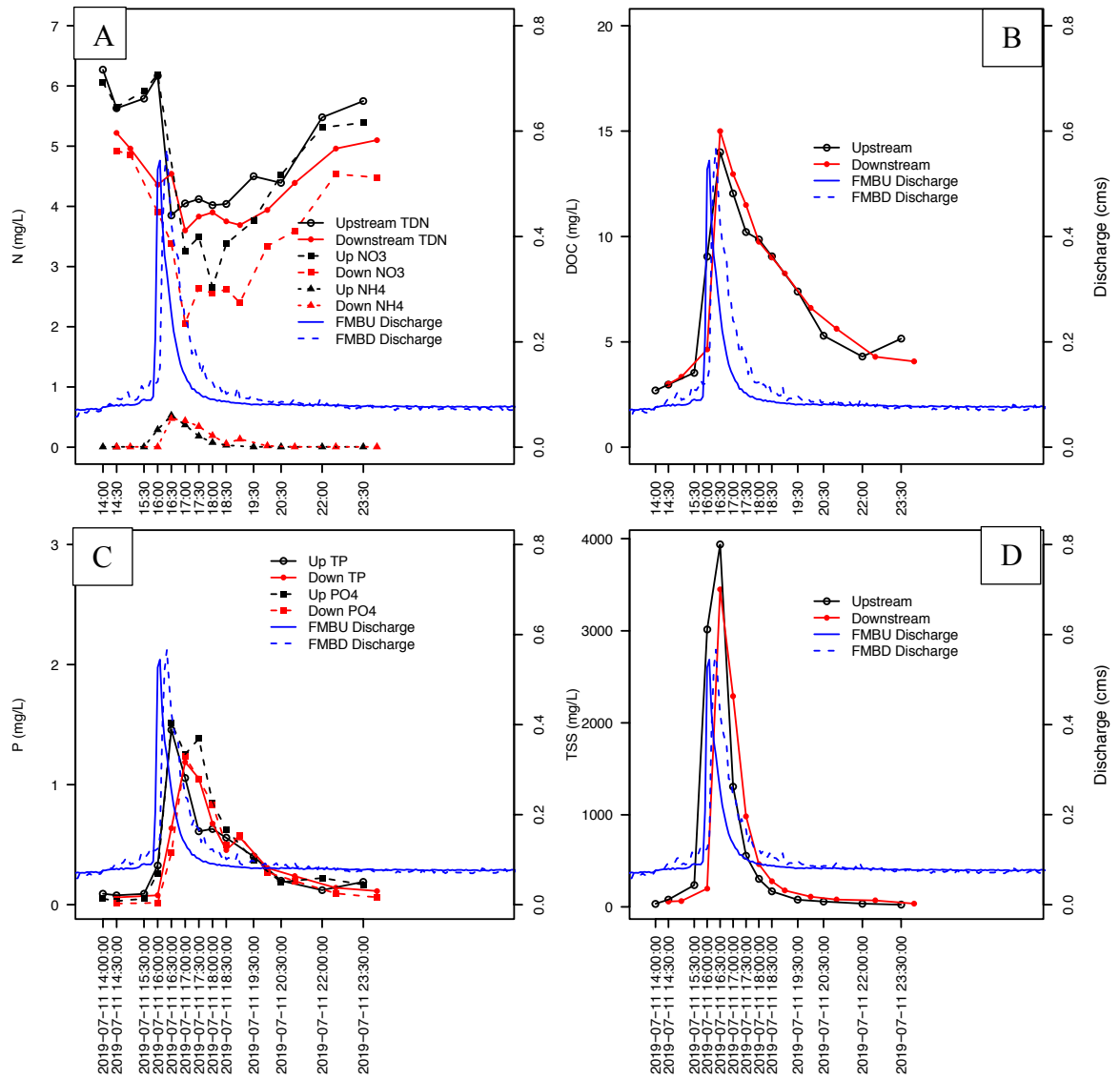


Fig. 18: (A) Nitrogen, (B) DOC, (C) phosphorous, and (D) TSS dynamics through the 07/11/2019 storm.

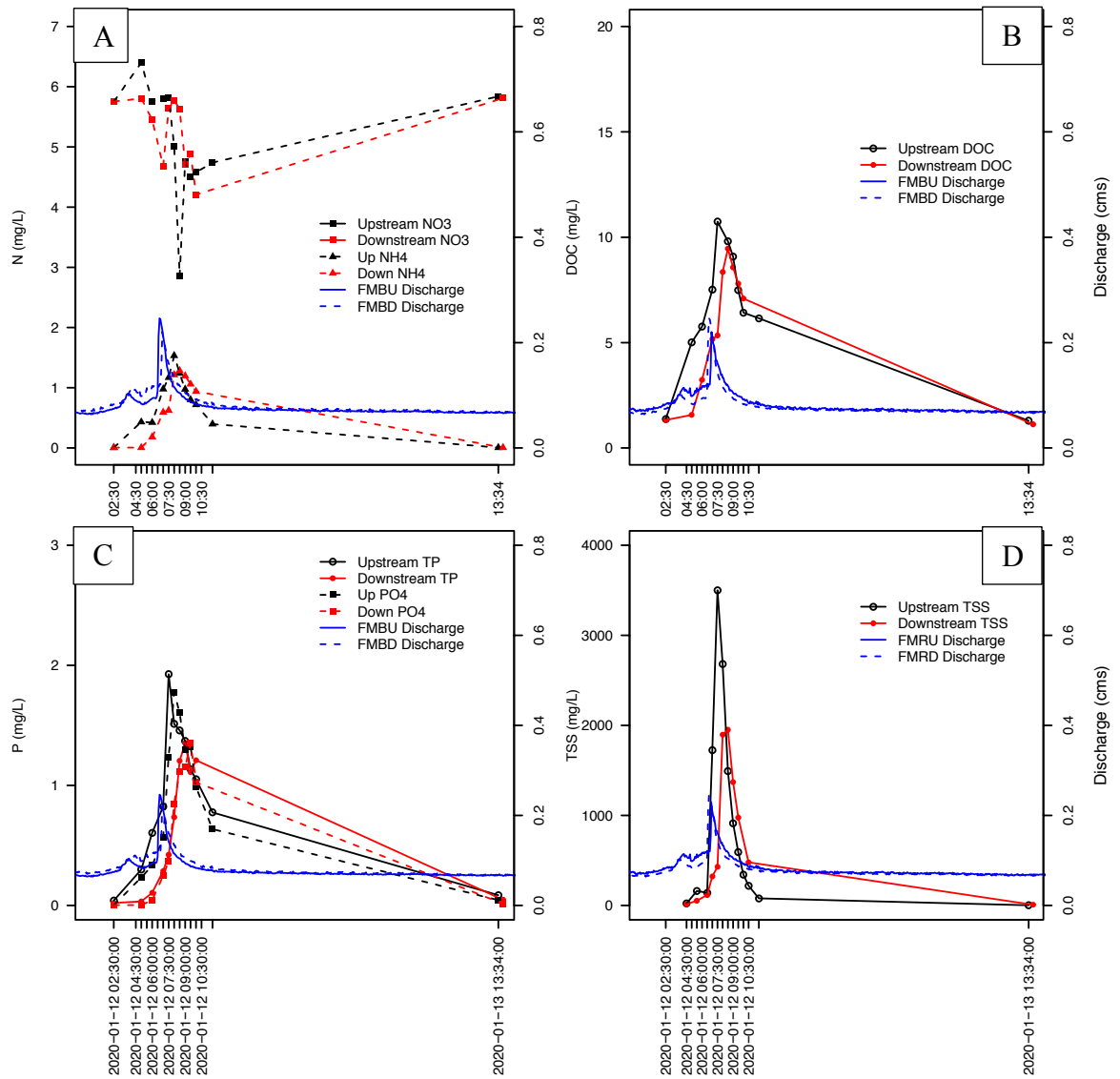


Fig. 19: (A) Nitrogen, (B) DOC, (C) phosphorous, and (D) TSS dynamics through the 01/12/2020 storm.

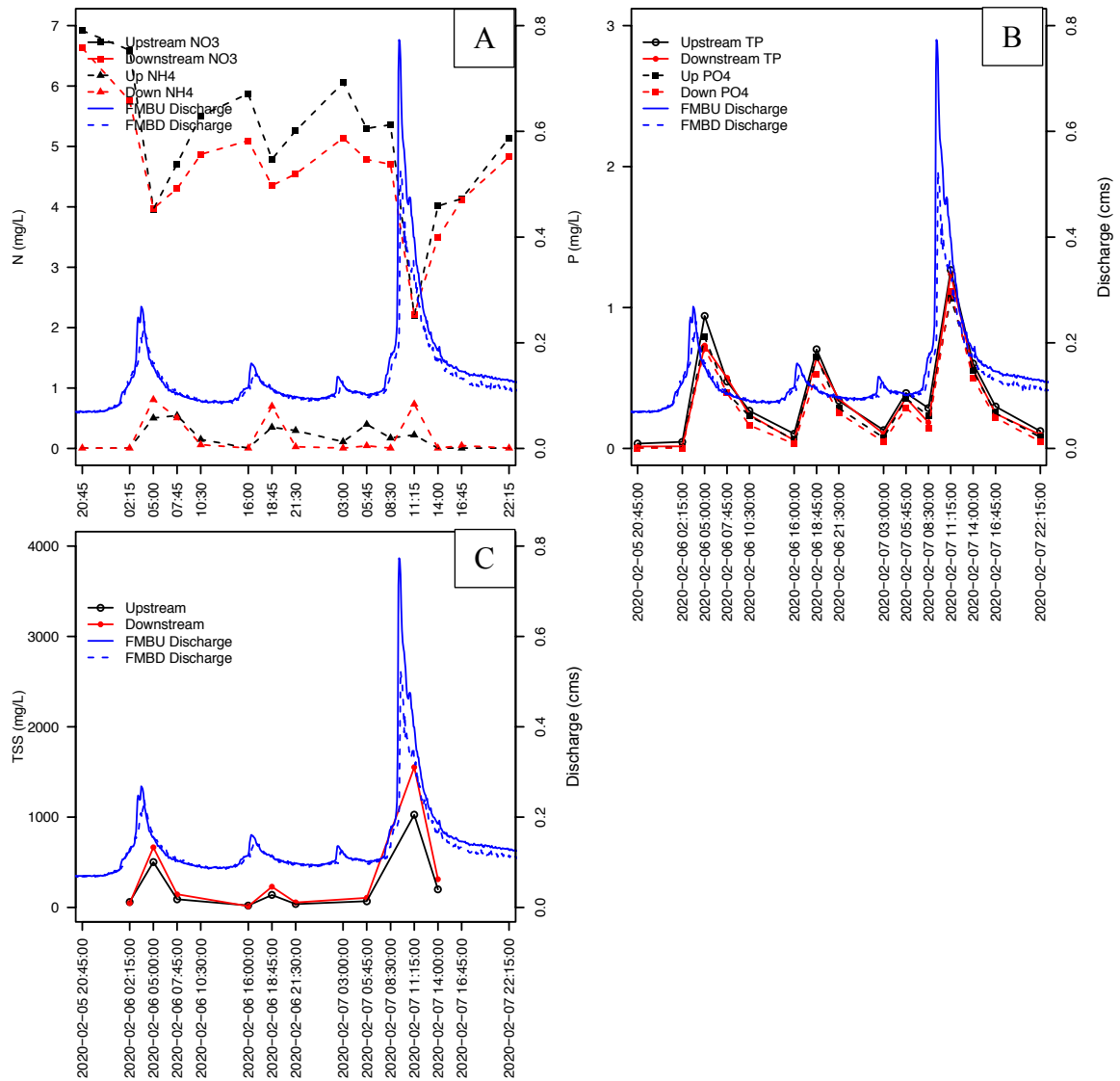


Fig. 20: (A) Nitrogen, (B) phosphorous, and (C) TSS dynamics through the 02/05/2019 storm.

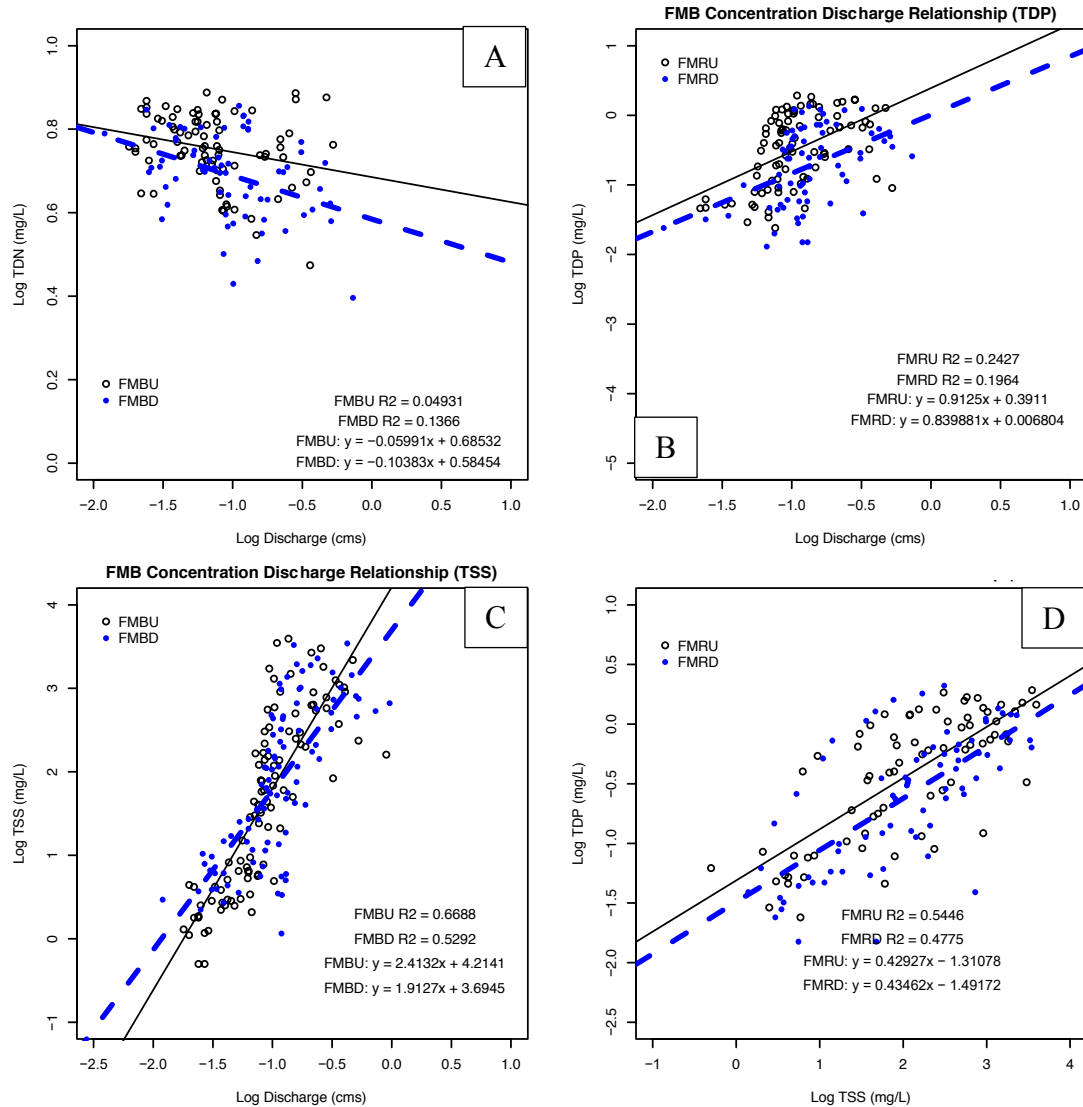


Fig. 21: (A) Concentration-discharge relationships between upstream and downstream sites for TDN. Discharge and concentration were log transformed to create a normal distribution to fit a linear model. The upstream linear model is represented by a solid black line and the downstream linear model is represented by a dashed blue line. (B) Concentration-discharge relationships between upstream and downstream sites for TDP. Discharge and concentration were log transformed to create a normal distribution to fit a linear model. The upstream linear model is represented by a solid black line and the downstream linear model is represented by a dashed blue line. (C) Concentration-discharge relationships between upstream and downstream sites for TSS. Discharge and concentration were log transformed to create a normal distribution to fit a linear model. The upstream linear model is represented by a solid black line and the downstream linear model is represented by a dashed blue line. (D) Concentrations-concentration relationships between upstream and downstream sites for TDP and TSS. Concentrations were log transformed to create a normal distribution to fit a linear model. The upstream linear model is represented by a solid black line and the downstream linear model is represented by a dashed blue line.

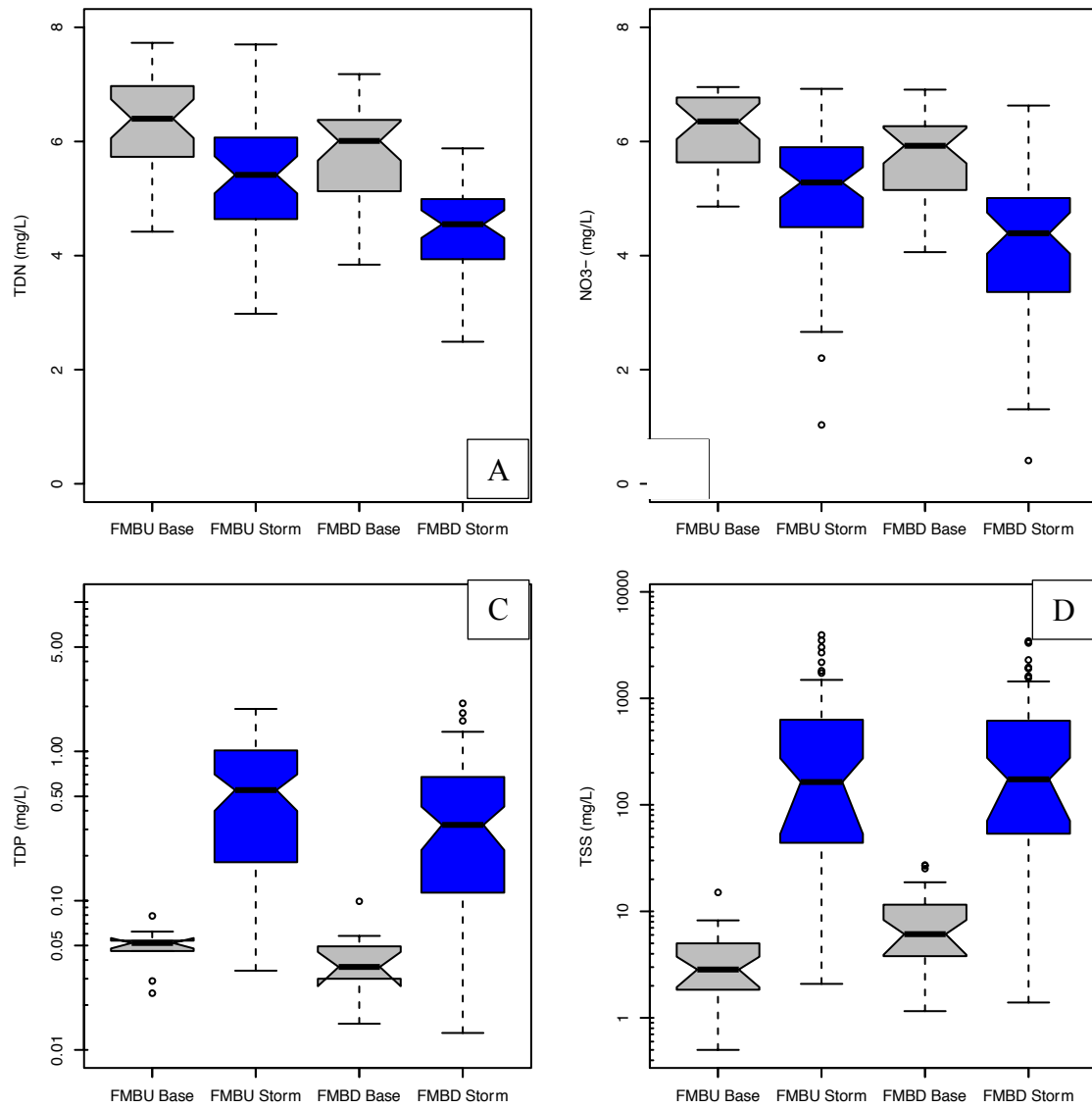


Fig. 22: Boxplots of FMBU/D baseflow (grey) versus stormflow (blue) concentrations. (A) TDN and (B) nitrate dilute during stormflow conditions. (C) TDP and (D) TSS increased by magnitudes during stormflow conditions.

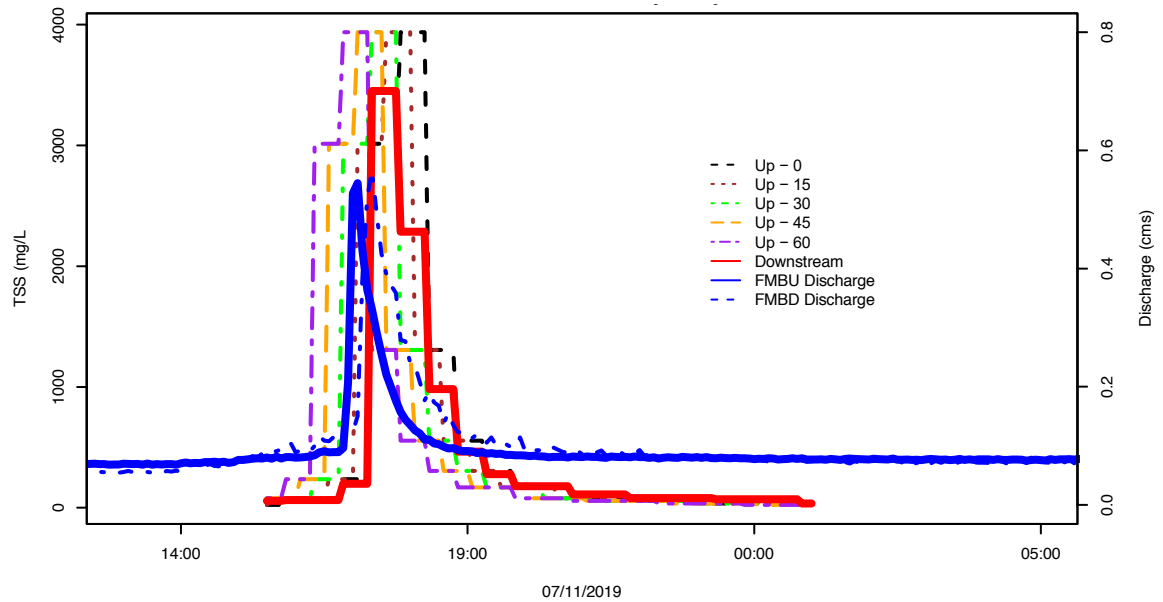


Fig. 23: 07/11/2019 storm TSS plotted to indicate the sensitivity analysis. The legend indicates 0, 15, 30, 45, and 60. These were the minutes that the upstream concentrations were moved back to account for timing errors. The plot only portrays TSS although the analysis covered all parameters. 30 minutes was selected to be the appropriate time step as this was most likely the result of mis-labeling and the ISCO time-steps were 30 minutes.

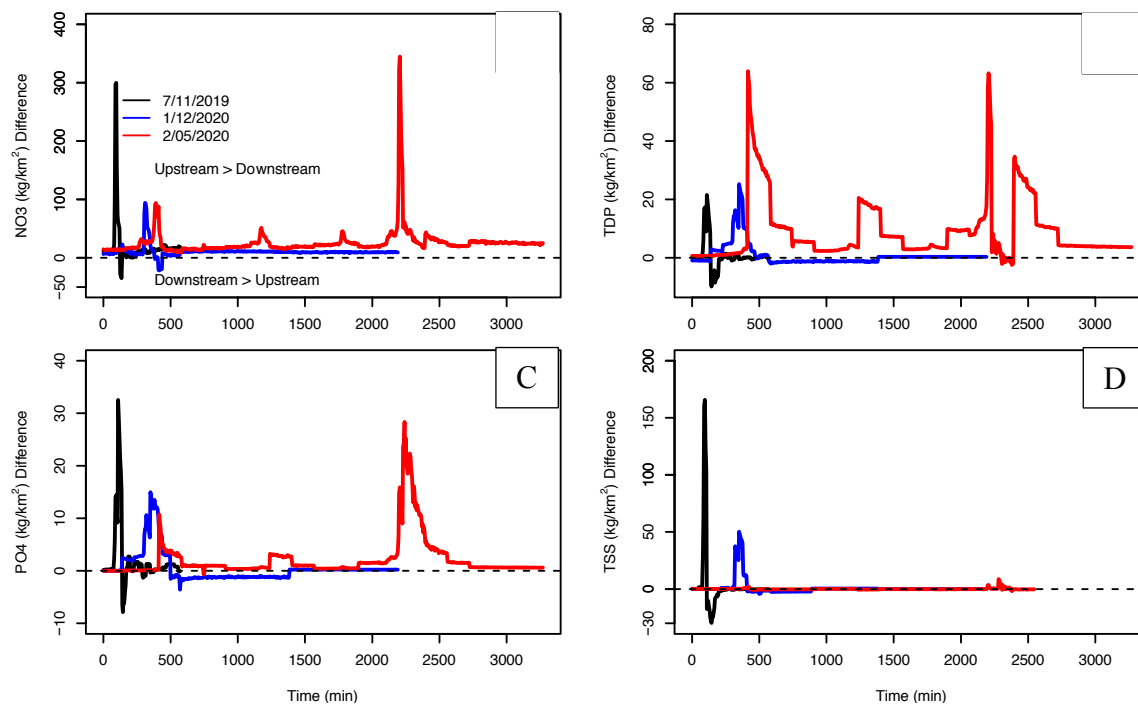


Fig. 24: Three storms load differences, normalized for watershed areas from FMBU/D, are shown in relation to storm length – time (min). Upstream loads were subtracted from paired downstream loads for each five-minute discharge interval. Concentrations were determined from intermittent grab samples and spread over the interval evenly before and after the discrete sample. A positive value indicates upstream loads were greater than downstream loads for that five-minute interval. A negative value indicate that downstream loads were greater than upstream. Largely, all storms for each parameter A) NO₃⁻, B) TDP, C) PO₄⁻, and D) TSS suggest greater incoming loads than downstream export.

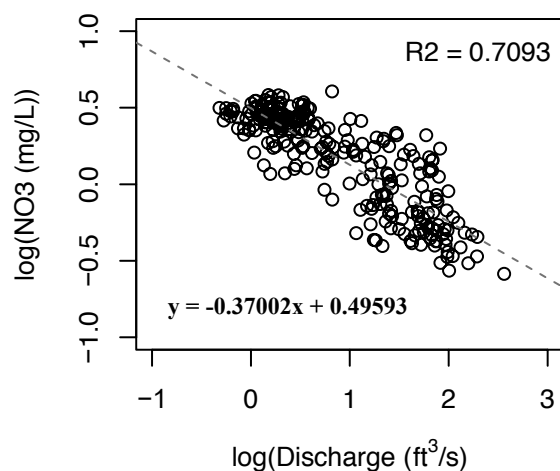


Fig. 25: C-Q relationship for Nitrate and discharge (collected high frequency data from USGS – See table 18 for reference) at PTRG

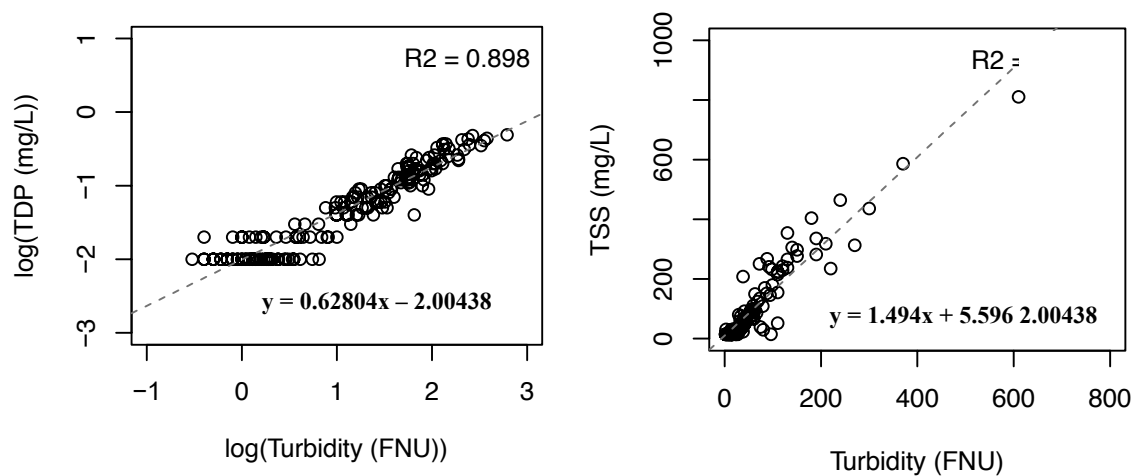


Fig. 26: C-C relationships for TDP & TSS to turbidity (collected high frequency data from USGS – See table 18 for reference) at PTRG.

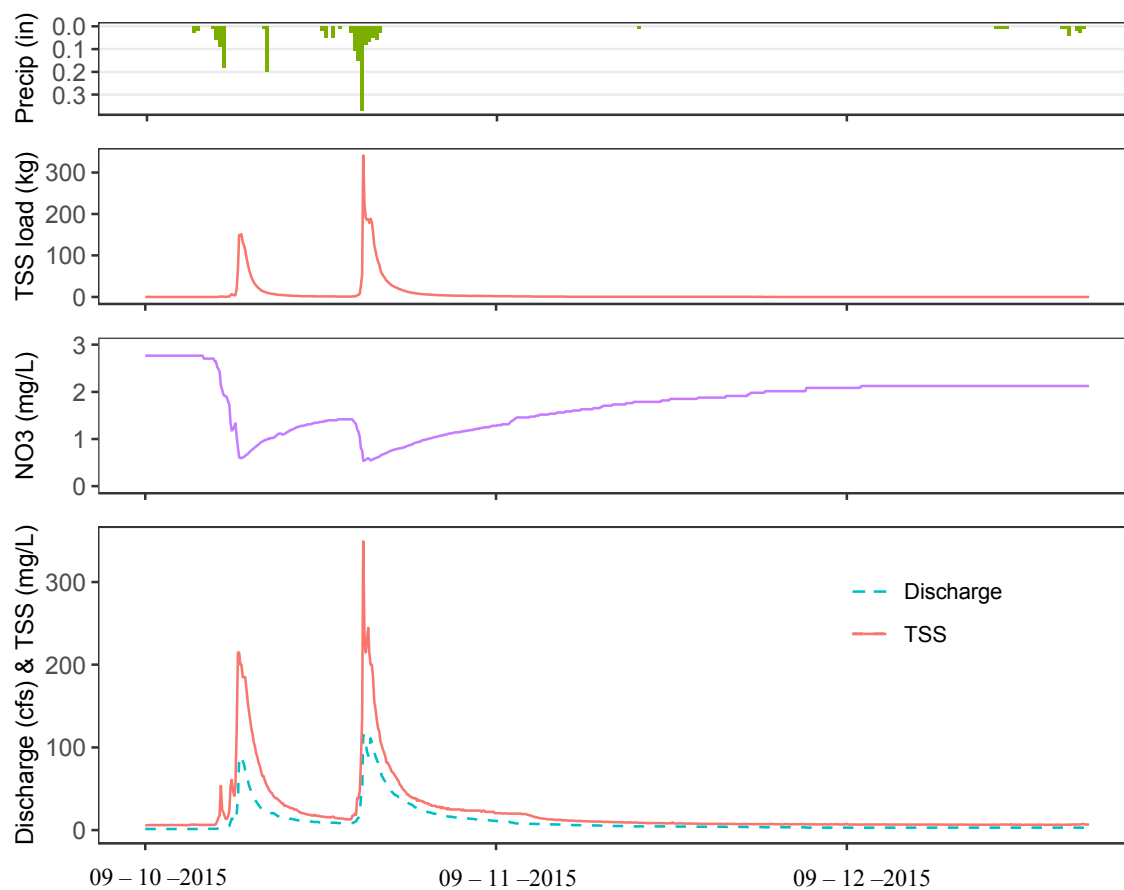


Fig. 27: Example storm timeseries plot (09/10/2015) of high-frequency data derived from concentration curves (Fig 25 & 26) at PTRG.

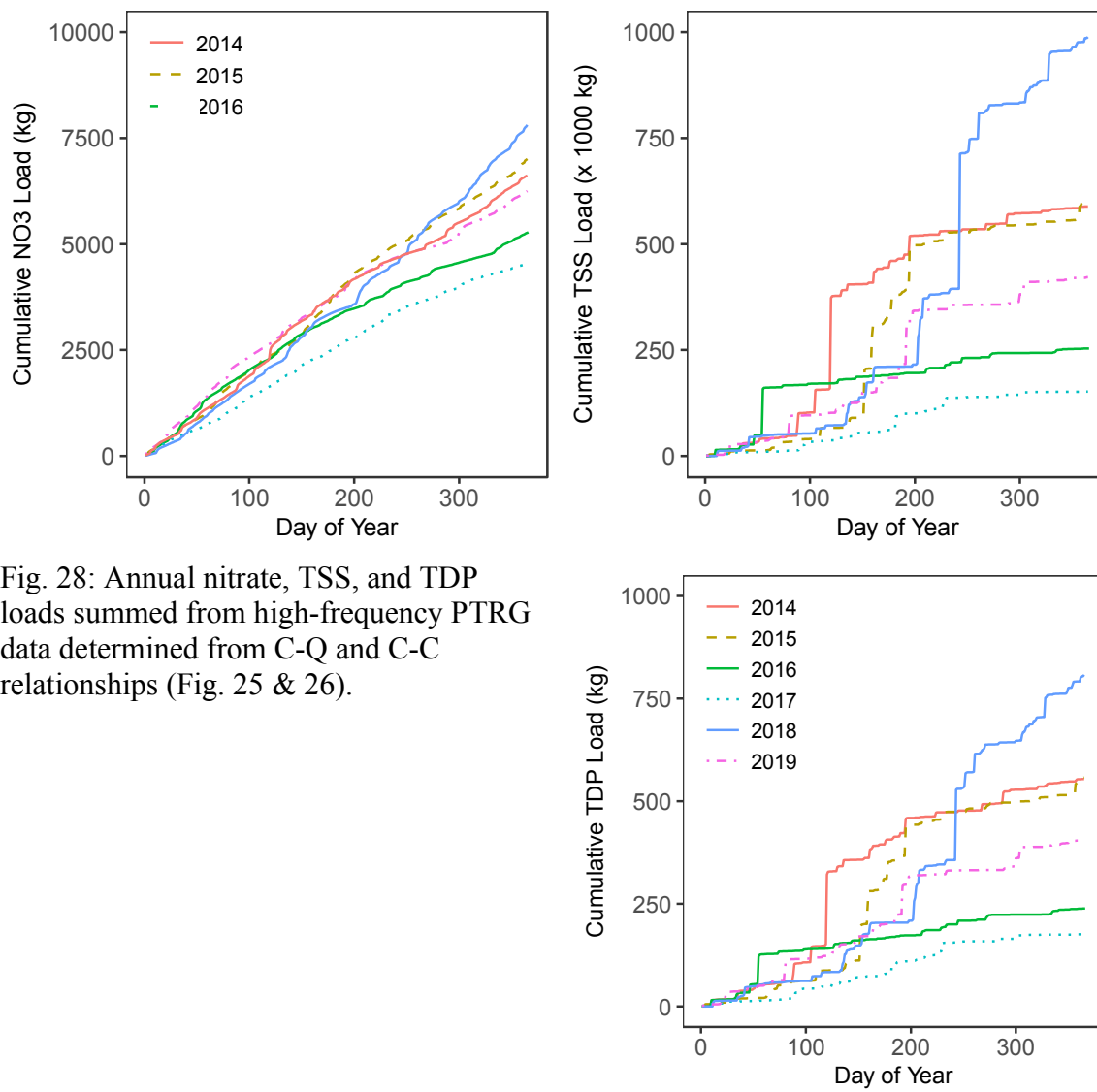


Fig. 28: Annual nitrate, TSS, and TDP loads summed from high-frequency PTRG data determined from C-Q and C-C relationships (Fig. 25 & 26).

8. References

- Aitkenhead-Peterson, J. A., Steele, M. K., Nahar, N., & Santhy, K. (2009). Dissolved organic carbon and nitrogen in urban and rural watersheds of south-central Texas: Land use and land management influences. *Biogeochemistry*, 96(1), 119–129. <https://doi.org/10.1007/s10533-009-9348-2>
- Anon. (2015). Determination of Total Suspended Solids (TSS) and Total Volatile Solids (TVS) in Waters of Fresh / Estuarine / Coastal Waters, 10.
- Ator, S. W., Blomquist, J. D., Webber, J. S., & Chanan, J. G. (2020). Factors driving nutrient trends in streams of the Chesapeake Bay watershed. *Journal of Environmental Quality*, 49(4), 812–834. <https://doi.org/10.1002/jeq2.20101>
- Asmala, E., Autio, R., Kaartokallio, H., Pitkänen, L., Stedmon, C. A., & Thomas, D. N. (2013). Bioavailability of riverine dissolved organic matter in three Baltic Sea estuaries and the effect of catchment land use. *Biogeosciences*, 10(11), 6969–6986. <https://doi.org/10.5194/bg-10-6969-2013>
- Baker, M. E., Schley, M. L., & Sexton, J. O. (2019). Impacts of Expanding Impervious Surface on Specific Conductance in Urbanizing Streams. *Water Resources Research*, 55(8), 6482–6498. <https://doi.org/10.1029/2019WR025014>
- Barnes, R. T., Smith, R. L., & Aiken, G. R. (2012). Linkages between denitrification and dissolved organic matter quality, Boulder Creek watershed, Colorado. *Journal of Geophysical Research: Biogeosciences*, 117(1), 1–14. <https://doi.org/10.1029/2011JG001749>
- Bash, J. S., & Ryan, C. M. (2002). Stream restoration and enhancement projects: Is anyone monitoring? *Environmental Management*, 29(6), 877–885.
- Beechie, T. J., Sear, D. A., Olden, J. D., Pess, G. R., Buffington, J. M., Moir, H., ... Pollock, M. M. (2010). Process-based Principles for Restoring River Ecosystems. *BioScience*, 60(3), 209–222.
- Behnke, J. (1975). A summary of the biogeochemistry of nitrogen compounds in ground water. *Journal of Hydrology*, 27(1–2), 155–167. [https://doi.org/10.1016/0022-1694\(75\)90104-3](https://doi.org/10.1016/0022-1694(75)90104-3)
- Benitez-Nelson, C. R. (2000). The biogeochemical cycling of phosphorus in marine systems. *Earth Science Reviews*, 51(1–4), 109–135.
- Bernhardt, E. S., Palmer, M. A., Allan, J. D., Alexander, G., Barnas, K., Brooks, S., ... Sudduth, E. (2005) Synthesizing U.S. River Restoration. *SCIENCE*, 408.

- Bhattarai, R., Kalita, P. K., & Patel, M. K. (2009). Nutrient transport through a Vegetative Filter Strip with subsurface drainage. *Journal of Environmental Management*, 90(5), 1868–1876. <https://doi.org/10.1016/j.jenvman.2008.12.010>
- Bhuiyan, F., Hey, R. D., & Wormleaton, P. R. (2010). Bank-Attached Vanes for Bank Erosion Control and Restoration of River Meanders. *Journal of Hydraulic Engineering*, 136(9), 583–596. [https://doi.org/10.1061/\(asce\)hy.1943-7900.0000217](https://doi.org/10.1061/(asce)hy.1943-7900.0000217)
- Boesch, D. F., Brinsfield, R. B., & Magnien, R. E. (2001). Chesapeake Bay Eutrophication: Scientific Understanding, Ecosystem Restoration, and Challenges for Agriculture. *Journal of Environmental Quality*, 30, 303–320.
- Booth, D. B., & Jackson, C. R. (1997). Urbanization of Aquatic Systems: Degradation Thresholds, Stormwater Detection, and the Limits of Mitigation. *Journal of the American Water Resources Association*, 33(5), 1077–1090.
- Bratt, A. R., Finlay, J. C., Hobbie, S. E., Janke, B. D., Worm, A. C., & Kemmitt, K. L. (2017). Contribution of Leaf Litter to Nutrient Export during Winter Months in an Urban Residential Watershed. *Environmental Science and Technology*, 51(6), 3138–3147. <https://doi.org/10.1021/acs.est.6b06299>
- Bried, J. T., & Ervin, G. N. (2011). Randomized intervention analysis for detecting non-random change and management impact: Dragonfly examples. *Ecological Indicators*, 11(2), 535–539.
- Brien, P. C. O., & Fleming, T. R. (2019). A Paired Prentice-Wilcoxon Test for Censored Paired Data Published by : International Biometric Society Stable URL : <https://www.jstor.org/stable/2531957> REFERENCES Linked references are available on JSTOR for this article : You may need to log in to JSTO, 43(1), 169–180.
- Brown, K. B. (2001). Urban Stream Restoration Practices: An Initial Assessment. *The Center For Watershed Protection*.
- Burcher, C. L., & Benfield, E. F. (2006). Physical and biological responses of streams to suburbanization of historically agricultural watersheds. *Journal of the North American Benthological Society*, 25(2), 356–369. [https://doi.org/10.1899/0887-3593\(2006\)25\[356:PABROS\]2.0.CO;2](https://doi.org/10.1899/0887-3593(2006)25[356:PABROS]2.0.CO;2)
- Calvi, C., Dapeña, C., Martinez, D. E., & Quiroz Londoño, O. M. (2018). Relationship between electrical conductivity, 18O of water and NO₃ content in different streamflow stages. *Environmental Earth Sciences*, 77(6), 1–12. <https://doi.org/10.1007/s12665-018-7427-1>

- Carpenter, S., Caraco, N., Correll, D. ., Howarth, R. W., Sharples, A. N., & Smith, V. H. (1998). Nonpoint pollution of surface waters with phosphorus and nitrogen. *Ecological Application*, 8, 559–568.
- Carpenter, S. R. ., Frost, T. M. ., Heisey, D., & Kratz, T. K. . (2011). Randomized Intervention Analysis and the Interpretation of Whole-Ecosystem Experiments. *Ecological Society of America*, 70(4), 1142–1152.
- Casey, R. E., Lev, S. M., & Snodgrass, J. W. (2013). Stormwater ponds as a source of long-term surface and ground water salinisation. *Urban Water Journal*, 10(3), 145–153. <https://doi.org/10.1080/1573062X.2012.716070>
- Chesapeake Bay Program. (2018a). 2016–2017 Bay barometer: Health and restoration in the Chesapeake Bay watershed. Edgewater, MD: Chesapeake Bay Program. Retrieved from <https://www.chesapeakebay.net/documents/bay-barometer-v6-web.pdf>
- Conway, T. M. (2007). Impervious surface as an indicator of pH and specific conductance in the urbanizing coastal zone of New Jersey, USA. *Journal of Environmental Management*, 85(2), 308–316. <https://doi.org/10.1016/j.jenvman.2006.09.023>
- Cooper, C. A., Mayer, P. M., & Faulkner, B. R. (2014). Effects of road salts on groundwater and surface water dynamics of sodium and chloride in an urban restored stream. *Biogeochemistry*, 121(1), 149–166. <https://doi.org/10.1007/s10533-014-9968-z>
- Copeland, R., McComas, D., Thorne, C., Soar, P., Jonas, M., & Fripp, J. (2001). Hydraulic design of stream restoration projects. *US Army Corps of Engineers*, (September).
- Coulter, C. B., Kolka, R. K., & Thompson, J. A. (2004). Water quality in agricultural, urban, and mixed land use watersheds. *Journal of the American Water Resources Association*, 40(6), 1593–1601. <https://doi.org/10.1111/j.1752-1688.2004.tb01608.x>
- Craig, L. S., Palmer, M. A., Richardson, D. C., Filoso, S., Bernhardt, E. S., Bledsoe, B. P., ... Wilcock, P. R. (2008). Stream restoration strategies for reducing river nitrogen loads. *Frontiers in Ecology and the Environment*, 6(10), 529–538. <https://doi.org/10.1890/070080>
- Day, T. J. (1977). Field Procedures and Evaluation of a Slug Dilution Gauging Method in Mountain Streams. *Journal of Hydrology New Zealand*.
- Davis, R. T., Tank, J. L., Mahl, U. H., Winikoff, S. G., & Roley, S. S. (2015). The Influence of Two-Stage Ditches with Constructed Floodplains on Water Column

- Nutrients and Sediments in Agricultural Streams. *Journal of the American Water Resources Association*, 51(4), 941–955. <https://doi.org/10.1111/1752-1688.12341>
- De Cicco LA, Lorenz D, Hirsch RM, Watkins W (2018). *dataRetrieval: R packages for discovering and retrieving water data available from U.S. federal hydrologic web services*. doi: [10.5066/P9X4L3GE](https://doi.org/10.5066/P9X4L3GE), al.,
- Derrick, B., White, P., & Toher, D. (2019). Parametric and non-parametric tests for the comparison of two samples which both include paired and unpaired observations. *Journal of Modern Applied Statistical Methods*, 18(1), 1–23. <https://doi.org/10.22237/JMASM/1556669520>
- Diaz, R. J. (2001). Overview of hypoxia around the world. *Journal of Environmental Quality*, 30(2), 275–281.
- Dohner, E., Abby, M., Barbour, M., Simpson, J., Byrne, J., Dates, G., ... Faalasli, E. (1997). Volunteer Stream Monitoring : A Methods Manual., *Environmental Protection*, 1–227.
- Dow, C. L., & Zampella, R. A. (2000). Specific conductance and pH as indicators of watershed disturbance in streams of the New Jersey Pinelands, USA. *Environmental Management*, 26(4), 437–445. <https://doi.org/10.1007/s002670010101>
- Duan, S., Kaushal, S. S., Groffman, P. M., Band, L. E., & Belt, K. T. (2012). Phosphorus export across an urban to rural gradient in the Chesapeake Bay watershed. *Journal of Geophysical Research: Biogeosciences*, 117(1), 1–12.
- Ekka, S. A., Haggard, B. E., Matlock, M. D., & Chaubey, I. (2006). Dissolved phosphorus concentrations and sediment interactions in effluent-dominated Ozark streams. *Ecological Engineering*, 26(4), 375–391. <https://doi.org/10.1016/j.ecoleng.2006.01.002>
- Epstein, D. M., Kelso, J. E., & Baker, M. A. (2016). Beyond the urban stream syndrome: organic matter budget for diagnostics and restoration of an impaired urban river. *Urban Ecosystems*, 19(4), 1623–1643. <https://doi.org/10.1007/s11252-016-0556-y>
- Filoso, S., & Palmer, M. A. (2011). Assessing stream restoration effectiveness at reducing nitrogen export to downstream waters. *Ecological Applications*, 21(6), 1989–2006.
- Filoso, S., Smith, S. M. C., Williams, M. R., & Palmer, M. A. (2015). The Efficacy of Constructed Stream-Wetland Complexes at Reducing the Flux of Suspended Solids to Chesapeake Bay. *Environmental Science and Technology*, 49(15), 8986–8994.
- Fox, R. J., Fisher, T. R., & Gustafson, A. B. (2014). Searching for the missing nitrogen : Biogenic nitrogen gases in groundwater and streams Searching for the missing

- nitrogen : biogenic nitrogen gases in groundwater and streams, (December).
<https://doi.org/10.1017/S0021859614000070>
- Gordon M., W., & John P., M. (1960). Magnitude and Frequency of Forces in Geomorphic Processes. *The Journal of Geology*, 68(1), 54–74.
- Glibert, P. M., Wazniak, C. E., Hall, M. R., & Sturgis, B. (2007). Seasonal and interannual trends in nitrogen and brown tide in Maryland's coastal bays. *Ecological Applications*, 17(5), 79–87.
- Grebliunas, B. D., & Perry, W. L. (2016). The role of C:N:P stoichiometry in affecting denitrification in sediments from agricultural surface and tile-water wetlands. *SpringerPlus*, 5(1). <https://doi.org/10.1186/s40064-016-1820-6>
- Groffman, P. M., Bain, D. J., Band, L. E., Belt, K. T., Grace, S., Grove, J. M., ... Zipperer, W. C. (2003). Down by the riverside: urban riparian ecology, 1(6), 315–321.
- Groffman, P. M., Law, N. L., Belt, K. T., Band, L. E., & Fisher, G. T. (2004). Nitrogen Fluxes and Retention in Urban Watershed Ecosystems. *Ecosystems*, 7(4), 393–403.
- Graeber, D., Gelbrecht, J., Pusch, M. T., Anlanger, C., & von Schiller, D. (2012). Agriculture has changed the amount and composition of dissolved organic matter in Central European headwater streams. *Science of the Total Environment*, 438, 435–446. <https://doi.org/10.1016/j.scitotenv.2012.08.087>
- Gutshall, M. A., & Oberholtzer, W. L. (2011). Floodplain restoration: basics, benefits, and practical applications. *Sustain*, 24(Spring/Summer), 14–23.
- Hadley Wickham, Romain François, Lionel Henry and Kirill Müller (2019). dplyr: A Grammar of Data Manipulation. R package version 0.8.3. <https://CRAN.R-project.org/package=dplyr>
- Hamilton, S. K., Kurzman, A. L., Arango, C., Jin, L., & Robertson, G. P. (2007). Evidence for carbon sequestration by agricultural liming. *Global Biogeochemical Cycles*, 21(2), 1–12. <https://doi.org/10.1029/2006GB002738>
- Haq, S., Kaushal, S. S., & Duan, S. (2018). Episodic salinization and freshwater salinization syndrome mobilize base cations, carbon, and nutrients to streams across urban regions. *Biogeochemistry*, 141(3), 463–486. <https://doi.org/10.1007/s10533-018-0514-2>
- Hatt, B. E., Fletcher, T. D., Walsh, C. J., & Taylor, S. L. (2004). The influence of urban density and drainage infrastructure on the concentrations and loads of pollutants in small streams. *Environmental Management*, 34(1), 112–124. <https://doi.org/10.1007/s00267-004-0221-8>

- Heathwaite, A. L., & Jones, P. J. (1996). Contribution of Nitrogen Species and Phosphorous Fractions to Stream Water Quality in Agricultural Catchments. *Hydrological Processes*, 10, 971–983.
- Helvey, J. D., J. N. Kochenderfer, and P. J. Edwards. "Effects of forest fertilization on selected ion concentrations in central Appalachian streams." *Sugar Maple: Tree and Bole Weights, Volumes, Centers of Gravity, and Logging Residue* 132 (1976): 278.
- Hobbie, S. E., Finlay, J. C., Benjamin, D., Nidzgorski, D. A., Millet, D. B., Lawrence, A., ... Millet, D. B. (2017). Contrasting nitrogen and phosphorus budgets in urban watersheds and implications for managing urban water pollution. *Proceedings of the National Academy of Sciences*, 114(20), E4116–E4116.
- Hope, D., Zhu, W., Gries, C., Oleson, J., Kaye, J., Grimm, N. B., & Baker, L. A. (2005). Spatial variation in soil inorganic nitrogen across an arid urban ecosystem. *Urban Ecosystems*, 8(3–4), 251–273. <https://doi.org/10.1007/s11252-005-3261-9>
- Hupp, C. R., Noe, G. B., Schenk, E. R., & Benthem, A. J. (2013). Recent and historic sediment dynamics along Difficult Run, a suburban Virginia Piedmont stream. *Geomorphology*, 180–181, 156–169.
- Ide, J., Takeda, I., Somura, H., Mori, Y., Sakuno, Y., Yone, Y., & Takahashi, E. (2019). Impacts of Hydrological Changes on Nutrient Transport From Diffuse Sources in a Rural River Basin, Western Japan. *Journal of Geophysical Research: Biogeosciences*, 124(8), 2565–2581. <https://doi.org/10.1029/2018JG004513>
- Imberger, S. J., Cook, P. L. M., Grace, M. R., & Thompson, R. M. (2014). Tracing carbon sources in small urbanising streams: Catchment-scale stormwater drainage overwhelms the effects of reach-scale riparian vegetation. *Freshwater Biology*, 59(1), 168–186. <https://doi.org/10.1111/fwb.12256>
- Jacobson, R. B., & Coleman, D. J. (1986). Stratigraphy and Recent Evolution of Maryland Piedmont Flood Plains. *American Journal of Science*, 286(2), 617–637.
- James, L. A. (2013). Legacy sediment: Definitions and processes of episodically produced anthropogenic sediment. *Anthropocene*, 2, 16–26.
- Jan, Y., Mar, F. E. B., & May, A. P. R. (2020). Baltimore MD Precipitation Baltimore MD Precipitation *** PLEASE NOTE *** Climate data on this page are PRELIMINARY (unofficial). CERTIFIED (official) climate data are available from the National Centers for Environmental Information (NCEI) - <http://www.ncdc.noaa.gov/> *** PLEASE NOTE *** Last updated 7 / 1 / 2020 Baltimore MD Precipitation.
- Janke, B. D., Finlay, J. C., Hobbie, S. E., Baker, L. A., Sterner, R. W., Nidzgorski, D., & Wilson, B. N. (2014). Contrasting influences of stormflow and baseflow pathways

- on nitrogen and phosphorus export from an urban watershed. *Biogeochemistry*, 121(1), 209–228.
- Johnson, L. B., Richards, C., Host, G. E., & Arthur, J. W. (1997). Landscape influences on water chemistry in Midwestern stream ecosystems. *Freshwater Biology*, 37(1), 193–208. <https://doi.org/10.1046/j.1365-2427.1997.d01-539.x>
- Jordan, T. E., Correll, D. L., & Weller, D. E. (1997). and fossil fuel combustion Cambridge, 33(11), 2579–2590.
- Kail, J., Hering, D., Muhar, S., Gerhard, M., & Preis, S. (2007). The use of large wood in stream restoration: Experiences from 50 projects in Germany and Austria. *Journal of Applied Ecology*, 44(6), 1145–1155.
- Kaushal, S. S., Groffman, P. M., Mayer, P. M., Striz, E. A., & Gold, A. J. (2008). Effects of Stream restoration on Denitrification in an Urbanizing Watershed. *Ecological Applications*, 18(3), 789–804.
- Kaushal, S. S., & Belt, K. T. (2012). The urban watershed continuum: Evolving spatial and temporal dimensions. *Urban Ecosystems*, 15(2), 409–435.
- Kemp, W. M., Boynton, W. R., Adolf, J. E., Boesch, D. F., Boicourt, W. C., Brush, G., ... Stevenson, J. C. (2005). Eutrophication of Chesapeake Bay: Historical trends and ecological interactions. *Marine Ecology Progress Series*, 303, 1–29.
- Khamis, K., Bradley, C., & Hannah, D. M. (2018). Understanding dissolved organic matter dynamics in urban catchments: insights from in situ fluorescence sensor technology . *Wiley Interdisciplinary Reviews: Water*, 5(1), e1259. <https://doi.org/10.1002/wat2.1259>
- Knapp, C. W., Dodds, W. K., Wilson, K. C., O'Brien, J. M., & Graham, D. W. (2009). Spatial Heterogeneity of Denitrification Genes in a Highly Homogenous Urban Stream. *Environmental Science and Technology*, 43(12), 4273–4279. <https://doi.org/10.1021/es9001407>
- Koenig, L. E., Shattuck, M. D., Snyder, L. E., Potter, J. D., & McDowell, W. H. (2017). Deconstructing the Effects of Flow on DOC, Nitrate, and Major Ion Interactions Using a High-Frequency Aquatic Sensor Network. *Water Resources Research*, 53(12), 10655–10673. <https://doi.org/10.1002/2017WR020739>
- Kondolf, G. M., & Micheli, E. R. (1995). Evaluating Stream Resoration Projects. *Environmental Management*, 19(1), 1-15.
- Konrad, C. P., Booth, D. B., & Washington. (2002). Hydrologic trends associated with urban development for selected streams in the Puget Sound Basin, Western

- Washington. *Water-Resources Investigations Report ;02-4040*, (vi, 40), vi, 40 .
<https://doi.org/10.1007/s10661-010-1363-1>
- Koskelo, A. I., Fisher, T. R., Sutton, A. J., & Gustafson, A. B. (2018). Biogeochemical storm response in agricultural watersheds of the Choptank River Basin, Delmarva Peninsula, USA. *Biogeochemistry*, 139(3), 215–239. <https://doi.org/10.1007/s10533-018-0464-8>
- Kuhnle, R. A., Bingner, R. L., Alonso, C. V., & Wilson, C. G. (2006). Goodwin Creek Experimental Watershed – Effect of Conservation Practices on Sediment Load, 300(6).
- Lake, P. S., Bond, N., & Reich, P. (2007). Linking ecological theory with stream restoration. *Freshwater Biology*, 52(4), 597–615. <https://doi.org/10.1111/j.1365-2427.2006.01709.x>
- Lambert, T., Pierson-Wickmann, A. C., Gruau, G., Jaffrezic, A., Petitjean, P., Thibault, J. N., & Jeanneau, L. (2014). DOC sources and DOC transport pathways in a small headwater catchment as revealed by carbon isotope fluctuation during storm events. *Biogeosciences*, 11(11), 3043–3056. <https://doi.org/10.5194/bg-11-3043-2014>
- Lammers, R. W., & Bledsoe, B. P. (2017). What role does stream restoration play in nutrient management? *Critical Reviews in Environmental Science and Technology*, 47(6), 335–371. <https://doi.org/10.1080/10643389.2017.1318618>
- Langland, M. J., Duris, J. W., Zimmerman, T. M., & Chaplin, J. J. (2020). *Effects of Legacy Sediment Removal on Nutrients and Sediment in Big Spring Run, Lancaster County, Pennsylvania, 2009-15 U.S. Geological Survey; 2020. Report No.: Scientific Investigations Report 2020-5031.*
- Liang, D., Wang, X., Bockelmann-Evans, B. N., & Falconer, R. A. (2013). Study on nutrient distribution and interaction with sediments in a macro-tidal estuary. *Advances in Water Resources*, 52, 207–220.
- Lepori, F., Palm, D., Brännäs, E., & Malmqvist, B. (2005). Does restoration of structural heterogeneity in streams enhance fish and macroinvertebrate diversity? *Ecological Applications*, 15(6), 2060–2071.
- Letson, David. (1992). Point/Nonpoint Source Pollution Reduction Trading: An Interpretive Survey. *Natural Resources Journal*, 32(2), 219-232.
- Long, D. T., Voice, T. C., Chen, A., Xing, F., & Li, S. G. (2015). Temporal and spatial patterns of Cl⁻ and Na⁺ concentrations and Cl/Na ratios in salted urban watershed. *Elementa*, 3, 1–14. <https://doi.org/10.12952/journal.elementa.000049>

- LaMorte, W. W. (2017). Mann Whitney U Test (Wilcoxon Rank Sum Test). Boston University School of Public Health. https://sphweb.bumc.bu.edu/otlt/mph-modules/bs/bs704_nonparametric/BS704_Nonparametric4.html
- LU, S., HU, H., SUN, Y., & YANG, J. (2009). Effect of carbon source on the denitrification in constructed wetlands. *Journal of Environmental Sciences*, 21(8), 1036–1043. [https://doi.org/10.1016/S1001-0742\(08\)62379-7](https://doi.org/10.1016/S1001-0742(08)62379-7)
- Mallin, M. A., Johnson, V. L., & Ensign, S. H. (2009). Comparative impacts of stormwater runoff on water quality of an urban, a suburban, and a rural stream. *Environmental Monitoring and Assessment*, 159(1–4), 475–491. <https://doi.org/10.1007/s10661-008-0644-4>
- Mark, N. L., Paul, D. A., Keith, W. M., & M. Brian, G. (2002). Does land use affect our streams ? A watershed example from Gwinnett County , Georgia , 1998 – 2001. *US Geological Survey Water Resources Investigation Report 02-4281*, (December), 1998–2001.
- Mattern, K., Lutgen, A., Sienkiewicz, N., Jiang, G., Kan, J., Peipoch, M., & Inamdar, S. (2020). Stream restoration for legacy sediments at gramies run, Maryland: Early lessons from implementation, water quality monitoring, and soil health. *Water (Switzerland)*, 12(8), 1–28. <https://doi.org/10.3390/W12082164>
- Mayer, P. M., Groffman, P. M., Striz, E. A., & Kaushal, S. S. (2010). Nitrogen Dynamics at the Groundwater–Surface Water Interface of a Degraded Urban Stream. *Journal of Environment Quality*, 39(3), 810. <https://doi.org/10.2134/jeq2009.0012>
- McMillan, S. K., & Noe, G. B. (2017). Increasing floodplain connectivity through urban stream restoration increases nutrient and sediment retention. *Ecological Engineering*, 108(March), 284–295. <https://doi.org/10.1016/j.ecoleng.2017.08.006>
- Meals, D. W., Dressing, S. A., & Davenport, T. E. (2010). Lag Time in Water Quality Response to Best Management Practices: A Review. *Journal of Environmental Quality*, 39(1), 85–96. <https://doi.org/10.2134/jeq2009.0108>
- Mendes, M., & Pala, A. (2003). Type I Error Rate and Power of Three Normality Tests, 2(2), 135–139.
- Merritts, D., Walter, R., Rahnis, M., Hartranft, J., Cox, S., Gellis, A., ... Becker, S. (2011). Anthropocene streams and base-level controls from historic dams in the unglaciated mid-Atlantic region, USA. *Philosophical Transactions of the Royal Society A: Mathematical, Physical and Engineering Sciences*, 369(1938), 976–1009.
- Merritts, D., Walter, R., & College, M. (2016). Big Spring Run Legacy Sediment Removal and Aquatic Ecosystem Restoration Project Big Spring Run Before Wetland Restoration.

- Moore, R. D. (2005). Introduction to salt dilution gauging for streamflow measurement Part 3: Slug injection using salt in solution. *Streamline*, 8(4), 1–6.
- Moore, J., Bird, D. L., Dobbis, S. K., & Woodward, G. (2017). Nonpoint Source Contributions Drive Elevated Major Ion and Dissolved Inorganic Carbon Concentrations in Urban Watersheds. *Environmental Science & Technology Letters*, 4(6), 198–204.
- Moore, J., Fanelli, R. M., & Sekellick, A. J. (2020). High-Frequency Data Reveal Deicing Salts Drive Elevated Specific Conductance and Chloride along with Pervasive and Frequent Exceedances of the U.S. Environmental Protection Agency Aquatic Life Criteria for Chloride in Urban Streams. *Environmental Science and Technology*, 54(2), 778–789. <https://doi.org/10.1021/acs.est.9b04316>
- Mouri, G., Shinoda, S., & Oki, T. (2012). Assessing environmental improvement options from a water quality perspective for an urban-rural catchment. *Environmental Modelling and Software*, 32, 16–26. <https://doi.org/10.1016/j.envsoft.2011.11.018>
- Murtaugh, P. A. (2017). Paired Intervention Analysis in Ecology. *Journal of Agricultural , Biological , and Environmental Statistics*, 5(3), 280–292.
- National Pollution Discharge Elimination System (NPDES). (1978). Phosphorous, all Forms (colorimetric, ascorbic acid, two reagent). *Method 365.3*, 3–7.
- Newcomer Johnson, T. A., Kaushal, S. S., Mayer, P. M., & Grese, M. M. (2014). Effects of stormwater management and stream restoration on watershed nitrogen retention. *Biogeochemistry*, 121(1), 81–106. <https://doi.org/10.1007/s10533-014-9999->
- Oh, N., & Raymond, P. A. (2006). Contribution of agricultural liming to riverine bicarbonate export and CO₂ sequestration in the Ohio River basin, 20(August), 1–17. <https://doi.org/10.1029/2005GB002565>
- Olaru, M., Șandru, M., & Pirnea, I. C. (2014). Monte Carlo Method Application for Environmental Risks Impact Assessment in Investment Projects. *Procedia - Social and Behavioral Sciences*, 109, 940–943.
- Orihel, D. M., Baulch, H. M., Casson, N. J., North, R. L., Parsons, C. T., Seckar, D. C. M., & Venkiteswaran, J. J. (2017). Internal phosphorus loading in Canadian fresh waters: a critical review and data analysis. *Canadian Journal of Fisheries and Aquatic Sciences*, 2029(September), 1–25.
- Palmer, M. A., Filoso, S., & Fanelli, R. M. (2014). From ecosystems to ecosystem services: Stream restoration as ecological engineering. *Ecological Engineering*, 65, 62–70. <https://doi.org/10.1016/j.ecoleng.2013.07.059>

- Palmer, M. A., Hondula, K. L., & Koch, B. J. (2014). Ecological Restoration of Streams and Rivers: Shifting Strategies and Shifting Goals. *Annual Review of Ecology, Evolution, and Systematics*, 45(1), 247–269.
- Paul, M. J., & Meyer, J. L. (2009). Streams in the Urban Landscape. *Ecology*, 32(2001), 333–365.
- Petrone, K. C. (2010). Catchment export of carbon, nitrogen, and phosphorus across an agro-urban land use gradient, Swan-Canning River system, southwestern Australia. *Journal of Geophysical Research*, 115(G1), G01016.
- Petrone, K. C., Fellman, J. B., Hood, E., Donn, M. J., & Grierson, P. F. (2011). The origin and function of dissolved organic matter in agro-urban coastal streams. *Journal of Geophysical Research: Biogeosciences*, 116(1).
<https://doi.org/10.1029/2010JG001537>
- Radtke, B. D. B., Wilde, F. D., Davis, J. V., & Popowski, T. J. (1998). 6.6 Alkalinity and Acid Neutralizing Capacity. *USGS TWRI Book 9*, 1–33.
- Raymond, P. A., & Bauer, J. E. (2001). Use of ^{14}C and ^{13}C natural abundances for evaluating riverine, estuarine, and coastal DOC and POC sources and cycling: A review and synthesis. *Organic Geochemistry*, 32(4), 469–485.
[https://doi.org/10.1016/S0146-6380\(00\)00190-X](https://doi.org/10.1016/S0146-6380(00)00190-X)
- Reynolds, L. V. (2020). Guidance for Stream Restoration, (September).
- Roni, P., Beechie, T. J., Bilby, R. E., Leonetti, F. E., Pollock, M. M., & Pess, G. R. (2002). A Review of Stream Restoration Techniques and a Hierarchical Strategy for Prioritizing Restoration in Pacific Northwest Watersheds. *North American Journal of Fisheries Management*, 22(1), 1–20.
- Rose, L. A., Karwan, D. L., & Godsey, S. E. (2018). Concentration–discharge relationships describe solute and sediment mobilization, reaction, and transport at event and longer timescales. *Hydrological Processes*, 32(18), 2829–2844.
<https://doi.org/10.1002/hyp.13235>
- RStudio Team (2019). RStudio: Integrated Development for R. RStudio, Inc., Boston, MA URL <http://www.rstudio.com/>.
- Sandström, S., Futter, M. N., Kyllmar, K., Bishop, K., O’Connell, D. W., & Djodjic, F. (2020). Particulate phosphorus and suspended solids losses from small agricultural catchments: Links to stream and catchment characteristics. *Science of the Total Environment*, 711. <https://doi.org/10.1016/j.scitotenv.2019.134616>
- Schueler, T. R. (1994). The Importance of Imperviousness. *Watershed Protection Techniques*, 1(3), 100–111.

- Scudlark, J. R., Russell, K. M., Galloway, J. N., Church, T. M., & Keene, W. C. (1998). MID-ATLANTIC U . S . COAST — METHODS EVALUATION AND PRELIMINARY MEASUREMENTS, 32(10).
- Shields, C. A., Band, L. E., Law, N., Groffman, P. M., Kaushal, S. S., Savvas, K., ... Belt, K. T. (2008). Streamflow distribution of non-point source nitrogen export from urban-rural catchments in the Chesapeake Bay watershed. *Water Resources Research*, 44(9), 1–13.
- Shier, R. (2004). The Wilcoxon signed rank sum test, 5–7.
- Smith, R. M., Kaushal, S. S., Beaulieu, J. J., Pennino, M. J., & Welty, C. (2017). Influence of infrastructure on water quality and greenhouse gas dynamics in urban streams. *Biogeosciences*, 14(11), 2831–2849. <https://doi.org/10.5194/bg-14-2831-2017>
- Standard Methods for the Examination of Water and Waste Water (2005). Method 2540 D, APHA, 21st Edition.
- Stanley, E. H., Powers, S. M., Lottig, N. R., Buffam, I., & Crawford, J. T. (2012). Contemporary changes in dissolved organic carbon (DOC) in human-dominated rivers: Is there a role for DOC management? *Freshwater Biology*, 57(SUPPL. 1), 26–42. <https://doi.org/10.1111/j.1365-2427.2011.02613.x>
- Steele, M. S., Governor, L., Jensen, W. P., & Secretary, D. (2004). State of Maryland ' s Comprehensive Water Monitoring Strategy, (September).
- Sweet, W., Dusek, G., Marcy, D., Carbin, G., & Marra, J. (2019). 2018 State of U.S. High Tide Flooding with a 2019 Outlook, (June), 23.
- Taylor, P. G., & Townsend, A. R. (2010). Stoichiometric control of organic carbon-nitrate relationships from soils to the sea. *Nature*, 464(7292), 1178–1181. <https://doi.org/10.1038/nature08985>
- Teufl, B., Weigelhofer, G., Fuchsberger, J., & Hein, T. (2013). Effects of hydromorphology and riparian vegetation on the sediment quality of agricultural low-order streams: Consequences for stream restoration. *Environmental Science and Pollution Research*, 20(3), 1781–1793. <https://doi.org/10.1007/s11356-012-1135-2>
- Thompson, D. M. (2008). The influence of lee sediment behind large bed elements on bedload transport rates in supply-limited channels, 99, 420–432. <https://doi.org/10.1016/j.geomorph.2007.12.004>
- Thompson, S. E., Basu, N. B., Lascrain, J., Aubeneau, A., & Rao, P. S. C. (2011). Relative dominance of hydrologic versus biogeochemical factors on solute export

- across impact gradients. *Water Resources Research*, 47(7), 1–20.
<https://doi.org/10.1029/2010WR009605>
- Trimble, S. W. (1997). Contribution o stream channel erosion to sediment yield from an urbanizing watershed. *Science*, 278(21 Nov.), 1442–1444.
- U. S. Environmental Protection Agency. (1971). Total Suspended Solids (TSS): EPA Method 160.2 (Gravimetric, Dried at 103-105 Degrees C), (Issued), 7–9.
- U.S. EPA (United States Environmental Protection Agency). (2000). The Quality of Our Nations Waters. 1998 Report to Congress, 1–20.
- Van Meter, K. J., & Basu, N. B. (2015). Catchment legacies and time lags: A parsimonious watershed model to predict the effects of legacy storage on nitrogen export. *PLoS ONE*, 10(5), 1–22. <https://doi.org/10.1371/journal.pone.0125971>
- Vanni, M. J., Renwick, W. H., Jenifer, L., Auch, J. D., & Schaus, M. H. (2001). Dissolved and particulate nutrient flux from three adjacent agricultural watersheds : A five-year study, 85–114.
- Vervier, P., Dobson, M., & Pinay, G. (1993). Role of interaction zones between surface and ground waters in DOC transport and processing: considerations for river restoration. *Freshwater Biology*, 29(2), 275–284. <https://doi.org/10.1111/j.1365-2427.1993.tb00763.x>
- Voli, M., Merritts, D., Walter, R., Ohlson, E., Datin, K., Rahnis, M., ... Hartranft, J. (2009). A New Paradigm for Water Resources Management. *American Resources Association*, 11(5).
- Volk, J. A., Savidge, K. B., Scudlark, J. R., Andres, A. S., & Ullman, W. J. (2006). Nitrogen Loads through Baseflow, Stormflow, and Underflow to Rehoboth Bay, Delaware, 1755, 1742–1755. <https://doi.org/10.2134/jeq2005.0373>
- Walsh, C. J., Roy, A. H., Feminella, J. W., Cottingham, P. D., Peter, M., & Ii, R. P. M.(2005). The urban stream syndrome : current knowledge and the search for a cure The urban stream syndrome : current knowledge and, 24(3), 706–723.
- Walter, R. C., & Merritts, D. J. (2008). Natural Streams and the legacy of water-powered mills. *American Association for the Advancement of Science*, 319(5861), 299–304.
- Ward, C. P., Nalven, S. G., Crump, B. C., Kling, G. W., & Cory, R. M. (2017). Photochemical alteration of organic carbon draining permafrost soils shifts microbial metabolic pathways and stimulates respiration. *Nature Communications*, 8(1), 1–7. <https://doi.org/10.1038/s41467-017-00759-2>

- Weigmann, D. L., Helfrich, L. A., & Downey, D. M. (1993). Guidelines for Liming Acidified Streams and Rivers.
- Wild, C. (1988). The Wilcoxon Rank-Sum Test, 2, 1–10.
- Williams, M. R., Bhatt, G., Filoso, S., & Yactayo, G. (2017). Stream Restoration Performance and Its Contribution to the Chesapeake Bay TMDL: Challenges Posed by Climate Change in Urban Areas. *Estuaries and Coasts*, 40(5), 1227–1246.
- Wittmann, K. J., Gundacker, C., Hölinger, M., & Sayed, H. El. (1996). Extinction processes and secondary biotopes in urban areas: the endangered oligorheophilic molluscan fauna of the River Danube. *Large Rivers*, 10(1–4), 485–491.
- Weitzman, J. N., Forshay, K. J., Kaye, J. P., Mayer, P. M., Koval, J. C., & Walter, R. C. (2014). Potential nitrogen and carbon processing in a landscape rich in milldam legacy sediments. *Biogeochemistry*, 120(1–3), 337–357.
- Wollheim, W. M., Pellerin, B. A., Vörösmarty, C. J., & Hopkinson, C. S. (2005). N retention in urbanizing headwater catchments. *Ecosystems*, 8(8), 871–884.
- Wohl, E., & Merritts, D. J. (2007). What Is a Natural River? *Geography Compass*, 1(4), 871–900.
- Wood, P. J., & Armitage, P. D. (1997). Biological effects of fine sediment in the lotic environment. *Environmental Management*, 21(2), 203–217.
<https://doi.org/10.1007/s002679900019>
- Worrall, F., Davies, H., Bhogal, A., Lilly, A., Evans, M., Turner, K., ... Merrington, G. (2012). The flux of DOC from the UK - Predicting the role of soils, land use and net watershed losses. *Journal of Hydrology*, 448–449, 149–160.
<https://doi.org/10.1016/j.jhydrol.2012.04.053>
- Zahawi, R. A., & Holl, K. D. (2009). Comparing the performance of tree stakes and seedlings to restore abandoned tropical pastures. *Restoration Ecology*, 17(6), 854–864. <https://doi.org/10.1111/j.1526-100X.2008.00423.x>
- Zarnetske, J. P., Haggerty, R., Wondzell, S. M., & Baker, M. A. (2011). Labile dissolved organic carbon supply limits hyporheic denitrification. *Journal of Geophysical Research: Biogeosciences*, 116(4). <https://doi.org/10.1029/2011JG001730>
- Zhi, W., Li, L., Dong, W., Brown, W., Kaye, J., Steefel, C., & Williams, K. H. (2019). Distinct Source Water Chemistry Shapes Contrasting Concentration-Discharge Patterns. *Water Resources Research*, 55(5), 4233–4251.
<https://doi.org/10.1029/2018WR024257>

9. Curriculum Vitae

PATRICK W. MCMAHON**EDUCATION****Towson University**

Thesis-Driven Master of Science in Environmental Science
GPA: 4.00/4.00

Summer 2017 – Spring 2021

University of Maryland, College Park, MD

Fall 2010 – Spring 2013

Bachelor of Science in Environmental Science and Technology, Concentration in Ecological Technology Design
GPA: 3.941/4.00

AWARDS

Towson University: Dean's List

Fall 2017 – Spring 2019

University of Maryland: Dean's List

Fall 2010 – Spring 2013

University of Maryland: Magna Cum Laude

Spring 2013

WORK EXPERIENCE**Towson University**

Adjunct Professor

Fall 2019 – Spring 2021

- Modified lesson plans and exams for Geology 121 laboratory exercises
- Lectured college students (30+) in classroom and outdoor settings
- Provided guidance through laboratory material

Towson University

Summer 2017 – Fall 2019

Research Assistant

- Performed thesis research on the hydrogeochemistry of Maryland streams to characterize the effectiveness of stream restoration practices
- Versed in stream sampling practices, protocols, and equipment: MF Pro, Mini DOT, Pro DSS, Thermo Orion, and all HOBO sensors
- Worked with many laboratory instruments including: Dionex ICS-500, Elementar Vario EL III, Mettler Toledo Automatic Titrator, Shimadzu TOC-Vcsh, SEAL AQ1

Teaching Assistant (taught for Geology 121 lab sections)

- Strengthened my abilities to present scientific ideas and to supervise large classes
- Gained an understanding of teaching complex ideas to students with diverse educational backgrounds

Maryland Environmental Service

October 2016 – June 2017

Environmental Specialist

- Inspected various environmental stormwater reduction technologies through the Clean Water Partnership in Prince Georges County
- Monitored and instructed contractors in the successful completion of numerous construction projects
- Crafted reports on the status, issues, and progress of construction on best management practices in relation to stormwater

Anacostia Watershed Society

Environmental Scientist – Project Coordinator

April 2014 – March 2016

- Environmental educator to students of various scholastic levels: day-to-day teaching and lesson plan development
- Managed restoration projects, including budget, permitting, and contractors, from the inception to completion
- Developed protocols for monitoring and maintenance on low impact development (LID) and restoration practices
- Performed research and analysis (physical and biological) on many restoration projects in order to measure success
- Conducted the day to day maintenance and construction of various LID and restoration efforts
- Worked closely with plants, terrestrial and aquatic, (germination, care, and planting) as well as wildlife populations

RESEARCH EXPERIENCE

- McMahon P., Moore J., et al (2019) Export of Nitrogen and Sediments Following Legacy Sediment Removal and Floodplain Reconnection Restoration Projects. *American Geophysical Union Fall Meeting*, San Francisco, CA.
- McMahon P., Moore J., et al (2019) Export of Nitrogen and Sediments Following Legacy Sediment Removal and Floodplain Reconnection Restoration Projects. Maryland Water Monitoring Council Annual Conference, Baltimore, MD.
- McMahon P., Moore J., et al (2019) Export of Suspended Solids Following Legacy Sediment Removal and Floodplain Reconnection Restoration Projects. *Wolman Club Meeting*, Lancaster, PA
- McMahon P., Moore J., et al (2018) Export of Nutrients Following Legacy Sediment Removal and Floodplain Reconnection Restoration Projects. *Maryland Water Monitoring Council*, Baltimore, MD.
- McMahon P., Moore J., et al (2018) Export of Nutrients Following Legacy Sediment Removal and Floodplain Reconnection Restoration Projects. *American Geophysical Union*, Washington, DC.

